CYTOKINE DETECTION METHODOLOGIES ON OPTICAL FIBER SUBSTRATE

BY

KAIXIN ZHANG

A THESIS SUBMITTED TO MACQUARIE UNIVERSITY

FOR THE DEGREE OF

DOCTOR OF PHILOSOPHY

DEPARTMENT OF PHYSICS AND ASTRONOMY

Feb 2019

MACQUARIE University
SYDNEY·AUSTRALIA

Contents

List of acronyms

Ab	Antibody
Ag	Antigen
AP	Alkaline phosphatase
APTES	Aminopropyltriethoxysilane
AuNP	Gold nanoparticle
BAS	Biotin-streptavidin system
BCIP	5-Bromo-4-choloro-3-indolyl phosphate
BSA	Bovine serum albumin
CTLs	Cytotoxic T lymphocytes
CNS	Central nervous system
CSF	Cerebrospinal fluid
DG	Dragon Green
DMEM	Dulbecco's modified Eagle's medium
ELISA	Enzyme-linked immunosorbent assay
ELISPOT	Enzyme-linked immunospot
FBS	Fetal Bovine Serum
G-CSF	Granulocyte colony stimulating factor
GM-CSF	Granulocyte-macrophage colony-stimulating factor
HER	Human epidermal growth factor receptor
H_2O_2	Hydrogen peroxide
HQ	Hydroquinone
HRP	Horseradish peroxidase
HIV	Human immunodeficiency virus
IFN	Interferon
IL	Interleukin
LPS	Lipolysaccharide

MA	6-mercaptohexanoic acid
NBT	Nitro blue tetrazolium
NGF	Nerve growth factor
NHS	N-hydroxysuccinimide
OSCC	Oropharyngeal squamous cell carcinoma
OSM	Oncostatin M
PBS	Phosphate-buffered saline
PC	Polycarbonate
PDMS	Polydimethylsiloxane
PMMA	Polymethyl methacrylate
PS	Polystyrene
PTSD	Post-traumatic stress disorder
SCF	Stem cell factor / KIT ligand
SCI	Spinal cord injury
SPIO	Superparamagnetic iron oxide
SPR	Surface plasmon resonance
TGF-β	Transforming growth factor β
TNF	Tumour necrosis factor
UV-vis	Ultraviolet–visible

Abstract

Sensitive and localized measurements of cytokines are important in biomedicine, medical research and clinical applications. The classic cytokine detection methods including ELISA, ELISPOT, and Western blot are reliable but with limited sensitivity, and they are only applicable to accessible biological fluids such as blood plasma. However, the cytokines are locally released (i.e. at the site of injury or disease), and measurements of their systemic levels in body fluids provide only a limited insight into the undergoing processes. Thus, to understand the role of the immune system in disease or multiple health conditions which lead to immunoreactivity and the expression of cytokines, the development of a method with sufficient sensitivity that can directly measure the locally released cytokine is highly desirable.

The focus of my Ph.D. research program is the development of sensitive cytokine immunosensors based on optical fiber allowing localized and spatially resolved cytokines detection. Specifically, my research project aims to advance the sensitivity of the cytokine immunosensor and explore the biological application of the designed immunosensor from *in vitro* to *in vivo*. The first paper (Chapter 2) demonstrated a cytokine detection device based on aminopropyltriethoxysilane-gold nanoparticle-6-mercaptohexanoic acid modified silica optical fiber for the monitoring of locally variable cytokine interleukin-6 concentrations using a sandwich immunoassay scheme. In the second paper (Chapter 3), we further extended the application of the way for fabrication immunosensor in the first paper and designed an optical fiber-based immunosensing device for repeated monitoring of spatially localized cytokine interleukin-1beta release in the rat brain. To further enhance the performance of the immuosensor, in the third paper (Chapter 4), a more sensitive and robust immunosensing system was designed based on biotin-streptavidin coupling for spatially localized femtogram mL^{-1} level detection of interleukin-6 in serum samples, then in the fourth paper (Chaper5), we further extended the application of the immunosensor that prepared by the biotin-streptavidin system in the rat spinal cord.

Key words: cytokine, immunosensing, localized and spatially resolved detection, optical fiber, rat

Statement of candidate

I certify that the work in this thesis has not previously been submitted for a degree nor has it been submitted as part of requirements for a degree to any other university or institution other than Macquarie University.

I also certify that the thesis is an original piece of research and it was authored by myself. Except when acknowledged otherwise, help and assistance that I have received in the course of my research work and in the preparation of the thesis itself has, where appropriate, been acknowledged.

In addition, I certify that all information sources and literature used in the course of this research is also indicated where appropriate in this record of my thesis.

_____

Kaixin ZHANG

Acknowledgements

I would like to express my sincere gratitude to my supervisor Professor Ewa M. Goldys for the continuous support of my Ph.D study. I am very thankful for her patience, motivation, and immense knowledge that helped me in all the time of research and writing of this thesis. Without her help, I could not achieve my project so smoothly and have so much freedom to carry out the research in my own way.

I am also thankful to Dr. Guozhen Liu, for her valuable assistance to my project and kind help at the beginning of my Ph.D study. I appreciate the advice and encouragement she provided. I have learned a lot from her, and because of that, I become stronger and more independent in striving towards my goals.

I would like to thank to my collaborators, Professor Steven Maier, Professor Mark Hutchinson, Professor Matthew Frank, Professor Michael Baratta for providing me great financial support when I was in their lab. Their helpful ideas and constructive comments also have contributed a lot to improve the quality of my papers. In addition, I have to say a big thank you to Dr Michael Baratta, Mr Nathan Leslie, and Ms Bella, for offering me great help in their lab and making my life much easier when I travelled in US, and also, a big thanks to Mr Azim Arman, who did a good collaboration in the application of our designed immunosensor, and also helped a lot when I travelled at Adelaide.

I also would like to thank to my acting supervisor professor Alex Fuerbach who has helped a lot during the submission of my thesis and given the valuable suggestions to this thesis. And also, I would like to extend my gratitude to my colleagues, Dr. Ayad Anwer for his patient training and management on most lab facilities and experimental procedures and Dr Annemarie Nadort for her valuable input to my project. I am also thankful to Dr Wenjie Chen, Ms Yuxiang Zhu, Ms Zosia Wargocka, Mr Fuyuan Zhang, Ms Yuan Liu, Ms Fang Gao, Mr Fei Deng, Dr Andrew Care, Mr. Kashif Islam, Dr Kai Zhang, Dr. Ke Ma, Mr. Fei Wang, Dr Xianlin Zheng, Dr Deming Liu, Dr. Liuen Liang, Dr. Wei Deng, Dr. Xiaoteng Jia, Ms Yan Wang, Ms Yameng Zheng, Ms Xin Xu, Mr Shilun Feng and my other wonderful colleagues and friends, who have contributed directly or indirectly to this success, and who have shared their time and their thoughts with me.

A special thanks to my family. Words cannot express how grateful I am to my parents for all of the sacrifices that they have made on my behalf. Their prayer for me was what sustained me thus far. In addition, I would like to express my deepest appreciation to my beloved wife Yueyue who has spent sleepless nights with and gives me continuous support, encouragement and strength to keep me moving forward.

Finally, I wish to acknowledge Macquarie University for awarding me the international Macquarie University Research Excellence Scholarship (iMQRES) and Postgraduate Research Fund (PGRF), and the financial support from ARC Centre of Excellence for Nanoscale BioPhotonics (CNBP) and department of Physics and Astronomy, which enable me to attend the national and international conferences during this project.

1
Introduction

Cytokines are small molecular proteins secreted by many different cells of the immune system (neutrophils, macrophages, monocytes, T-cells, and B-cells) to regulate both local and systemic inflammatory responses [1], thus cytokines are usually recognized as biomarkers to characterize the immune function, understand and predict disease, and monitor the effects of treatment [2-4]. Therefore, cytokine detection is important as elevated concentrations of cytokines may indicate the activation of cytokine pathways associated with inflammation or disease progression. However, the detection of cytokines is challenging because of their dynamic secretion process and low abundance *in vivo*, with physiological concentrations normally in the pM range. Standard methods based on the idea of an immunoassay greatly rely on the popular enzyme-linked immunosorbent assay (ELISA), enzyme-linked immunospot (ELISPOT), and western blot etc., as these methods are reliable and accurate. But the application of these methods is usually limited in *in vitro* sample analysis and the requirement of the large volume sample makes it inadequate to detect trace cytokine in complicated samples. Thus, broad interest exists in developing simple, sensitive and rapid cytokine analysis platforms that afford comprehensive characterization and quantitative analysis of cytokines secretion from *in vitro* to *in vivo.*

This thesis reports a cytokine immunosensing method that performed on the optical fiber surface allowing sensitively localized and spatially resolved cytokine detection from *in vitro* to *in vivo*. Firstly, a covalent chemical bonding method was introduced for the sensing surface fabrication, and a spatially resolved ELISA sandwich assay was built on the optical fiber surface. By using detection antibody conjugated to bright fluorescent Dragon Green beads for signal amplification, this variant of spatial ELISA was successfully used for the detection of cytokine with the low limit of detection of 1 pg mL^{-1} and sample volume of 1 μL. In particular, as the fiber could be inserted into a perforated brain implanted cannula that enables fluid exchange between the outside and inside of the cannula, that a novel platform for *in vivo* detection of cytokine release within discrete brain regions, was established by this variant of spatial ELISA. This novel immunosensing technology represents an opportunity for unlocking the function of neuroimmune signaling. In addition, to further enhance the performance of the immunosensor, biotin-streptavidin was introduced to advance the fabrication of the sensing surface, and a robust and ultrasensitive immunosensor was achieved, making the sensitivity from pg mL^{-1} to fg mL^{-1} level. Moreover, this developed sensing platform was further applied for the cytokine detection in the cell culture medium and in a spinal cord of an anesthetized rat.

This chapter reviews the current status of the immunosensing method developments for the detection of cytokine. It briefly introduces the significance for the cytokine detection; the standard immunoassay for cytokine detection; new developed cytokine immunosensors based on the novel technology; remaining challenges and opportunities for the cytokine immunosensing and a detailed thesis outline is provided at the end of this chapter.

1.1 Cytokines

1.1.1 Definition, Types & Function

Cytokines are hormone-like polypeptides with a wide variety of molecular weight ranges from approximately 6 to 70 kDa. They are secreted by many different cells of the immune system (neutrophils, macrophages, monocytes, T-cells, and B-cells) to regulate both local and systemic inflammatory responses [1]. Until now, around 200 cytokines are discovered, and the number of identified proteins continues to grow. As the diverse structure and function of the cytokines, currently, there is no unified way to class and name these cytokines, the ways commonly used for the cytokines classification are usually based on the cells that are their targets, their cell of origin, the category of activity they influence, their spectrum of activity, or on specific features of their ligand-receptor interaction. Based on the type of receptor cytokines utilize, existent cytokines can be grouped in interferons, interleukins, chemokines, and tumor necrosis factor. And typical cytokines belonging to each group are shown in table 1-1 [5].

Table1-1 A list of cytokines and chemokines grouped by their receptor types [5].

Interleukins
– Class I receptors: β-chain (IL-3, IL-5, GM-CSF), γ-chain (IL-2, IL-4, IL-7, IL-9, IL-13, IL-15, IL-21), IL-6-like (IL-6, IL-11, IL-30, IL-31), IL-12 family (IL-12, IL-23, IL-27, IL-35)
– Class II receptors: IL-10 family (IL-10, IL-19, IL-20, IL-22, IL-24, IL-26, IFN type III)
– Ig superfamily or IL-1 receptor family: (IL-1α, IL-1β, IL-1RA, IL-18)
– IL-17 receptor family: (IL-17, IL-25)
Interferons (around 36 total)
– Type I: Alpha, beta (IFNAR1, IFNAR2)
– Type II: Gamma (IFNGR1, IFNGR2)

– Type III: Lambda
Chemokines
– CCL (CCL1–CCL28)
– CXC family
TNF receptors (p55 and p75) family: (TNF-α, LTα, LTβ, FasL, CD40L, TRAIL, LIGHT)
TGF-β receptors (Type 1 & Type 2)

As a biological communication factor, cytokines may act locally on the cells that secrete them (autocrine action), on nearby cells (paracrine action), or in some cases on distant cells (endocrine action)[6-8], so they are considered as important mediators and modulators of many physiological systems. Table 1-2 displays some key cytokines with performing specific roles dependent upon cell type and location [9]. Usually, they functionalize as intercellular messengers in the immune system where they integrate the function of several cell types in various body compartments into a coherent immune response (Figure 1-1). The complex interactions among the immune and inflammatory response cells such as lymphoid cells, hematopoietic cells, and various pro-inflammatory and anti-inflammatory cells are always mediated by the secretions of cytokines [10]. Therefore, in response to pathogens, cytokines secreted by immune cells usually can act as first danger signals, alerting, and initiating immunological pathways.

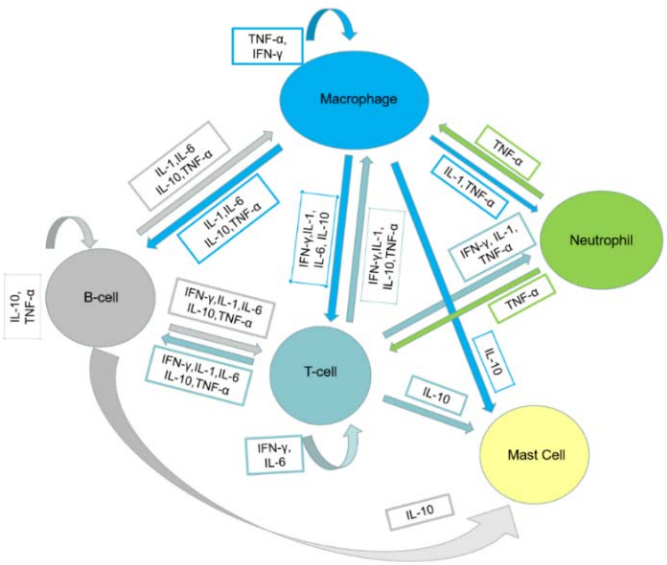

Figure 1-1 An abbreviated version of the cytokine network in biological communications between different cell types in the immune system [11].

Table 1-2 Functions of some key cytokines [9].

	Cytokine	Target cell	Main Function
Interleukins	IL-1	B cells, NK cells, T-cells	Pyrogenic, pro-inflammatory, proliferation and differentiation, BM cell proliferation
	IL-2	Activated T and B cells,	Proliferation and activation
	IL-3	Stem cells	Hematopoietic precursor proliferation and differentiation
	IL-4	B cells, T cells,macrophages	Proliferation of B and cytotoxic T cells, enhances MHC class II expression, stimulates IgG and IgE production
	IL-5	Eosinophils, B-cells	Proliferation and maturation, stimulates IgA and IgM production
	IL-6	Activated B-cells, plasma cells	Differentiation into plasma cells, IgG production
	IL-7	Stem cells	B and T cell growth factor
	IL-8	Neutrophils	Chemotaxis, pro-inflammatory
	IL-9	T cell	Growth and proliferation
	IL-10	B cells, macrophages	Inhibits cytokine production and mononuclear cell function, anti-inflammatory
	IL-11	B cells	Differentiation, induces acute phase proteins
	IL-12	NK cells	Activates NK cells
Interferons	IFN-α	Various cells	Anti-viral
	IFN-β	Various cells	Anti-viral, anti-proliferative
	IFN-γ	Various cells	Anti-viral, macrophage activation, increases neutrophil and monocyte function, MHC-I and -II expression on cells
Tumour necrosis factors	TNF-α	Macrophages	Phagocyte cell activation, endotoxic shock
	TNF-β	Tumor cells, Phagocytes, tumor cells	Tumour cytotoxicity, cachexia Chemotactic, phagocytosis, oncostatic, induces other cytokine
Chemokines	TGF-β	Activated T and B cells	Inhibit T and B cell proliferation, inhibit hematopoiesis, promote wound healing

1.1.2 Role of cytokines in diseases

Since cytokines are potent mediators, participating in acute and chronic inflammation via a complex and sometimes seemingly contradictory network of interactions, figuring out how these pathways work may help facilitate more accurate identification of agents mediating inflammation and the treatment of inflammatory diseases. It is well known that some cytokines play key roles in diseases. For example, IL-2, IFN- γ, IL-12 are associated with elimination of intracellular infections, especially for those caused by viruses or parasites, modulation of organ-specific autoimmune diseases or mediating allograft rejection and recurrent abortions [12]; IL3, IL-4, IL-5, and IL-13 are involved in promoting antibody-mediated responses, which are responsible for atopic disorders, progression to acquired immunodeficiency syndrome, chronic graft versus host disease and cancer metastasis or the hypereosinophilic syndrome; The balance of the microenvironment in the body compartment is maintained by the suppressive or regulatory cytokines include mediators such as IL-10 or transforming growth factor β (TGF-β), which can help to reduce other types of immune responses. Furthermore, it is evidenced that cytokine activation or dysregulation is implied in a variety of disease states like sepsis [13, 14], rheumatoid arthritis [15-17], crohn's disease [18, 19], or multiple sclerosis [20-22]. Given the specific roles of cytokines mediating in disease, cytokines can be considered as useful biomarkers for health and disease, and maybe act as diagnostic, prognostic and therapeutic agents for disease treatment (Table 1-3) [16, 23]. As a result, cytokine measurements have been an important part of the process of defining the role which various cytokines play in health and disease.

Table 1-3 Cytokines as targets for therapeutic treatment of diseases.

Cytokine	Disease targets
IL-2	Metastatic melanoma, Renal cell carcinoma [24, 25]
IL-4	Asthma [26, 27]
IL-5	Asthma [28-30]
IL-6	Rheumatic diseases [31-33]
IL-10	Crohn's disease [34-36], Ulcerative colitis [37], Psoriasis [38-40], Rheumatoid arthritis [41]
IL-11	Crohn's disease, Ulcerative colitis, Psoriasis, Rheumatoid arthritis [37], Cancer [42]
IL-13	Asthma [37, 43], Radiation lung injury [44]
IFN-α	Hepatitis B and C [45]

IFN-β	Multiple sclerosis [45, 46]
IFN-γ	Chronic granulomatous disease [47], Crohn's disease [48], Multidrug resistant tuberculosis [49]
TNF-α	Rheumatoid arthritis [50, 51], Sepsis[52], Refractory asthma [53], Psoriasis [37]
G-CSF	Idiopathic neutropenia, Congenital neutropenia, Febrile neutropenia, Leukemic neutropenia, Aplastic neutropenia [37], Bone marrow suppression [45]
GM-CSF	Bone marrow suppression, Crohn's disease [45]
HER2-Specific Monoclonal Antibody	Adenocarcinoma of stomach, Breast cancer [54-57]
Erythropoietin	Anaemia [58, 59], Bone marrow failure [45]

1.2 Standard cytokine assays

As the significant importance of cytokine in the field of disease diagnosis and therapy, accurate and reliable methods for the measurement of cytokines are developed for the investigation of cytokine biochemistry, biology, and establishing the potency of cytokine medicinal products intended for therapeutic use. Currently, common approaches for cytokine quantification are generally based on the idea of an immunoassay. The classic standard methods including bioassay, ELISA, ELISPOT/FluoroSpot, western blot represent the dominant roles in the cytokine quantification field. Herein, we make a brief introduction of these classic methods and generally describe the advantages and limitations with respect to each standard cytokine quantification method.

1.2.1 Cytokine Bioassay

Cytokine bioassay is a type of technique based on the activity of the cytokine which can induce various biological responses and read-outs which can be obtained through these biological responses including proliferation tests, cytotoxicity tests, antiviral activity, induction of cell surface molecules, chemotactic activity and inhibition of cytokine secretion. It is usually considered as a semi-quantitative technique that shows a narrow analytical range. In a bioassay, a sensitive cells line is applied to test the activity of a sample and the results of this activity are compared to a standard cytokine preparation. The biological activity of cytokines is generally measured by *in vitro* adapted cell lines that are dependent and/or responsive to a specific growth factor or cellular proliferation of primary cell cultures (Table

1-4)[60]. *In vitro* assays for the measurement of the cytokines through other biological activities including induction of killing, induction of further cytokine secretion, degranulation, antiviral activity, chemotaxis, cytotoxicity, and promotion of colony formation, are also available right now. The bioassay provides a way that not only quantify the cytokine concentrations but also allow the detection of biological activities of the cytokines. However, the drawbacks of this assay are that this assay always requires a large sample size, and the procedure of this assay is time, labour and resource-intensive and usually difficult to perform it reproducibily. In addition, the biggest challenge for the cytokine bioassays is the poor specificity owing to the redundant and overlapping biological activities of cytokines [60, 61], for example, in addition to granulocyte-macrophage-colony-stimulating factor (GM-CSF). TF-1 cells can proliferate in response to oncostatin M (OSM), Stem cell factor / KIT ligand (SCF), nerve growth factor (NGF), IL-4, IL-5, IL-13, etc [62]. This combination of disadvantageous factors drives the development of more specific and sensitive assays by which to measure cytokines directly.

Table 1-4 Bioassays for measurement of potency of some key cytokines

Cytokine	Adapted cell lines	read-outs biological responses	Overlapping/modulating cytokines
IL-2	CTLL-2, murine cytotoxic T cell	Proliferation	IL-12, IL-15, TGF-β1, TGF-β2
IL-4	CT.h4S, murine cytotoxic T cell transfected with human IL-4 receptor	Proliferation	IL-2, TNF-α/β, IFN-α/β, TGF-β
IL-6	B9, murine hybridoma	Proliferation	IL-11, IL-13, OSM
IL-10	Ba8.1C1, murine pro-B cell transfected with human IL-10 receptor	Proliferation	----
IL-12	KIT-225, human chronic T-lymphocyte leukemia	Proliferation	IL-2, IL-4, IL-7, IL-15, IL-21, IL-23
IL-18	KG-1, human myelomonocytic leukemia	IFN-c production	IL-12, IL-21
IFN-α	A549, human lung carcinoma, or 2D9, human glioblastoma, or Daudi, Burkitts lymphoma, or Transfected A549 or HEK 293 (human embryo kidney) cells	Antiviral activity, or production of protein MxA	IFN-β, IFN-x, IFN-c
IFN-γ	A549, human lung carcinoma, or 2D9, human glioblastoma, or Colo205, human colon adenocarcinoma	Antiviral activity	IFN-α, IFN-β
TNF-α	L-929, murine fibroblast or WEHI164 clone 13, murine fibroblast, or KYM-1, human rhabdomyosarcoma, or U-138MG, human glioblastoma	Cytotoxic activity, Stimulation of ICAM-1 expression	IL-1α, IL-1β, IFN-c, TNF-β
GM-CSF	MO7e, human megakaryoblastic leukemia, or TF-1, human erythroleukemia	Proliferation	IL-4, IL-5, IL-6, IL-13, IL-15, GM-CSF, NGF, SCF, LIF, EPO, OSM, TNFα/β, IFN-α/β, TGF-β

EPO: Erythropoetin, GM-CSF: Granulocyte macrophage colony stimulating factor, IFN- Interferon, LIF: Leukemia inhibitory factor, NGF: Nerve growth factor, OSM: Oncostatin M, SCF: Stem cell factor, TGF: Transforming growth factor, TNF: Tumour necrosis factor.

1.2.2 ELISA assay

ELISA assays firstly developed in 1971 [63, 64], enable quantitative detection of a cytokine within biological samples in a liquid environment within a reaction chamber. ELISAs can be performed with a number of modifications to the basic procedure, and current ELISAs for cytokine detection can be classified into three major styles, they are direct, indirect and sandwich ELISA (Figure 1-2). All the three formats ELISA rely on the specific interaction between the antigen and antibody, and each of them has specific roles in their application. The direct ELISA is typically used when analyzing immune response to an antigen, while the indirect ELISA is commonly used for determining total antibody concentration in sample. For the quantification of the cytokine concentrations, a sandwich mode of operation is usually used in the ELISA assay that a capture antibody with specificity for the cytokine of interest is immobilized on the solid phase, usually the bottom of a transparent plate, upon the capture of specific cytokine, detection antibody is added which is enzymatically converted, resulting in an optical change (colored or fluorescent) that permits the quantitative and qualitative detection of the desired cytokine. The sandwich ELISA comprises two specific antibodies (to bind two different epitopes on the cytokine) that enable analysis of complex samples with high specificity for cytokines detection and without the need of sample pre-fractionation [65]. Even though this sandwich ELISA is sensitive and robust for the cytokine measurement, several limitations of the interpretation of ELISA data must be mentioned. For example, the ELISA can only be used for measurement of cytokines in cell culture medium or accessible biological fluids such as serum and saliva, it can provide a total cytokine level, but cannot provide direct information on the identities and frequencies of individual cytokine-producing cells. Moreover, the ELISA methods suffer from the large sample volumes, high reagent costs, and varying binding affinity of antibodies because of differences in the internal structure of recombinant cytokines used to generate these antibodies and the fact that the method only allows the measurement of one cytokine at a time in a specified sample volume.

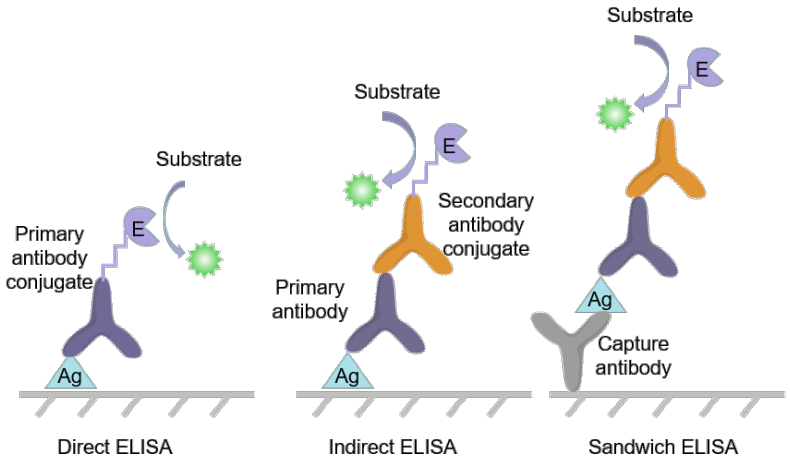

Figure 1-2 Diagram of common ELISA formats (direct vs. sandwich assays). In the assay, the cytokine of interest is immobilized by direct adsorption to the assay plate or by first attaching a capture antibody to the plate surface. Detection of the antigen can then be performed using an enzyme-conjugated primary antibody (direct detection) or a matched set of unlabelled primary and conjugated secondary antibodies (indirect detection).

1.2.3 ELISPOT/FluoroSPOT

The enzyme-linked immuno-spot (ELISPOT) assay is a sensitive method that initially was used for accurate quantification of antigen-secreting immune system cells. It allows determining the frequency of cytokine precursor cells among a heterogeneous population. In this assay (Figure 1-3), a stimulated cell suspension is laid on a microplate well coated with primary antibodies that are capable of directly capture the cytokine of interest [66]. Upon 2-4 hours incubation, cells are removed through extensive washing and the cytokine binding to the solid phase antibody is visualized by a second enzyme-labeled detection antibody. This technique is adaptable to a high throughput and capable of detecting one cytokine-producing cell from 10^5 plated cells. Moreover, it can also provide an estimate of the frequency of antigen responsive cells among those plated [67, 68]. This role of ELISPOT has already been used in the assessment of cytotoxic T lymphocytes (CTLs) precursor frequencies prior and after peptide-based vaccinations in patients with cancer and also in human immunodeficiency virus (HIV) vaccine trials [69-71]. In addition, lots of variations of the ELISPOT assays have also been developed by investigators, a typical example of this variations is FluoroSpot. The FluoroSpot assay is a modification of the ELISPOT assay that is visualized by a bound fluorophore labeled detection antibody instead

of an enzymatic reaction. The position of each cytokine-producing cell is visualized as a fluorescent spot and then the number and size of these spots can be achieved by a special ELISPOT reader consisting of a light microscope with incident fluorescence illumination. This technique shows high sensitivity towards the cytokine detection and now is available for measurement of two different cytokines from a given cell by using different capture antibodies.

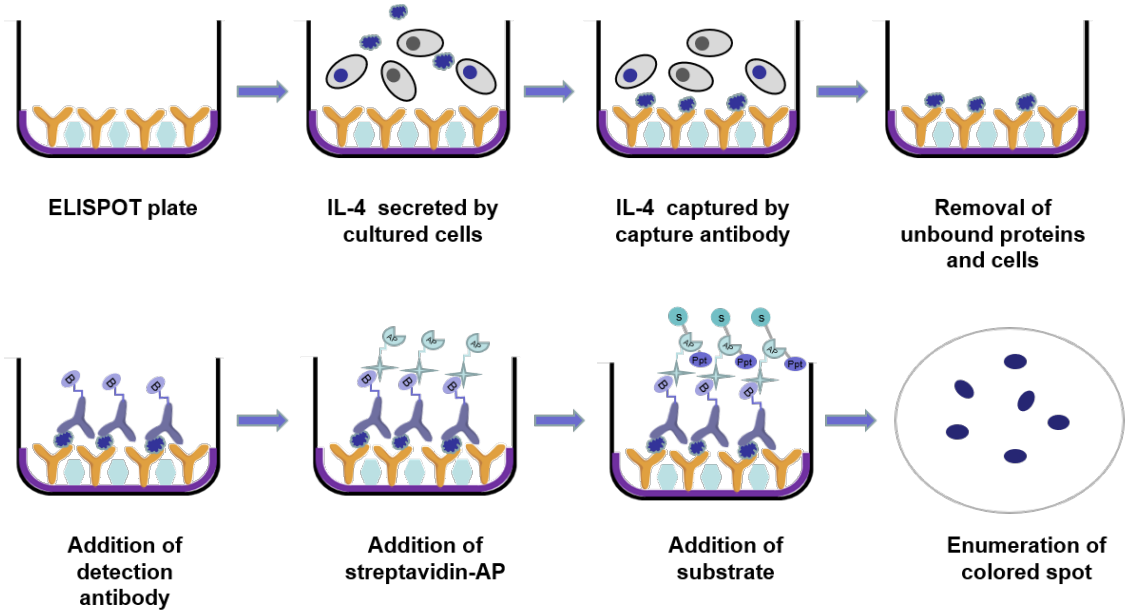

Figure 1-3 methodological principle of the ELISPOT assay (eg: detection of IL-4 released by cells using ELISPOT technique). The plates are coated with primary antibody (anti-IL-4), and thereafter nonspecific binding sites blocked. Cells are added in the presence or absence of specific stimulus, during the incubation, cells become activated and start to secrete the cytokine IL-4 which can be captured by anti-IL-4 antibodies coated on the plate. Cells and non-binding proteins are removed and the detection antibody biotinylated anti-human IL-4 is added to combine the IL-4. After the streptavidin-AP added to binds the biotinylated detection antibody, a precipitating substrate (usually NBT/BCIP) is added to react with AP to produce colored spots that can be read on an ELISPOT reader. Abbreviations: AP, Alkaline phosphatse; NBT, Nitro blue tetrazolium; BCIP, 5-Bromo-4-choloro-3-indolyl phosphate.

1.2.4. Western Blot

Western blot is a powerful biochemical technique capable of protein detection and semi-quantification. Unlike ELISA, ELISPOT/FluoreSPOT, which are applied for cytokine detection in solution, western blot is widely used for the analysis of cytokines within cells,

tissues, and complex biological samples. In this technique, denatured cytokines are firstly separated in polyacrylamide gels through gel electrophoresis, then they are transferred to the nitrocellulose or polyvinylidene difluoride membranes producing a band for each of protein (Figure 1-4). And finally, the membrane is stained with labelled antibodies specific to the cytokine of interest. For the signal read-out system, there are many methods including colorimetric, radioactive, and fluorescent available for the signal reads-out whereas chemiluminescent is commonly used as chemiluminescence is a sensitive and robust method for relative quantitation of the protein of interest. After the primary antibody binds to the protein of interest, the secondary antibody, is usually linked to horseradish peroxidase which is used to cleave a chemiluminescent agent. The reaction product produces luminescence, which is related to the amount of protein, thus the amount of cytokine present can be achieved by a standard calibration curve. This technique may not be as sensitive as ELISA in cytokine detection, but the more significant thing is that it provides useful information on the cytokine molecular weight, which enables this technique to monitor the cytokine molecule degradation and distinguish splice variants and inactive precursors from the active forms. A typical example is that this technique can be successfully used to distinguish the IL-1 β precursor (31KDa) and mature IL-1β (17 KDa), indirectly providing information about protein activation [72].

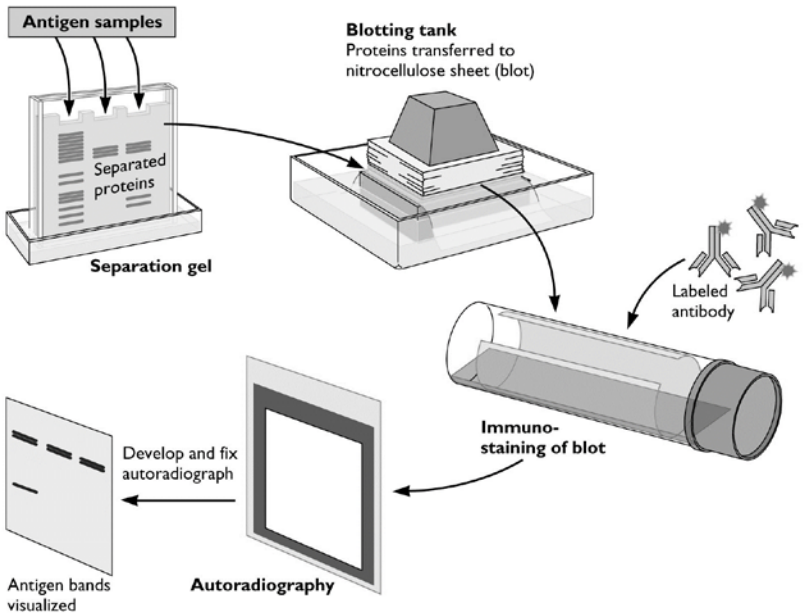

Figure 1-4 the procedure of western blot technique for protein detection.
(https://www.mybiosource.com/learn/westernblotting)

1.3 Immunosensors for cytokine detection

The most common techniques, bioassays, ELISA, ELISPOT/FluoroSpot and western blot, are reliable, but all of them suffer from a long sample preparation time and the requirement of a large sample volume also makes them inadequate to detect trace level of cytokines in a complex biological sample. As a result, these limitations drive people to develop sensitive and rapid robust cytokine immunosensors beyond the traditional immunoassays to realize the comprehensive characterization and quantitative analysis of cytokines released in both healthy and pathological conditions. It is known that to make a successful immunosensor, establishment of a proper sensing surface and a reasonable transducer for subsequent signaling are always the crucial elements that need to be considered. In this chapter, the way of the sensing surface fabrication and signaling strategies for a cytokine immunosensor are briefly reviewed.

1.3.1 Fabrication of the sensing surface

The key factor for fabrication of an immunosensor is the construction of a highly effective recognition sensing surface capable of fast and reliable interaction with its binding cytokine of interest. This always involves the distribution and immobilization of the antibody on a solid substrate. As the antibody is a big Y structure (Figure 1-5) and only specific sites can interact with the antigen, thus the orientation, stability, and density of the bound antibodies will greatly affect the performance of the immunosensor such as sensitivity, specify, and the shelf life of the immunosensor. As a result, the choice of the immobilization method is a key consideration. Currently, immobilization methods can be concisely categorized into physical absorption, bioaffinity attachment, and covalent chemical bonding. Strategies for immobilization of antibodies on a solid substrate while maintaining its identity, structural conformation, and functionality are an evolving field of research. This can promote the advances in the development of rapid and highly sensitive immunosensors. In this part, the strengths and limitations of the developments in antibody immobilization methods are discussed for providing a useful guideline for the selection of suitable antibody immobilization.

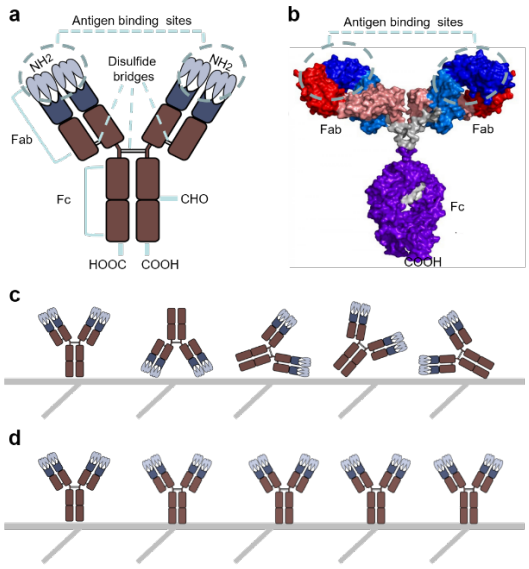

Figure 1-5 (a) Schematic representation of an antibody molecule. (b) three-dimension view of an antibody. (c) random orientation of the antibodies on the substrate (d) optimal orientation of the antibody on the substrate. Fab-fragment, antigen binding; Fc-fragment, crystallizable; CHO-carbohydrate moiety.

1.3.1.1. Physical absorption

Physical absorption of antibody on a solid surface is the easiest method for immobilization. It occurs through non-covalent interactions between the antibodies and target solid supports including plastic surfaces (polystyrene and silicone), membranes (nitrocellulose and nylon), and various metallic surfaces. Interactions for the physical absorption methods usually include various non-covalent bridges, such as pi-pi interactions, hydrophobic interactions, van der Waals forces, ionic and hydrogen bonds etc, which are largely determined by the chemical properties of the solid phase and the surface characteristics of the antibody, as well as the solvent used in the immobilization system. Even though this immobilization method is characterized by fast, simple and does not involve any chemical steps that might affect the antibodies integrity, it provides immunosensor with a relative low sensitivity, as adsorbed antibodies are usually randomly oriented, and the steric hindrance of the active site or the lack of biocompatibility between the immobilized antibody and the substrates, may change the antibody folding resulting in a loss of its biological activity. In addition, sometimes, because of the week binding forces involved, only a slight change of the immobilization condition such as solvent, temperature and pH used in the immobilization system, might have a significant effect on the absorption

of the antibody. Moreover, in biological media, the adsorbed antibodies tend to slowly leach from the surface in exchange for molecules with a higher affinity for the surface [73-75]. As a result, the use of adsorption as immobilization technique sometimes is limited by the relatively poor reproducibility and low operational stability. However, despite these drawbacks of antibody adsorption, this method is still widely used in many applications such as ELISA, antibody arrays, and immunosensors because of their simple procedure and high antibody-binding capacity in a certain immobilization environment. It is of note that currently some novel substrates are developed for the purpose of antibody adsorption with improved orientation. For example, Kamil Awsiuk recently reports regioregular poly(3-alkylthiophenes) films with a semi-crystalline surface structure with edge-on texture that promotes end-on immunoglobulin orientation, leading to a 71% higher performance than the conventional film on the biorecognition of immobilized IgG[76].

1.3.1.2. Covalent chemical bonding immobilization

Covalent binding of the antibody on a substrate is also commonly used. Although it is harsher than the physical absorption strategy, covalent chemical bonding immobilization provides the highest irreversible surface loading. Usually, this covalent immobilization takes place by formation of the amide linkage, as amino groups on the antibody surface can be readily combined with some reactive moieties, such as carboxyl, aldehyde, epoxy, and N-hydroxysuccinimide (NHS) on various solid substrate. So far, some ready-to-use substrates such as carboxyl, aldehyde- and epoxy-activated solid substrates, have already been widely employed for biomolecules (antibody, enzyme, DNA) immobilizations. The covalent immobilization method provides a way to achieve a stable sensing surface and it solves the problems of instability, aggregation, diffusion, or inactivation of antibodies which are trapped on sensor surfaces by polymer matrices, or Langmuir-Blodget films or adsorbed on surfaces. However, as there is a large number of similar amino acid residues on the antibody, bindings between the crosslinker on the substrate with the functional groups on the antibody, usually are not selective, resulting in a significant amount of different binding orientations and in some instances loss of functional activity of the immobilized antibodies. It is reported that the capacities of antigen binding of randomly-coupled antibodies on the substrate were 2~3 times lower than that of well-oriented antibodies [77, 78]. As covalent immobilization that results in specifically-oriented antibodies involves binding of the Fc fragment, several strategies have been developed for the site-specific immobilization of antibodies, where carbohydrate chains or disulphide bridges of antibodies are used for the immobilization

(Figure 1-6) [79]. For example, activation of the C-terminus carboxylic acid group of the antibody via 1-ethyl-3-(3-dimethylaminopropyl)carbodiimide (EDC) and N-hydroxysuccinimide (NHS) allows binding to amino-rich surfaces [80], and a selective partial reduction of hinge-region disulfide bonds of the antibody, generated free pendent sulfhydryl groups, which can be immobilized on a variety of solid supports using sulfhydryl-specific heterobifunctional linkers in a very selective site-specific manner [81]. These methods have advanced the orientations of the antibodies and enhanced the performance of the sensing surface, however, more complicated experimental procedures are involved for example, they require chemical treatments of antibodies, the reaction process needs to be properly controlled, and laborious and tedious protocols are involved in the purification of the chemical activated antibodies. In addition, these commonly used covalent methods are also predicted to generate cross-linking of the antibody itself, and possible loss of biological activity may happen due to the chemical reactions involved. Therefore, when it comes to the antibody immobilization, it would be better to consider all factors in a comprehensive way to choose the most suitable method for immobilization.

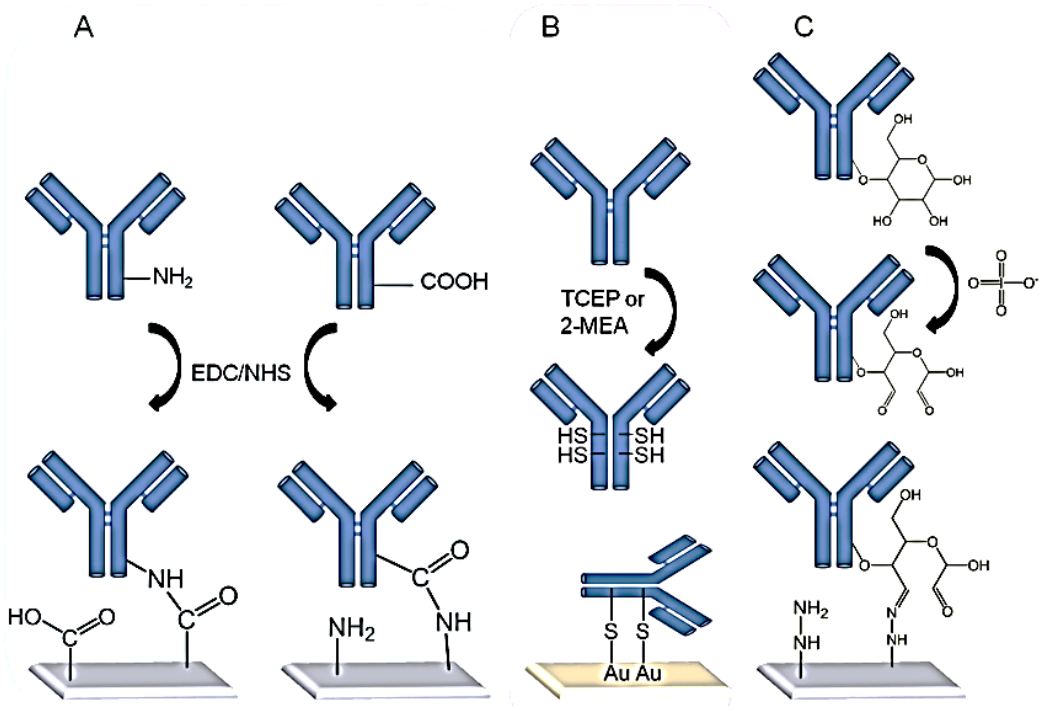

Figure 1-6 Oriented antibody immobilization strategies. (a) EDC/NHS coupling of antibody amine and carboxyl groups to surface carboxyl and amine groups. (b) Reduction of antibody disulfides, with TCEP or 2-MEA, to reactive thiols for binding gold substrates. (c) Periodate oxidation of carbohydrates in the Fc region of antibodies followed by coupling to hydrazide surface chemistry [79].

1.3.1.3. Bioaffinity attachment

Bioaffinity attachment is also convenient way to immobilize the capture antibody on the target substrate. This method is based on the high-affinity constants between certain biomolecules and the target of the substrate, so the capture antibody usually needs to be firstly modified with some affinity tags which helps the antibody firmly attached on the certain substrate. Biotin is a commonly used tag, which has been widely used for antibody immobilization. These antibodies with biotin tag can be strongly attached to the substrates which coated with streptavidin or avidin because of the strong affinity between biotin and streptavidin or avidin. It is reported that the interaction between biotin and (strept) avidin is characterized by a dissociation constant of $10^{\wedge -15}$M, which is the highest dissociation constant reported, around 1000 to 1000000 times higher than for the affinity between an antigen and its specific antibodiy [82]. This high affinity ensures high coupling efficiency between the biotin/biotin-derivatives and (strept)avidin and enables these biotin-streptavidin complex not to be disturbed by extreme changes in pH, temperature, organic solvents and other denaturing agents [83]. Although in the biotin-(strept)avidin system, the random biotin labeled antibody leads to a random immobilization, the biospecific connection between biotinylated antibodies and (strept)avidin coated substrates results in convenient and simple preparation, elimination of toxic compounds and highly efficient antibody utilization. The immobilization of antibody through affinity interactions also can be achieved by using protein G or A binding proteins, as protein G and protein A can specifically bind the Fc region of an antibody, especially of IgGs [84, 85]. This specific binding can make the antibodies maintain a high level of accessibility to antigen binding sites, therefore immunosensors employing protein G or protein A for antibody immobilization regularly show higher sensitivity compared to that of using conventional methods such as random covalent immobilization [86, 87]. However, the main concern of this immobilization approach is the additional immobilization process for binding proteins coating on the surface of a substrate prior to immobilization of the target antibody. But unlike the natural antibodies, binding proteins like protein G or A is easily obtained, and they can be engineered in large quantities, which enable this approach to be widely used for the antibody immobilization. A typical example of the engineered binding protein is the chemical modification of the protein G with a thiolate tag, which enables the formation of the protein G layer on a gold surface to be able to efficiently capture the target antibodies [88, 89]. Another common way is to engineer the N-terminus of the protein G with cysteine residues that can directly form a well-ordered protein G film on a gold like surface [90], which enhanced the orientation of the

subsequent antibody immobilization, resulting in a better performance of the sensing surface. Even though the immobilization method by affinity can help to control the orientation of the antibody and retain the antibodies binding abilities, the affinity between the binding protein and the target antibodies might be not strong enough when they meet some harsh conditions, such as the extreme change of the pH and, temperature, organic solvents and other denaturing agents. Therefore, the environment conditions of the sensing surface used should be carefully considered when this binding method is applied for antibody immobilization.

1.3.1.4 Other strategies

Apart from the methods mentioned above for the fabrication of the sensing surface, there are still some other ways that are available to use. The light-induced antibody immobilization is an attractive approach that can precisely control the areas of immobilization [91]. UV-irradiation of the antibodies results in the cleavage of the disulfide bridge and resulted Fab fragments with thiol groups can be well orientated on a gold like or thiol-reactive surface [92]. Localized and specific conjugation of antibodies can also be achieved by a photoactivable electrogenerated polymer film coated surface allowing the covalent immobilization of biomolecules through light mediation [93]. Another light induced immobilization example employs a protein-photo-reactive crosslinker coated substrate where antibodies can be covalently immobilized upon light irradiation [94]. To some extent, antibody coupling via photo-immobilization technique overcomes some limitations of conventional approaches, such as random chemical reactions or reversible protein binding, and provides a versatile tool for the fabrication of sensing surface, but it is essential to keep in mind that light irritation may also impair the structure of the antibody, resulting in a loss of activity. Immobilization through recombinant antibodies in forms of full-length antibodies, single chain antibody fragments (scFv) or Fab fragments provides another alternative strategy for the sensing surface fabrication. Methods for the oriented immobilization of these recombinant antibodies have already been investigated by employing genetic fusions such as histidine [95-97] or cysteine tags [98]. Such recombinant antibody can be immobilized on the substrates by the same immobilization methods as mentioned in the section of physical absorption, bioaffinity attachment and covalent chemical bonding.

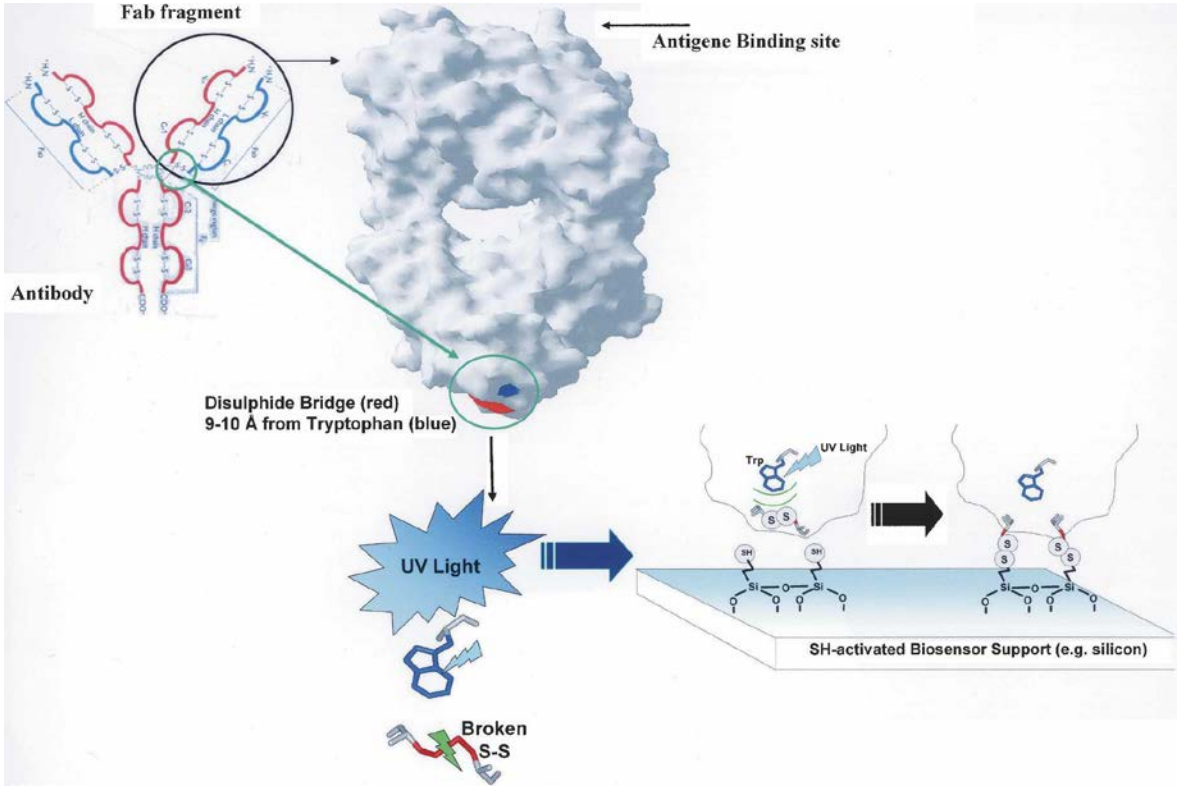

Figure 1-7. An example of the light-induced antibody immobilization. UV light-induced immobilization of Fab fragment onto a thiol-derivatized surface. The disulfide bridge (red) located near a Tryptophan residue (blue) is located far away from the antigen binding site [92].

1.3.2 Signalling strategies for cytokine detection.

As the cytokine immunosensor is designed to detect the direct binding of an antibody or antigen to form an immunocomplex at the transducer surface, signal transducing in immunosensors can be achieved by different methods by detecting different surface properties changes or signal generation, which occurs following the formation of antigen-antibody complex (Figure 1-8) [99]. Then the cytokine can be quantified with the generated signal that is proportional to the analyte concentration. Currently, lots of signalling strategies such as using electrochemical, thermometric, optical, piezoelectric and magnetic signal are available for cytokine detection. As electrochemical and optical signalling strategies are always considered as the popular ways for signal readout, this chapter focuses on the cytokine immunosensors where the transducing mechanisms are related to the measurement of electrons and photons.

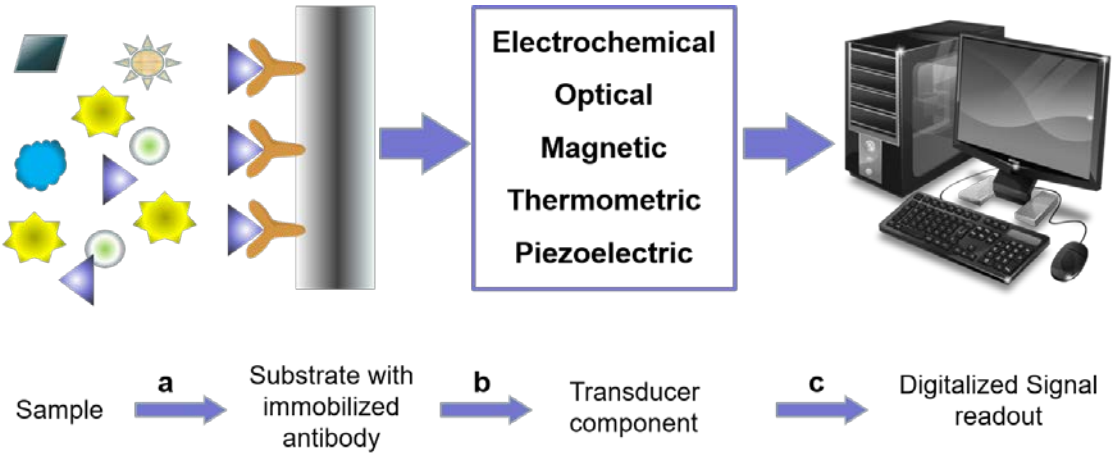

Figure 1-8. A schematic illustration of the mechanism of a standard immunosensor. (a) The formation of antibody /antigen immunocomplex, (b) this then creates a change and thereby a signal. (c) the signal is then transduced either electrochemically, optically, magnetically or piezoelectrically and thermometrically (d) The generated signal is finally collected on a digital readout [99].

1.3.3.1 Electrochemical based immunsensing

Electrochemical cytokine immunosensors are affinity based biosensors when they use a specific transducer with a recognition element that binds the cytokines with specificity and selectivity. The detection of binding a target cytokine to probe in solution is governed by detecting the changes of the electric current, voltage difference or a resistivity change at a localized sensing surface (Figure 1-9). Therefore, the signal from the electrochemical cytokine immunosensors can be obtained by amperometric, potentiometric and impedimetric transducers converting the chemical information into a measurable electronical signal. For successful fabrication of a cytokine electrochemical immunsensor, signal amplification and noise reduction are the key factors that need to be considered as the changes of the electrochemical signal caused by antigen–antibody reaction is relatively weak [100].Currently, the most popular methods for the signalling are voltammetry (linear sweep, differential pulse, stripping, square wave), and amperometry methods. These methods usually involve in three basic steps. Firstly, it need a tracer antibody that binding an electroactive species, such as metal nanoparticle, enzyme, or quantum dot; secondly, the electroactive species modified antibody is able to specific combine the target of cytokine, possibly through an intermediate primary antibody, and thus immobilized on an electrode surface; Finally, a given potential is applied, which drives a redox reaction of the labelled electroactive species resulting in a current signal that is proportional to the concentration of the antibody-bound cytokines, thus the concentration of the targeted cytokine can be

quantified. Differences among the various voltammetry methods are the waveform of the applied voltage and phase of the waveform during which currents are recorded. It is of note that the method stripping voltammetry is a special case that can be applied for multiplex-cytokine detection. As the electroactive ionic species such as the metal ionic species can be discriminated from multiple metal species when they are given a necessary potential for oxidation, multiplex-cytokine sensing can be realized by using different metal or nanoparticle tags to the respective secondary antibodies.

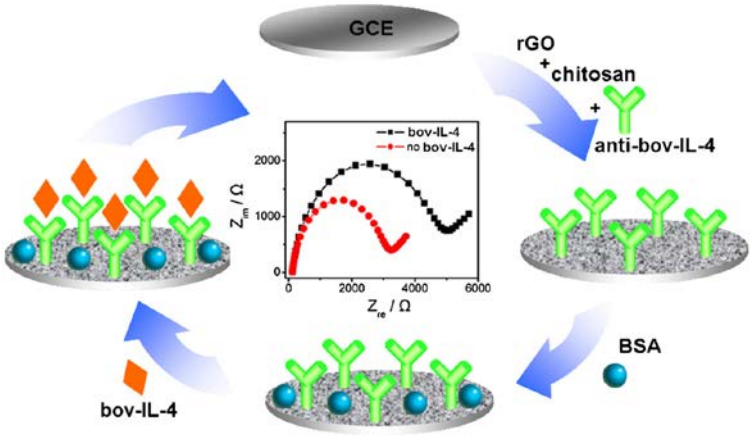

Figure 1-9 An example of electrochemical immunosensor: electrochemical immunosensors for cytokine detection (eg IL-4). Impedance immunosensor for bovine IL-4 using an electrode modified with reduced graphene oxide and chitosan [101].

Improved electrochemical immunosensors employing nanoparticle labels, magnetic beads and nanostructured surfaces provide new opportunities for highly sensitive protein detection [102-116]. Most of the cytokine electrochemical detection strategies are based on the classic sandwich immunoassay method in which the sensing surface is coated by capture antibody or aptamer to specifically capture the target of cytokine (Figure 1-10). After the capture of the target of cytokine, a tracer enzyme or nanoparticle-labelled antibody is introduced to bind the captured cytokine to form the sandwich immunocomplex. Amplification strategies such as employing multiply-labelled antibodies, enzyme labelled magnetic beads or gold nanoparticles are commonly introduced to enhance the sensitivity of the detection.

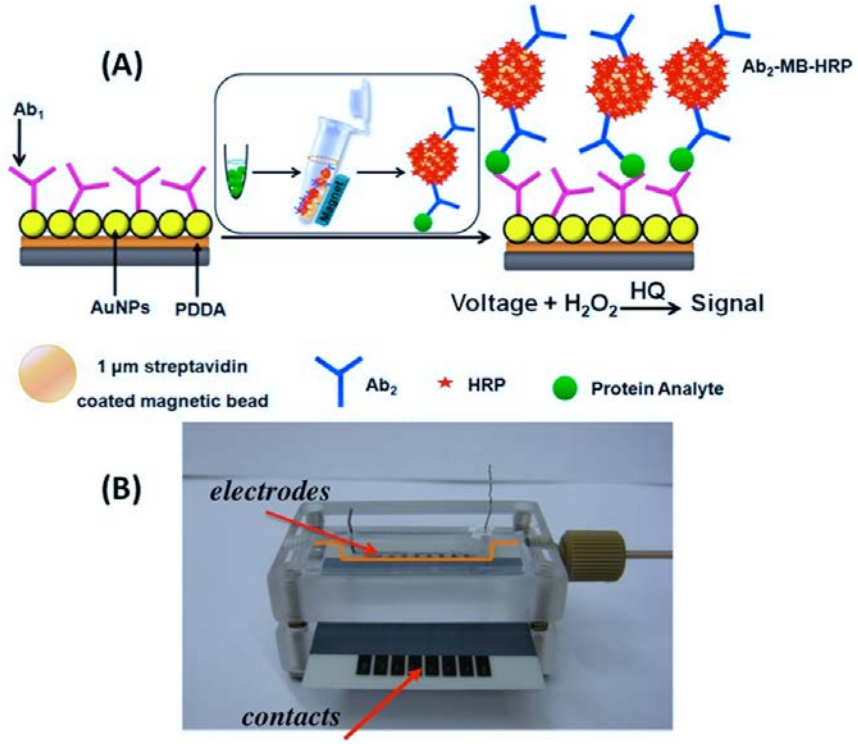

Figure 1-10 Example of an improved electrochemical-based immunosensor for cytokine detection. (A) Magnetic beads coated with massively horseradish peroxidase (HRP) enzyme labels that can catalyse hydrogen peroxide (H_2O_2) to water in the presence of hydroquinone (HQ) to benzoquinone that is reduced to hydroquinone at −0.3 V vs Ag/AgCl. (B) Multiplexed channels for multiplex cytokine sensing [117].

Even though electrochemical based immunsensing showed excellent sensitivity, selectivity and reliability, making the electrochemical based immunosing technique to be a very attractive tool in cytokine detection, these immunosensors might be vulnerable to interference from the experimental conditions such as different pH, ionic strength and co-existing molecules in biological fluids. In addition, the functionality of the capture antibody immobilized on the sensing surface may decline in the presence of external redox mediators that are essentially mixed with the sample solution for electrochemical immunosensing platforms. As a result, it would be great if these electrochemical immunosensors could perform in a normal physiological solution, so that the sensing surface can maintain their best binding performance.

1.3.3.2. Surface plasmon resonance (SPR) based immunsensing

SPR is a powerful surface optical technique to monitor biomolecular interactions with a high degree of accuracy, precision, and sensitivity. It requires a system with polarized light passing through a prism with a metal layer that acts like a mirror [118]. The light from a specific angle (the resonance angle), will interact with the free electrons in the metal layer (usually Au film) resulting in a dip in the light property. Therefore, binding events cause changes in refractive index close to the surface which affect the reflected light intensity, angle and wavelength, which can be measured to probe the interactions between biomolecules (Figure 1-11). Generally, SPR for cytokine detection can be classified into two formats that are direct detection and indirect detection. In direct format, antibodies are directly immobilized on the sensor surface and subjected to the binding interaction with the cytokine of interest. The change in resonance angle due to the formation of antibody-cytokine immunocomplex is directly proportional to the concentration of target cytokine. Direct method is easy to perform, however, it is not suitable for direct cytokine detection. This is because the concentration of cytokine in physiological state is very low (usually at pM range), while direct method for cytokine detection can only provide a low limit of detection at nM range or above, because the cytokine-antibody interaction is not enough to generate a sufficient measurable change in the refractive index [119]. Consequently, indirect SPR methods may provide alternative choices for the cytokine detection. Among indirect methods, a sandwich method is commonly used for signal amplification. Cytokine capture antibody (Ab1) was firstly immobilized on the sensing surface, then binding of cytokine to the capture antibody was detected as the Ab1-Cytokine-Ab2 immunocomplex, where Ab2 is the detection antibody, which usually labeled with some nanoparticles to amplify the SPR signal. Based on this sandwich method, Deckert and F. Legay, developed a SPR immunosensor to monitor the activities of different batches of recombinant IL-6, protein A was introduced to improve the orientation of the capture antibody, and a detection limit of 4 $ng.mL^{-1}$ was achieved. This method showed high reproducibility in IL-6 detection indicating a reliable IL-6 SPR immunosensor was fabricated. A similar SPR immunosensor for IL-8 detection was also developed [120], and it was applied to detect the ten-fold pre-concentration of the initial samples from the patients with oropharyngeal squamous cell carcinoma (OSCC) because this IL-8 SPR immunosensor only got a detection limit of 184 pM, which is not sensitive enough to detect the IL-8 existing in the healthy individuals (30 pM) and patients with OSCC (86 pM) [121]. Therefore, sensitivity and limit of detection for the cytokine SPR immunosensor need to be further improved by introducing specific

amplification strategies. A classic way for improving the performance of these cytokine SPR immunosensor is using the nanoparticles labeled detection antibody to amplify the SPR signal. A typical SPR example for this amplification strategy is developed by Choi's group [122]. They fabricated a SPR immunosensor for the detection of prostate specific antigen using a biotin labelled detection antibody, and this detection antibody was further coupled with streptavidin coated Au nanoparticles which greatly enhanced the SPR signal. And the limit of detection for this SPR immunosensor can be up to 1 $ng.mL^{-1}$ in human serum samples. Furthermore, this group employs magnetic nanoparticles coated with detection antibody for off-line capture of prostate specific antigen, and the SPR signal was further amplified to enable the SPR immunosensor monitor the prostate specific antigen in serum at $fg.mL^{-1}$ level. It can be seen that these amplified SPR immunosensors are very promising as they can be used for the detection of some disease biomarkers for further disease diagnosis. Development of point of care testing device for this SPR immunosensors will be of great value. Even though there still remains the expense of optical detection, and the requirements for a robust, stable, portable SPR device, new development of the optical technology might be helpful to decrease the cost, and it seems that a robust point of care device will become commercially available, allowing for convenient cytokine detection and early remediation of many health challenges in the near future.

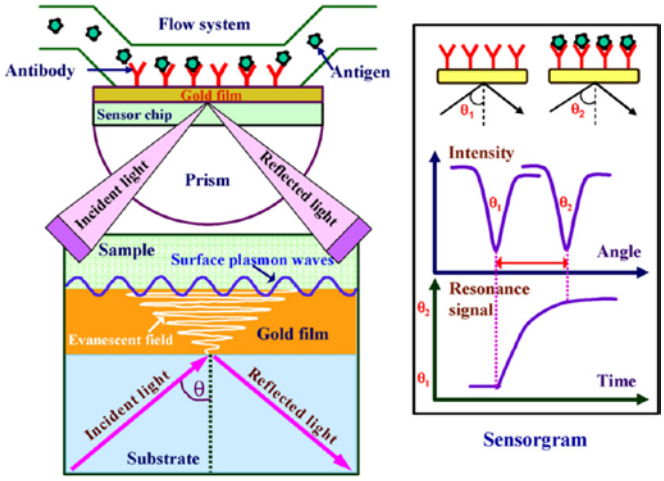

Figure 1-11 Schematic view of the SPR immunoassay technique [123] .

1.3.3.3. Fluorescence based immunosensing

Fluorescence based immunosensing is the most popular method which monitors antibody-antigen binding. It utilises fluorescent molecules which bind either directly to the target antigen or as an indirect label to measure via spectrometry, and quantification of

antigen can be further achieved by measuring the changes of fluorescence signal. Currently, most of the commercially available cytokine assays like ELISA, ELISPOT and cytokine bioassay are based on the fluorescence signalling. Fluorescence based immunosensing represents the most widely studied methodology for cytokine detection because of its high sensitivity. This fluorescence based immunosensing platform has been widely employed using antibody sandwich assay for the detection of cytokines such as, IL-1, IL-6, IL-8 and TNF-α [124]. Improvements for the fluorescence-based cytokine immunosensing using novel signalling materials has also been extensively explored. Typical example for enhancing the performance of the fluorescence immunosensing is applying some nanoparticles that integrate with some bright fluorescent dyes to get the signal amplification. For example, Zhang et. al developed a novel sandwich fluoroimmunosensor for the detection of IL-6. They use functionalized Rubpy-encapsulated fluorescent core–shell silica nanoparticles labels as the signal reporter, and IL-6 was quantified by specific affinity between the captured IL-6 antigens and the fluorescent functionalized core-shell nanoparticles labeled anti-IL 6 antibodies [125]. This approach has offered potential advantages of sensitivity, simplicity and reproducibility for the measurement of IL-6 in serum samples. Another immunosensor with enhanced performance for the detection of TNF-α was developed by Cunningham's group [126]. They employed the photonic crystals coupled with colloidal quantum dot emitters as the signal reporter which made a 20-fold enhancement of emitted light by fluorescent molecules, resulting in high signal-to-noise ratio for TNF-α detection. Improvements in photonic crystal performance can be made to further lower the detection limits as some unique photonic crystal properties such as size-controlled fluorescence, high fluorescence quantum yields, and stability against photobleaching. Generally, the fluorescence based immunosensing for cytokine detection can achieve the limit of detection in the range from $fg.mL^{-1}$ to $ng.mL^{-1}$, which is generally sufficient enough for many cytokines in physiological condition.

1.4 Optical fiber-based cytokine sensor

Optical fibers are chemically passive, have small physical dimensions (diameters in the range of tens to few hundreds μm), and are able to access challenging environments [127, 128]. Configured as fiber-optics sensors, they offer an advantage of long interaction length which, in some situations, can yield enhanced signals. Moreover, optical fiber biosensors can be used in combination with different types of spectroscopic techniques, e.g., absorption,

fluorescence, phosphorescence, Raman, and surface plasmon resonance (SPR) [129]. By combination with the spectroscopic techniques, optical fibers have also been widely explored as a promising platform for cytokine detection [130-133]. A recent report describes a fiber-optics SPR sensor for the detection of IL-1, IL-6, and TNF-α in a buffered saline solution and a spiked cell culture medium [134]. In this study, the detection limit of IL-6 of 0.44 ng mL^{-1} was achieved. The optical fiber-based sensors have also been applied to the monitoring of biologically relevant molecules in real time. For example, a label-free fiber-optic localized SPR sensor for the detection of IFN-γ was fabricated using spherical gold nanoparticles on a polished end-face of the optical fiber [135]. This label-free immunoassay sensor was characterized by a short detection time (5 min), high resolution, and sensitivity (2 pg mL^{-1} for IFN-γ) due to the signal amplification from AuNPs. A recently reported photonic lab-on-a-chip sensor allowed rapid determination of IL-2 levels secreted by lymphocytes based on the measurement of optical absorbance [136]. However, all these fabricated fiber sensors are targeted for the detection of cytokines in buffered saline solution or in the accessible biological liquid (e.g. cell culture medium, serum), none of these devices is capable of spatially localized cytokine detection along the fiber length based on the quantification of the signal on the sensing interface, so it would be of great significance to develop the fiber sensor with the ability of spatially localized detection.

1.5 Challenges and opportunities for cytokine immunosensor

Even though the fabrication of the cytokine immunosensor has been extensively investigated, there are still challenges for the development of cytokine immunosensor. The sensitivity of the immunosensor is always an issue for cytokines detection because cytokines released into the extracellular milieu are always at a very low concentration range (pM) [137]. Apart from the sensitivity issue, in fact, sometimes it is very hard for the immunosensors to measure physiological concentrations of cytokines accurately and reproducibly because of some other challenges such as significant interference from the rheumatoid factors [138], heterophilic antibodies [139], and specific or non-specific cytokine binding proteins [140]. Even though some developed immunosensors claimed that they can get a limit detection level at $pg.mL^{-1}$ or even lower at $fg.mL^{-1}$, the lack of the standardization and a proper way for validation reduce the reliability of these cytokine immunosensors. It is essential to keep in mind that only when validated and carefully controlled methods for cytokine immunosensors are made can we expect to make progress in the development of these

immunosensors into practical work. In addition, evaluations of cytokine levels in tissue are always important, as cytokines are usually produced locally (i.e. at the site of injury or disease), the in-situ cytokine profile might be more relevant to the ongoing physiologic or pathologic processes than systemic cytokine levels. However, the majority of the developed immunosensors for cytokine detection are designed for *in vitro* cytokine detection which usually carried out on accessible biological fluids away from these local sites of action, which make the measured concentration maybe greatly reduced compared to the actual concentration which is present at the active site. Another challenge for many cytokine immunosensors is that they have only been developed in laboratory environments and only few immunosensors are commercially available for practical work. For any commercial application to be successful there must exist a technology that allows rapid production of a number of sensors with high quality. Many believe that the cytokine immunosensors have not lived up to the expectations because of their cost limitations, the lack of sensitivity and ability to be manufactured. Although the concept for fabrication of cytokine immunosensors is simple and elegant, development of such a device is daunting. It needs the efforts from a multidisciplinary field that combines the expertise of immunochemists, immunologists, materials scientists and engineers to develop the intimate interface between the biologic component and the transducer. When combined with the potential integration techniques made possible by the advances in optical, electronic and fabrication technology, it seems that a whole new range of point-of-care tests will become commercially available, allowing for mass-screening programs and detection and early remediation of many health and environmental challenges.

1.6 Thesis aims and outline

Standard methods (e.g. ELISA, ELISPOT and western blot) offer a reliable and accurate way for cytokine detection, but the requirements of the large sample volumes, and tedious operations steps hindered their applications especially in the circumstances that only a limit sample volume can be accessed. Most of the following developed platforms for cytokine detection have reduced the requirements for the sample volumes by introducing some new signal amplification strategies, such as using electrochemical, thermometric, optical, piezoelectric and magnetic signal, however, the application of most of these platforms still limited by their low sensitivity and reproducibility. In addition, there are only limit platforms that are able to be used *in vivo* and real time cytokine analysis is still daunting.

Thus, broad interest exists in developing simple, sensitive and rapid cytokine analysis platforms that afford comprehensive characterization and quantitative analysis of cytokines secretion from *in vitro* to *in vivo*. By using nanoparticles labeled detection antibody to amplify the detection signal, it is expected that immunosensor performed on optical fiber surface would be capable of spatially localized cytokine detection with high sensitivity and make the localized cytokine detection from *in vitro* to *in vivo*. Therefore, motivated by the above identified challenges and opportunities, my PhD program has been aligned to the fabrication of immunosensors on the optical fiber surface for sensitive detection of cytokines from *in vitro* to *in vivo*. The aims of my PhD study are to (1) design sensitive cytokine immunosensors on the optical fiber surface, (2) explore the biological applications of the fabricated immunosensor from *in vitro* to *in vivo*.

The whole thesis consists of six chapters. **Chapter 1** introduces the background and the significance for conducting this project.

Chapter 2 reports a sensitive cytokine immunosensor based on optical fiber allowing localized and spatially resolved detection of interleukin-6 *in vitro* and *ex vivo*. This chapter is in the format of a second-authored paper published in the journal of ACS sensors in 2017. We demonstrated a cytokine detection device based on APTES-AuNP- 6-mercaptohexanoic acid (MA) modified silica optical fiber for the monitoring of locally variable cytokine interleukin-6 concentrations using a sandwich immunoassay scheme. The sensor interface was stable for up to 9 days in PBS solution, and it was capable of detecting localized IL-6 secreted by BV2 cells with liposaccharide stimulation.

Chapter 3 further extends the application of the immunosensor we designed in chapter 2. This chapter is in the format of a first-authored paper published in the journal of Brain, Behavior, and Immunity in 2018. In this work, we designed an optical fiber-based immunosensing device for repeated monitoring of spatially localized cytokine IL-1β release in the rodent brain. We employed APTES-AuNP-MA modified silica optical fiber labeled with a IL-1β capture antibody on the surface interface that can be inserted into a stainless steel implanted cannula with micrometer-sized holes drilled along its length to enable fluid exchange between the outside and inside of the cannula. We showed that the immunocapture device can be introduced into the perforated guide cannula for repeated analyte measurements *in vivo*. An increase in fluorescence detection of spatially localized intrahippocampal IL-1β release was observed following a peripheral lipopolysaccharide

challenge in Sprague Dawley rats. This novel immunosensing technology represents an opportunity for unlocking the function of neuroimmune signaling.

Chapter 4 reports a more sensitive and robust immunosensing system based on biotin-streptavidin coupling for spatially localized femtogram mL^{-1} level detection of IL-6. This chapter is also in the format of a first-authored paper published in the journal of Biosensors and Bioelectronics in 2018. we report a more sensitive immunoassay on the optical fiber surface for accurate quantification of IL-6 in serum samples. A superior sensing surface coated with biotinylated capture antibody was fabricated according to biotin-streptavidin binding strategy. Compared with the antibody immobilization method through covalent reaction with 6-mercaptohexanoic acid reported in chapter 2 and chapter 3, the biotin-streptavidin system could boost the amount of capture antibody immobilized on the fiber surface, leading to increased sensitivity of the immunosensor. In addition, a more stable immunocapture was achieved by using biotin-streptavidin coupling strategy, as the sensing surface can be stable for up to 4 weeks in PBS solution.

Chapter 5 further extends the application of the immunosensor prepared by biotin-streptavidin system. This chapter is in the format of a first-authored paper published in the journal of Sensors and Actuators B-chemical in 2018. In this work, compared to the previous study in chapter 4, we have advanced the biotin-streptavidin coupling strategy for the immobilization of capture antibody on the sensing surface and characterised the properties of the sensing surface such as stability and reproducibility. The application of the fiber immunosensor was firstly tested ex-vivo by analysing the secretions of rat macrophages stimulated by lipopolysaccharide (LPS), then an in vivo test of a localized measurement of IL-1β in the rat spinal cord.

Chapter 6 summarises the key research outcomes of this thesis and discusses the future prospects of developing immunosensors for cytokine detection.

1.7 Reference

[1] J. Parkin, B. Cohen, An overview of the immune system, The Lancet 357(9270) (2001) 1777-1789.
[2] H.D. Schmidt, R.C. Shelton, R.S. Duman, Functional biomarkers of depression: diagnosis, treatment, and pathophysiology, Neuropsychopharmacology 36(12) (2011) 2375.
[3] I. Tabas, C.K. Glass, Anti-inflammatory therapy in chronic disease: challenges and opportunities, Science 339(6116) (2013) 166-172.
[4] W.-W. Lin, M. Karin, A cytokine-mediated link between innate immunity, inflammation, and cancer, The Journal of clinical investigation 117(5) (2007) 1175-1183.
[5] L.H. Butterfield, T.L. Whiteside, Cytokine Assays, eLS2016, pp. 1-11.
[6] J.J. Haddad, Cytokines and related receptor-mediated signaling pathways, Biochemical and biophysical research communications 297(4) (2002) 700-713.
[7] J.E. Blalock, The syntax of immune-neuroendocrine communication, Immunology today 15(11) (1994) 504-511.
[8] K. Gulati, S. Guhathakurta, J. Joshi, N. Rai, A. Ray, Cytokines and their Role in Health and Disease: A Brief Overview, MOJ Immunol 4(2) (2016) 00121.
[9] M.D. Turner, B. Nedjai, T. Hurst, D.J. Pennington, Cytokines and chemokines: At the crossroads of cell signalling and inflammatory disease, Biochimica et Biophysica Acta (BBA) - Molecular Cell Research 1843(11) (2014) 2563-2582.
[10] L.M. Coussens, Z. Werb, Inflammation and cancer, Nature 420(6917) (2002) 860.
[11] J.A. Stenken, A.J. Poschenrieder, Bioanalytical chemistry of cytokines – A review, Analytica Chimica Acta 853 (2015) 95-115.
[12] S. Romagnani, The th1/th2 paradigm, Immunology today 18(6) (1997) 263-266.
[13] B.G. Chousterman, F.K. Swirski, G.F. Weber, Cytokine storm and sepsis disease pathogenesis, Seminars in immunopathology, Springer, 2017, pp. 517-528.
[14] M. Surbatovic, N. Popovic, D. Vojvodic, I. Milosevic, G. Acimovic, M. Stojicic, M. Veljovic, J. Jevdjic, D. Djordjevic, S. Radakovic, Cytokine profile in severe Gram-positive and Gram-negative abdominal sepsis, Scientific reports 5 (2015) 11355.
[15] I.B. McInnes, C.D. Buckley, J.D. Isaacs, Cytokines in rheumatoid arthritis—shaping the immunological landscape, Nature Reviews Rheumatology 12(1) (2016) 63.
[16] S. Siebert, A. Tsoukas, J. Robertson, I. McInnes, Cytokines as therapeutic targets in rheumatoid arthritis and other inflammatory diseases, Pharmacological reviews 67(2) (2015) 280-309.
[17] S. Mateen, A. Zafar, S. Moin, A.Q. Khan, S. Zubair, Understanding the role of cytokines in the pathogenesis of rheumatoid arthritis, Clinica chimica acta 455 (2016) 161-171.
[18] M.F. Neurath, Cytokines in inflammatory bowel disease, Nature Reviews Immunology 14(5) (2014) 329.
[19] K.F. Baker, J.D. Isaacs, Novel therapies for immune-mediated inflammatory diseases: What can we learn from their use in rheumatoid arthritis, spondyloarthritis, systemic lupus erythematosus, psoriasis, Crohn's disease and ulcerative colitis?, Annals of the rheumatic diseases (2017) annrheumdis-2017-211555.
[20] C.A. Dendrou, L. Fugger, M.A. Friese, Immunopathology of multiple sclerosis, Nature Reviews Immunology 15(9) (2015) 545.
[21] A.P. Kallaur, S.R. Oliveira, D.F. Alfieri, T. Flauzino, J. Lopes, W.L.d.C.J. Pereira, C. de Meleck Proença, S.D. Borelli, D.R. Kaimen-Maciel, M. Maes, Cytokine profile in patients with progressive multiple sclerosis and its association with disease progression and disability, Molecular neurobiology 54(4) (2017) 2950-2960.

[22] B. Hemmer, M. Kerschensteiner, T. Korn, Role of the innate and adaptive immune responses in the course of multiple sclerosis, The Lancet Neurology 14(4) (2015) 406-419.
[23] I. Striz, E. Brabcova, L. Kolesar, A. Sekerkova, Cytokine networking of innate immunity cells: a potential target of therapy, Clinical science 126(9) (2014) 593-612.
[24] S. Lee, K. Margolin, Cytokines in cancer immunotherapy, Cancers 3(4) (2011) 3856-3893.
[25] T. Hughes, M. Klairmont, J. Broucek, G. Iodice, S. Basu, H.L. Kaufman, The prognostic significance of stable disease following high-dose interleukin-2 (IL-2) treatment in patients with metastatic melanoma and renal cell carcinoma, Cancer Immunology, Immunotherapy 64(4) (2015) 459-465.
[26] L. Hendeles, M. Asmus, S. Chesrown, Evaluation of cytokine modulators for asthma, Paediatric respiratory reviews 5 (2004) S107-S112.
[27] G.M. Walsh, Anti-IL-4/-13 based therapy in asthma, Taylor & Francis, 2015.
[28] M.J. Leckie, A. ten Brinke, J. Khan, Z. Diamant, B.J. O'connor, C.M. Walls, A.K. Mathur, H.C. Cowley, K.F. Chung, R. Djukanovic, Effects of an interleukin-5 blocking monoclonal antibody on eosinophils, airway hyper-responsiveness, and the late asthmatic response, The Lancet 356(9248) (2000) 2144-2148.
[29] R. Russell, C.E. Brightling, Anti-IL-5 for severe asthma: aiming high to achieve success, Chest 150(4) (2016) 766-768.
[30] D. Bagnasco, M. Ferrando, G. Varricchi, F. Puggioni, G. Passalacqua, G.W. Canonica, Anti-interleukin 5 (IL-5) and IL-5Ra biological drugs: efficacy, safety, and future perspectives in severe eosinophilic asthma, Frontiers in medicine 4 (2017) 135.
[31] P.E. Lipsky, Interleukin-6 and rheumatic diseases, Arthritis Research & Therapy 8(2) (2006) S4.
[32] L.H. Calabrese, S. Rose-John, IL-6 biology: implications for clinical targeting in rheumatic disease, Nature Reviews Rheumatology 10(12) (2014) 720.
[33] G.W. Kim, N.R. Lee, R.H. Pi, Y.S. Lim, Y.M. Lee, J.M. Lee, H.S. Jeong, S.H. Chung, IL-6 inhibitors for treatment of rheumatoid arthritis: past, present, and future, Archives of pharmacal research 38(5) (2015) 575-584.
[34] R.N. Fedorak, A. Gangl, C.O. Elson, P. Rutgeerts, S. Schreiber, G. Wild, S.B. Hanauer, A. Kilian, M. Cohard, A. LeBeaut, Recombinant human interleukin 10 in the treatment of patients with mild to moderately active Crohn's disease, Gastroenterology 119(6) (2000) 1473-1482.
[35] H. Herfarth, J. Schölmerich, IL-10 therapy in Crohn's disease: at the crossroads, Gut 50(2) (2002) 146-147.
[36] H. Tilg, C. Van Montfrans, A. Van den Ende, A. Kaser, S. Van Deventer, S. Schreiber, M. Gregor, O. Ludwiczek, P. Rutgeerts, C. Gasche, Treatment of Crohn's disease with recombinant human interleukin 10 induces the proinflammatory cytokine interferon γ, Gut 50(2) (2002) 191-195.
[37] Z. Zidek, P. Anzenbacher, E. Kmoníčková, Current status and challenges of cytokine pharmacology, British journal of pharmacology 157(3) (2009) 342-361.
[38] K. Asadullah, W. Sterry, K. Stephanek, D. Jasulaitis, M. Leupold, H. Audring, H.-D. Volk, W.-D. Döcke, IL-10 is a key cytokine in psoriasis. Proof of principle by IL-10 therapy: a new therapeutic approach, The Journal of clinical investigation 101(4) (1998) 783-794.
[39] H. Traupe, Psoriasis and the interleukin‐10 family: evidence for a protective genetic effect, but not an easy target as a drug, British Journal of Dermatology 176(6) (2017) 1438-1439.
[40] X. Wang, K. Wong, W. Ouyang, S. Rutz, Targeting IL-10 Family Cytokines for the Treatment of Human Diseases, Cold Spring Harbor perspectives in biology (2017) a028548.
[41] J. Vilček, M. Feldmann, Historical review: cytokines as therapeutics and targets of therapeutics, Trends in pharmacological sciences 25(4) (2004) 201-209.

[42] T.L. Putoczki, M. Ernst, IL-11 signaling as a therapeutic target for cancer, Immunotherapy 7(4) (2015) 441-453.
[43] Y. Vugmeyster, P. Szklut, L. Tchistiakova, W. Abraham, M. Kasaian, X. Xu, Preclinical pharmacokinetics, interspecies scaling, and tissue distribution of humanized monoclonal anti-IL-13 antibodies with different IL-13 neutralization mechanisms, International immunopharmacology 8(3) (2008) 477-483.
[44] S.I. Chung, J.A. Horton, T.R. Ramalingam, A.O. White, E.J. Chung, K.E. Hudak, B.T. Scroggins, J.R. Arron, T.A. Wynn, D.E. Citrin, IL-13 is a therapeutic target in radiation lung injury, Scientific reports 6 (2016) 39714.
[45] C.A. Dinarello, Historical insights into cytokines, European journal of immunology 37(S1) (2007) S34-S45.
[46] V. Annibali, R. Mechelli, S. Romano, M. Buscarinu, A. Fornasiero, R. Umeton, V. Ricigliano, F. Orzi, E. Coccia, M. Salvetti, IFN-β and multiple sclerosis: from etiology to therapy and back, Cytokine & growth factor reviews 26(2) (2015) 221-228.
[47] J.I. Gallin, J.M. Farber, S.M. Holland, T.B. Nutman, Interferon-γ in the management of infectious diseases, Annals of internal medicine 123(3) (1995) 216-224.
[48] D.W. Hommes, T.L. Mikhajlova, S. Stoinov, D. Štimac, B. Vucelic, J. Lonovics, M. Zákuciová, G. D'Haens, G. Van Assche, S. Ba, Fontolizumab, a humanised anti-interferon γ antibody, demonstrates safety and clinical activity in patients with moderate to severe Crohn's disease, Gut 55(8) (2006) 1131-1137.
[49] R. Condos, W.N. Rom, N.W. Schluger, Treatment of multidrug-resistant pulmonary tuberculosis with interferon-γ via aerosol, The Lancet 349(9064) (1997) 1513-1515.
[50] M.J. Elliott, R.N. Maini, M. Feldmann, A. Long‐Fox, P. Charles, P. Katsikis, F.M. Brennan, J. Walker, H. Bijl, J. Ghrayeb, Treatment of rheumatoid arthritis with chimeric monoclonal antibodies to tumor necrosis factor α, Arthritis & Rheumatism 36(12) (1993) 1681-1690.
[51] M. Feldmann, R.N. Maini, Anti-TNFα therapy of rheumatoid arthritis: what have we learned?, Annual review of immunology 19(1) (2001) 163-196.
[52] E.A. Panacek, J.C. Marshall, T.E. Albertson, D.H. Johnson, S. Johnson, R.D. MacArthur, M. Miller, W.T. Barchuk, S. Fischkoff, M. Kaul, Efficacy and safety of the monoclonal anti-tumor necrosis factor antibody F (ab′) 2 fragment afelimomab in patients with severe sepsis and elevated interleukin-6 levels, Critical care medicine 32(11) (2004) 2173-2182.
[53] J.B. Morjaria, A.J. Chauhan, K.S. Babu, R. Polosa, D.E. Davies, S.T. Holgate, The role of a soluble TNF-a receptor fusion protein (etanercept) in corticosteroid-refractory asthma: a double blind, randomised placebo-controlled trial, Thorax (2008).
[54] C.A. Hudis, Trastuzumab—mechanism of action and use in clinical practice, New England Journal of Medicine 357(1) (2007) 39-51.
[55] R.M. Hudziak, G.D. Lewis, M. Winget, B.M. Fendly, H.M. Shepard, A. Ullrich, p185HER2 monoclonal antibody has antiproliferative effects in vitro and sensitizes human breast tumor cells to tumor necrosis factor, Molecular and cellular biology 9(3) (1989) 1165-1172.
[56] A. Muntasell i Castellví, M. Cabo, S. Servitja Tormo, I. Tusquets Trias de Bes, M. Martínez-García, A. Rovira Guerín, F. Rojo, J. Albanell Mestres, M. López-Botet, Interplay between Natural killer cells and Anti-HER2 antibodies: Perspectives for breast cancer immunotherapy, Front Immunol. 2017 Nov 13; 8: 1544 (2017).
[57] A. Muntasell, M. Cabo, S. Servitja, I. Tusquets, M. Martínez-García, A. Rovira, F. Rojo, J. Albanell, M. López-Botet, Interplay between natural killer cells and anti-HER2 antibodies: perspectives for breast cancer immunotherapy, Frontiers in immunology 8 (2017) 1544.
[58] M. Urena, M.T. Del, O. Altisent, F. Campelo-Prada, A. Regueiro, R. DeLarochelliere, D. Doyle, S. Mohammadi, J.-M. Paradis, F. Dagenais, Combined erythropoietin and iron

therapy for anaemic patients undergoing transcatheter aortic valve implantation: the EPICURE randomised clinical trial, EuroIntervention: journal of EuroPCR in collaboration with the Working Group on Interventional Cardiology of the European Society of Cardiology 13(1) (2017) 44-52.
[59] F. Almeida, S. Santos, I. Beirão, Regulation of erythropoietin production and recent trends in anaemia therapy, Portuguese Journal of Nephrology HYpertension 29(2) (2015) 113-122.
[60] A. Meager, Measurement of cytokines by bioassays: theory and application, Methods 38(4) (2006) 237-252.
[61] M.L. Tsang, J. Weatherbee, Cytokine assays and their limitations, Alimentary pharmacology & therapeutics 10(Sup2) (1996) 55-61.
[62] R. Thorpe, M. Wadhwa, C. Bird, A. Mire-Sluis, Detection and measurement of cytokines, Blood reviews 6(3) (1992) 133-148.
[63] B. Van Weemen, A. Schuurs, Immunoassay using antigen—enzyme conjugates, FEBS letters 15(3) (1971) 232-236.
[64] E. Engvall, K. Jonsson, P. Perlmann, Enzyme-linked immunosorbent assay. II. Quantitative assay of protein antigen, immunoglobulin G, by means of enzyme-labelled antigen and antibody-coated tubes, Biochimica et Biophysica Acta (BBA)-Protein Structure 251(3) (1971) 427-434.
[65] K. Shah, P. Maghsoudlou, Enzyme-linked immunosorbent assay (ELISA): the basics, British Journal of Hospital Medicine 77(7) (2016) C98-C101.
[66] D.M. Klinman, T.B. Nutman, ELISPOT assay to detect cytokine ‐ secreting murine and human cells, Current Protocols in Immunology 10(1) (1994) 6.19. 1-6.19. 8.
[67] W. Herr, J. Schneider, A.W. Lohse, K.-H.M. zum Büschenfelde, T. Wölfel, Detection and quantification of blood-derived CD8+ T lymphocytes secreting tumor necrosis factor α in response to HLA-A2. 1-binding melanoma and viral peptide antigens, Journal of immunological methods 191(2) (1996) 131-142.
[68] W. Herr, B. Linn, N. Leister, E. Wandel, K.-H.M. zum Büschenfelde, T. Wölfel, The use of computer-assisted video image analysis for the quantification of CD8+ T lymphocytes producing tumor necrosis factor α spots in response to peptide antigens, Journal of immunological methods 203(2) (1997) 141-152.
[69] T. Asai, W.J. Storkus, T.L. Whiteside, Evaluation of the modified ELISPOT assay for gamma interferon production in cancer patients receiving antitumor vaccines, Clinical and diagnostic laboratory immunology 7(2) (2000) 145-154.
[70] N. Meidenbauer, D. Harris, L. Spitler, T. Whiteside, Generation of PSA ‐ reactive effector cells after vaccination with a PSA ‐ based vaccine in patients with prostate cancer, The Prostate 43(2) (2000) 88-100.
[71] N. Meidenbauer, W. Gooding, L. Spitler, D. Harris, T. Whiteside, Recovery of ζ-chain expression and changes in spontaneous IL-10 production after PSA-based vaccines in patients with prostate cancer, British journal of cancer 86(2) (2002) 168.
[72] K.S. Schneider, C.J. Thomas, O. Groß, Inflammasome activation and inhibition in primary murine bone marrow-derived cells, and assays for IL-1α, IL-1β, and caspase-1, The Inflammasome, Springer2013, pp. 117-135.
[73] V. Ball, P. Huetz, A. Elaissari, J. Cazenave, J. Voegel, P. Schaaf, Kinetics of exchange processes in the adsorption of proteins on solid surfaces, Proceedings of the National Academy of Sciences 91(15) (1994) 7330-7334.
[74] L. Cao, Carrier-bound immobilized enzymes: principles, application and design, John Wiley & Sons2006.
[75] S.F. Oliveira, G. Bisker, N.A. Bakh, S.L. Gibbs, M.P. Landry, M.S. Strano, Protein functionalized carbon nanomaterials for biomedical applications, Carbon 95 (2015) 767-779.

[76] K. Awsiuk, A. Budkowski, P. Petrou, M.M. Marzec, M. Biernat, T. Jaworska-Gołąb, J. Rysz, Orientation and biorecognition of immunoglobulin adsorbed on spin-cast poly (3-alkylthiophenes): Impact of polymer film crystallinity, Colloids and Surfaces B: Biointerfaces 148 (2016) 278-286.
[77] I.-H. Cho, E.-H. Paek, H. Lee, J.Y. Kang, T.S. Kim, S.-H. Paek, Site-directed biotinylation of antibodies for controlled immobilization on solid surfaces, Analytical biochemistry 365(1) (2007) 14-23.
[78] J.H. Kang, H.J. Choi, S.Y. Hwang, S.H. Han, J.Y. Jeon, E.K. Lee, Improving immunobinding using oriented immobilization of an oxidized antibody, Journal of Chromatography A 1161(1-2) (2007) 9-14.
[79] N.G. Welch, J.A. Scoble, B.W. Muir, P.J. Pigram, Orientation and characterization of immobilized antibodies for improved immunoassays, Biointerphases 12(2) (2017) 02D301.
[80] S.K. Vashist, E. Lam, S. Hrapovic, K.B. Male, J.H. Luong, Immobilization of antibodies and enzymes on 3-aminopropyltriethoxysilane-functionalized bioanalytical platforms for biosensors and diagnostics, Chemical reviews 114(21) (2014) 11083-11130.
[81] A. Makaraviciute, A. Ramanaviciene, Site-directed antibody immobilization techniques for immunosensors, Biosensors and Bioelectronics 50 (2013) 460-471.
[82] E.P. Diamandis, T.K. Christopoulos, The biotin-(strept) avidin system: principles and applications in biotechnology, Clinical chemistry 37(5) (1991) 625-636.
[83] H. Schetters, Avidin and streptavidin in clinical diagnostics, Biomolecular engineering 16(1-4) (1999) 73-78.
[84] W. Lee, D.-B. Lee, B.-K. Oh, W.H. Lee, J.-W. Choi, Nanoscale fabrication of protein A on self-assembled monolayer and its application to surface plasmon resonance immunosensor, Enzyme and microbial technology 35(6-7) (2004) 678-682.
[85] B.-K. Oh, W. Lee, Y.-K. Kim, W.H. Lee, J.-W. Choi, Surface plasmon resonance immunosensor using self-assembled protein G for the detection of Salmonella paratyphi, Journal of biotechnology 111(1) (2004) 1-8.
[86] U. Bilitewski, Protein-sensing assay formats and devices, Analytica chimica acta 568(1-2) (2006) 232-247.
[87] R. Danczyk, B. Krieder, A. North, T. Webster, H. HogenEsch, A. Rundell, Comparison of antibody functionality using different immobilization methods, Biotechnology and bioengineering 84(2) (2003) 215-223.
[88] G.T. Hermanson, Bioconjugate techniques, Academic press2013.
[89] J.M. Fowler, M.C. Stuart, D.K. Wong, Self-assembled layer of thiolated protein G as an immunosensor scaffold, Analytical chemistry 79(1) (2007) 350-354.
[90] J.M. Lee, H.K. Park, Y. Jung, J.K. Kim, S.O. Jung, B.H. Chung, Direct immobilization of protein G variants with various numbers of cysteine residues on a gold surface, Analytical chemistry 79(7) (2007) 2680-2687.
[91] M. Duroux, E. Skovsen, M.T. Neves‐Petersen, L. Duroux, L. Gurevich, S.B. Petersen, Light‐induced immobilisation of biomolecules as an attractive alternative to microdroplet dispensing‐based arraying technologies, Proteomics 7(19) (2007) 3491-3499.
[92] M.T. Neves‐Petersen, T. Snabe, S. Klitgaard, M. Duroux, S.B. Petersen, Photonic activation of disulfide bridges achieves oriented protein immobilization on biosensor surfaces, Protein Science 15(2) (2006) 343-351.
[93] T. Konry, M. Bouhifd, S. Cosnier, M. Whelan, A. Valsesia, F. Rossi, R.S. Marks, Electrogenerated indium tin oxide-coated glass surface with photosensitive interfaces: Surface analysis, Biosensors and Bioelectronics 22(9-10) (2007) 2230-2236.
[94] Y. Jung, J.M. Lee, J.-w. Kim, J. Yoon, H. Cho, B.H. Chung, Photoactivable antibody binding protein: site-selective and covalent coupling of antibody, Analytical chemistry 81(3) (2009) 936-942.

[95] K. Terpe, Overview of tag protein fusions: from molecular and biochemical fundamentals to commercial systems, Applied microbiology and biotechnology 60(5) (2003) 523-533.
[96] C. Steinhauer, C. Wingren, F. Khan, M. He, M.J. Taussig, C.A. Borrebaeck, Improved affinity coupling for antibody microarrays: Engineering of double‐(His) 6‐tagged single framework recombinant antibody fragments, Proteomics 6(15) (2006) 4227-4234.
[97] R. Vallina-Garcia, M. del Mar García-Suárez, M.T. Fernández-Abedul, F.J. Méndez, A. Costa-García, Oriented immobilisation of anti-pneumolysin Fab through a histidine tag for electrochemical immunosensors, Biosensors and Bioelectronics 23(2) (2007) 210-217.
[98] L. Torrance, A. Ziegler, H. Pittman, M. Paterson, R. Toth, I. Eggleston, Oriented immobilisation of engineered single-chain antibodies to develop biosensors for virus detection, Journal of virological methods 134(1-2) (2006) 164-170.
[99] T.R. Holford, F. Davis, S.P. Higson, Recent trends in antibody based sensors, Biosensors and Bioelectronics 34(1) (2012) 12-24.
[100] J. Zhou, J. Zhuang, M. Miró, Z. Gao, G. Chen, D. Tang, Carbon nanospheres-promoted electrochemical immunoassay coupled with hollow platinum nanolabels for sensitivity enhancement, Biosensors and Bioelectronics 35(1) (2012) 394-400.
[101] X. Chen, P. Qin, J. Li, Z. Yang, Z. Wen, Z. Jian, J. Zhao, X. Hu, X.a. Jiao, Impedance immunosensor for bovine interleukin-4 using an electrode modified with reduced graphene oxide and chitosan, Microchimica Acta 182(1-2) (2015) 369-376.
[102] H. Jiang, X. Weng, D. Li, Microfluidic whole-blood immunoassays, Microfluidics and nanofluidics 10(5) (2011) 941-964.
[103] B. Zhang, D. Tang, B. Liu, H. Chen, Y. Cui, G. Chen, GoldMag nanocomposite-functionalized graphene sensing platform for one-step electrochemical immunoassay of alpha-fetoprotein, Biosensors and Bioelectronics 28(1) (2011) 174-180.
[104] Q. Li, D. Tang, J. Tang, B. Su, G. Chen, M. Wei, Magneto-controlled electrochemical immunosensor for direct detection of squamous cell carcinoma antigen by using serum as supporting electrolyte, Biosensors and Bioelectronics 27(1) (2011) 153-159.
[105] X. Sun, Y. Zhu, X. Wang, Amperometric immunosensor based on deposited gold nanocrystals/4, 4′-thiobisbenzenethiol for determination of carbofuran, Food Control 28(1) (2012) 184-191.
[106] E. Sánchez-Tirado, G. Martínez-García, A. González-Cortés, P. Yáñez-Sedeño, J. Pingarrón, Electrochemical immunosensor for sensitive determination of transforming growth factor (TGF)-β1 in urine, Biosensors and Bioelectronics 88 (2017) 9-14.
[107] S. Eissa, N. Alshehri, A.M.A. Rahman, M. Dasouki, K.M.A. Salah, M. Zourob, Electrochemical immunosensors for the detection of survival motor neuron (SMN) protein using different carbon nanomaterials-modified electrodes, Biosensors and Bioelectronics 101 (2018) 282-289.
[108] S. Campuzano, M. Pedrero, G.-P. Nikoleli, J. Pingarrón, D. Nikolelis, Hybrid 2D-nanomaterials-based electrochemical immunosensing strategies for clinical biomarkers determination, Biosensors and Bioelectronics 89 (2017) 269-279.
[109] F. Mollarasouli, V. Serafín, S. Campuzano, P. Yáñez-Sedeño, J.M. Pingarrón, K. Asadpour-Zeynali, Ultrasensitive determination of receptor tyrosine kinase with a label-free electrochemical immunosensor using graphene quantum dots-modified screen-printed electrodes, Analytica chimica acta 1011 (2018) 28-34.
[110] M. Li, P. Wang, F. Li, Q. Chu, Y. Li, Y. Dong, An ultrasensitive sandwich-type electrochemical immunosensor based on the signal amplification strategy of mesoporous core–shell Pd@ Pt nanoparticles/amino group functionalized graphene nanocomposite, Biosensors and Bioelectronics 87 (2017) 752-759.
[111] M.A. Tabrizi, M. Shamsipur, R. Saber, S. Sarkar, N. Zolfaghari, An ultrasensitive sandwich-type electrochemical immunosensor for the determination of SKBR-3 breast

cancer cell using rGO-TPA/FeHCFnano labeled Anti-HCT as a signal tag, Sensors and Actuators B: Chemical 243 (2017) 823-830.
[112] Y. Liu, X. Weng, K.-K. Wang, Y. Xue, A.-J. Wang, L. Wu, J.-J. Feng, A novel enzyme-free sandwich-like electrochemical immunosensor for the detection of carbohydrate antigen 15-3 based on hierarchical AuPd nanochain networks, Sensors and Actuators B: Chemical 247 (2017) 349-356.
[113] M. Shamsipur, M. Emami, L. Farzin, R. Saber, A sandwich-type electrochemical immunosensor based on in situ silver deposition for determination of serum level of HER2 in breast cancer patients, Biosensors and Bioelectronics 103 (2018) 54-61.
[114] Y. Yang, Q. Yan, Q. Liu, Y. Li, H. Liu, P. Wang, L. Chen, D. Zhang, Y. Li, Y. Dong, An ultrasensitive sandwich-type electrochemical immunosensor based on the signal amplification strategy of echinoidea-shaped Au@ Ag-Cu2O nanoparticles for prostate specific antigen detection, Biosensors and Bioelectronics 99 (2018) 450-457.
[115] H. Lv, Y. Li, X. Zhang, Z. Gao, C. Zhang, S. Zhang, Y. Dong, Enhanced peroxidase-like properties of Au@ Pt DNs/NG/Cu2+ and application of sandwich-type electrochemical immunosensor for highly sensitive detection of CEA, Biosensors and Bioelectronics 112 (2018) 1-7.
[116] X. Liu, D. Wang, J. Chu, Y. Xu, W. Wang, Sandwich pair nanobodies, a potential tool for electrochemical immunosensing serum prostate-specific antigen with preferable specificity, Journal of Pharmaceutical and Biomedical Analysis (2018).
[117] R. Malhotra, V. Patel, B.V. Chikkaveeraiah, B.S. Munge, S.C. Cheong, R.B. Zain, M.T. Abraham, D.K. Dey, J.S. Gutkind, J.F. Rusling, Ultrasensitive detection of cancer biomarkers in the clinic by use of a nanostructured microfluidic array, Analytical chemistry 84(14) (2012) 6249-6255.
[118] A.J. Tudos, R.B. Schasfoort, Introduction to surface plasmon resonance, Handbook of surface Plasmon resonance (2008) 1-14.
[119] D.R. Shankaran, K.V. Gobi, N. Miura, Recent advancements in surface plasmon resonance immunosensors for detection of small molecules of biomedical, food and environmental interest, Sensors and Actuators B: Chemical 121(1) (2007) 158-177.
[120] C.-Y. Yang, E. Brooks, Y. Li, P. Denny, C.-M. Ho, F. Qi, W. Shi, L. Wolinsky, B. Wu, D.T. Wong, Detection of picomolar levels of interleukin-8 in human saliva by SPR, Lab on a Chip 5(10) (2005) 1017-1023.
[121] M.A.S. John, Y. Li, X. Zhou, P. Denny, C.-M. Ho, C. Montemagno, W. Shi, F. Qi, B. Wu, U. Sinha, Interleukin 6 and interleukin 8 as potential biomarkers for oral cavity and oropharyngeal squamous cell carcinoma, Archives of Otolaryngology–Head & Neck Surgery 130(8) (2004) 929-935.
[122] J.-W. Choi, D.-Y. Kang, Y.-H. Jang, H.-H. Kim, J. Min, B.-K. Oh, Ultra-sensitive surface plasmon resonance based immunosensor for prostate-specific antigen using gold nanoparticle–antibody complex, Colloids and Surfaces A: Physicochemical and Engineering Aspects 313 (2008) 655-659.
[123] D.R. Shankaran, N. Miura, Trends in interfacial design for surface plasmon resonance based immunoassays, Journal of Physics D: Applied Physics 40(23) (2007) 7187.
[124] H.R. Hill, T.B. Martins, The flow cytometric analysis of cytokines using multi-analyte fluorescence microarray technology, Methods 38(4) (2006) 312-316.
[125] X. Hun, Z. Zhang, Functionalized fluorescent core-shell nanoparticles used as a fluorescent labels in fluoroimmunoassay for IL-6, Biosensors and Bioelectronics 22(11) (2007) 2743-2748.
[126] N. Ganesh, I.D. Block, P.C. Mathias, W. Zhang, E. Chow, V. Malyarchuk, B.T. Cunningham, Leaky-mode assisted fluorescence extraction: application to fluorescence enhancement biosensors, Optics Express 16(26) (2008) 21626-21640.

[127] B. Culshaw, Fiber-optic sensors: applications and advances, Optics and photonics news 16(11) (2005) 24-29.
[128] G. Rajan, Optical fiber sensors: advanced techniques and applications, CRC press2015.
[129] C. Caucheteur, T. Guo, J. Albert, Review of plasmonic fiber optic biochemical sensors: improving the limit of detection, Analytical and bioanalytical chemistry 407(14) (2015) 3883-3897.
[130] Y.-C. Huang, C.-Y. Chiang, C.-H. Li, T.-C. Chang, C.-S. Chiang, L.-K. Chau, K.-W. Huang, C.-W. Wu, S.-C. Wang, S.-R. Lyu, Quantification of tumor necrosis factor-α and matrix metalloproteinases-3 in synovial fluid by a fiber-optic particle plasmon resonance sensor, Analyst 138(16) (2013) 4599-4606.
[131] T.M. Blicharz, W.L. Siqueira, E.J. Helmerhorst, F.G. Oppenheim, P.J. Wexler, F.F. Little, D.R. Walt, Fiber-optic microsphere-based antibody array for the analysis of inflammatory cytokines in saliva, Analytical chemistry 81(6) (2009) 2106-2114.
[132] R. Kapoor, C.-W. Wang, Highly specific detection of interleukin-6 (IL-6) protein using combination tapered fiber-optic biosensor dip-probe, Biosensors and Bioelectronics 24(8) (2009) 2696-2701.
[133] C.-W. Wang, R. Kapoor, U. Manne, V.V. Reddy, D. Oelschlager, V. Katkoori, W.E. Grizzle, Development of combination tapered fiber-optic biosensor dip probe for quantitative estimation of interleukin-6 in serum samples, Journal of biomedical optics 15(6) (2010) 067005.
[134] T.M. Battaglia, J.-F. Masson, M.R. Sierks, S.P. Beaudoin, J. Rogers, K.N. Foster, G.A. Holloway, K.S. Booksh, Quantification of cytokines involved in wound healing using surface plasmon resonance, Analytical chemistry 77(21) (2005) 7016-7023.
[135] H.-H. Jeong, N. Erdene, J.-H. Park, D.-H. Jeong, H.-Y. Lee, S.-K. Lee, Real-time label-free immunoassay of interferon-gamma and prostate-specific antigen using a Fiber-Optic Localized Surface Plasmon Resonance sensor, Biosensors and Bioelectronics 39(1) (2013) 346-351.
[136] R. Usuba, M. Yokokawa, T.N. Ackermann, A. Llobera, K. Fukunaga, S. Murata, N. Ohkohchi, H. Suzuki, Photonic lab-on-a-chip for rapid cytokine detection, ACS Sensors 1(8) (2016) 979-986.
[137] T. Schenk, H. Irth, G. Marko-Varga, L. Edholm, U. Tjaden, J. van der Greef, Potential of on-line micro-LC immunochemical detection in the bioanalysis of cytokines, Journal of pharmaceutical and biomedical analysis 26(5-6) (2001) 975-985.
[138] E.M. Bartels, I. Falbe Wätjen, E. Littrup Andersen, B. Danneskiold-Samsøe, H. Bliddal, S. Ribel-Madsen, Rheumatoid factor and its interference with cytokine measurements: problems and solutions, Arthritis 2011 (2011).
[139] N. Bolstad, D.J. Warren, K. Nustad, Heterophilic antibody interference in immunometric assays, Best Practice & Research Clinical Endocrinology & Metabolism 27(5) (2013) 647-661.
[140] J. Whicher, S. Evans, Cytokines in disease, Clinical chemistry 36(7) (1990) 1269-1281.

2

Detection of Interleukin-6 on APTES - AuNP-MA Modified Glass Fiber

2.1 Introduction

Interleukin-6 (IL-6), acting as a both pro-inflammatory and anti-inflammatory cytokine, plays a key role in the inflammatory response. Many diseases such as osteoarthrosis, asthma, psoriasis, cardiovascular disease, diabetes and inflammatory bowel disease are closely associated with IL-6, which can cause an increase in the IL-6 level. However, the cytokine IL-6 is usually locally released (i.e. at the site of injury or disease), and traditional ELISA detection method can only provide a systemic level in body fluids, offering a limited insight into the undergoing processes. To achieve the detection of the concentration of the locally released IL-6, we did a variant of traditional ELSA on the optical fiber to enable the localised released cytokine be detected.

This chapter demonstrated a cytokine detection device based on gold nanoparticle modified silica optical fiber for the monitoring of locally variable cytokine IL-6 concentrations using a sandwich immunoassay scheme. The feasibility of the fabricated cytokine assay for the spatially localized detection of IL-6 was studied by placing single drops (~1 μL) of the serum sample containing different concentrations of IL-6 onto various locations of the fabricated optical fiber surfaces, followed by incubation with the detection antibody. And the performance of the fiber immunosensor in IL-6 detection in serum and BV-2 cell culture medium was further explored.

Liu, G., **Zhang, K.**, Nadort, A., Hutchinson, M.R. and Goldys, E.M., 2017. Sensitive cytokine assay based on optical fiber allowing localized and spatially resolved detection of interleukin-6. ACS sensors, 2(2), pp.218-226.

Summary of the Author contributions to paper 1 following the order of author.

Paper 1	G. L	K. Z	A. N	M. H	E. G
Experiment Design	•	•	•	•	•
Sample Preparation	•	•			
Data Collection	•	•			
Analysis	•	•	•		
Figures	•	•			•
Manuscript	•			•	•

2.2 Full paper

ACS SENSORS

Article

pubs.acs.org/acssensors

Sensitive Cytokine Assay Based on Optical Fiber Allowing Localized and Spatially Resolved Detection of Interleukin-6

Guozhen Liu,*[†,‡] Kaixin Zhang,[†] Annemarie Nadort,[†] Mark R. Hutchinson,[§] and Ewa M. Goldys[†]

[†]ARC Centre of Excellence in Nanoscale Biophotonics (CNBP), Macquarie University, North Ryde 2109, Australia

[‡]Key Laboratory of Pesticide and Chemical Biology of Ministry of Education, College of Chemistry, Central China Normal University, Wuhan 430079, P. R. China

[§]ARC Centre of Excellence in Nanoscale Biophotonics (CNBP), The University of Adelaide, Adelaide 5005, Australia

Supporting Information

ABSTRACT: We demonstrated a cytokine detection device based on gold nanoparticle modified silica optical fiber for the monitoring of locally variable cytokine interleukin-6 (IL-6) concentrations using a sandwich immunoassay scheme. The fiber is designed to be introduced into an intrathecal catheter with micrometer-sized holes drilled along its length to enable fluid exchange between the outside and inside of the catheter. An exposed optical fiber (diameter 125 μm) modified with a layer of gold nanoparticles was functionalized with the IL-6 capture antibody to form the sensing interface. The immunocapture device was incubated with a cytokine solution to capture the analyte. The device was then exposed to the IL-6 detection antibody which was loaded on the fluorescently labeled magnetic nanoparticles, making it possible to quantify the cytokine concentration based on the intensity of fluorescence. A reliable method for quantifying the fluorescent signal on a 3D structure was developed. This device was applied to the detection of cytokine IL-6 with the low limit of detection of 1 pg mL^{-1} in a sample volume of 1 μL. The device has the linear detection range of 1−400 pg mL^{-1} and spatial resolution on the order of 200−450 μm, and it is capable of detecting localized IL-6 secreted by live BV2 cells following their liposaccharide stimulation. This biological detection system is suitable for monitoring multiple health conditions.

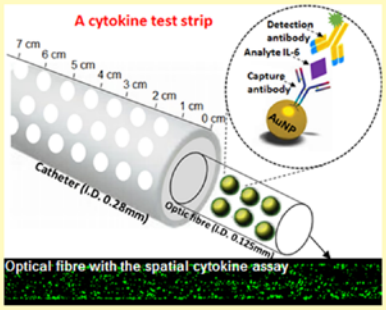

KEYWORDS: *optical fiber, cytokines, localized and spatially resolved detection, IL-6, immunosensors, cytokine test strip*

Cytokines are small proteins (~6−70 kDa) secreted by cells, with broad biological importance, in particular for cellular signaling.[1] Certain pro-inflammatory cytokines such as IL-1β, IL-6, and TNF-α in the spinal cord, dorsal root ganglions (DRG), injured nerves, or skin are known to be involved with abnormal spontaneous activity in injured nerve fibers or compressed/inflamed DRG neurons[2] and in the process of pathological pain.[3] Current cytokine detection methods are applicable to body fluids such as blood plasma. However, the cytokines are locally released and measurements of their average content in body fluids provide only a limited insight into the underpinning processes. Thus, in order to understand the role of the immune system in pain or multiple other health conditions which lead to immunoreactivity and the expression of cytokines, it would be useful to be able to monitor spatially localized concentration of cytokine in specific locations of the body, such as the spinal cord, reproductive tract, cancer stroma, and so forth. This is challenging because the cytokine concentration in body fluids is low, normally in the pM range,[4] and cytokine assays may suffer interference from heterophilic antibodies, rheumatoid factors, and specific or nonspecific cytokine binding proteins.[5]

Benefiting from cost-effective and simple parallel array-type operation, and relatively high sensitivity, conventional enzyme-linked immunosorbent assay (ELISA) has become the most common cytokine quantification tool, used, for example, for clinical diagnosis of the "cytokine storm" in patients.[6−8] However, ELISA typically requires long incubation time (several hours) and suffers from the complicated sample labeling process. Moreover, a large amount of sample must be available to achieve a sufficient signal-to-background ratio for detection. Thus, broad interest exists in developing simple, sensitive, and rapid cytokine analysis platforms for comprehensive characterization and quantitative analysis of cytokines secreted from immune cells.[9−22] Recently, a microfluidic microsphere-based biosensor for quasi real-time detection of TNF-α was reported by Konry and co-workers.[23] A label-free localized surface plasmon resonance (LSPR) biosensing technique to detect cell-secreted tumor necrosis factor (TNF)-α cytokines in clinical blood samples was also reported.[24] This technology can detect cytokines with a blood sample volume of 3 μL and a total assay time 3 times shorter than that of ELISA (5−6 h). Revzin and co-workers

Received: October 6, 2016
Accepted: December 20, 2016
Published: December 20, 2016

DOI: 10.1021/acssensors.6b00619
ACS Sens. 2017, 2, 218−226

Scheme 1. Scheme of the Preparation of the Cytokine Test Strip Based on the Optical Fiber for Detection of the Localized Analyte IL-6

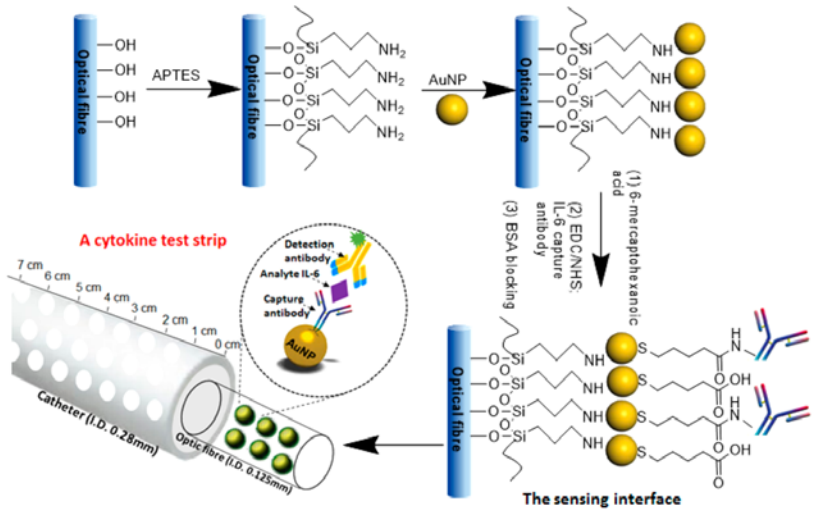

have reported a microscale device for detecting local release of interferon gamma (IFN-γ) from primary human leukocytes in real time.[15] However, this device is not suitable for measuring localized cytokines in vivo.

Optical fibers are chemically passive, have small physical dimensions (diameters in the range of tens to few hundred μm), and are able to access challenging environments.[25,26] Configured as fiber-optics sensors, they offer an advantage of long interaction length which, in some situations, can yield enhanced signals. Moreover, optical fiber biosensors can be used in combination with different types of spectroscopic techniques, e.g., absorption, fluorescence, phosphorescence, Raman, and surface plasmon resonance (SPR).[27] Optical fibers have also been explored as a promising platform for cytokine detection.[11,28−30] A recent report describes a fiber-optics SPR sensor for the detection of IL-1, IL-6, and TNF-α in a buffered saline solution and a spiked cell culture medium.[31] In this study, the detection limit of IL-6 of 0.44 ng mL^{-1} was achieved. The optical fiber-based sensors have also been applied to the monitoring of biologically relevant molecules in real time. For example, a label-free fiber-optic localized SPR sensor for the detection of IFN-γ was fabricated using spherical gold nanoparticles (AuNPs) on a polished end-face of the optical fiber.[12] This label-free immunoassay sensor was characterized by a short detection time (5 min), high resolution, and sensitivity (2 pg mL^{-1} for IFN-γ) due to the signal amplification from AuNPs. A recently reported photonic lab-on-a-chip sensor allowed rapid determination of IL-2 levels secreted by lymphocytes based on the measurement of optical absorbance.[32] However, none of these devices is capable of spatially localized cytokine detection along the fiber length based on the quantification of the fluorescent signal on the sensing interface.

In this study we designed an immunosening device (similar to a cytokine test strip) for monitoring of localized cytokine IL-6 concentration (Scheme 1). This cytokine capture device comprises a de-cladded optical fiber modified with a layer of AuNPs which are functionalized with the cytokine IL-6 capture antibody to form the sensing interface. This cytokine capture device can be inserted into a catheter with microscale holes drilled along its length to enable fluid exchange between the outside and inside of the catheter. It can be removed from a catheter at any stage and a new capture device may be then reintroduced for a second or subsequent measurement. The difference between the diameter of the catheter and the fiber is 155 μm resulting in very low friction between the fiber and the catheter. The removed capture device carries the analytes (cytokine IL-6) which are then detected. To achieve that, the fiber device is exposed to the IL-6 detection antibody which is loaded on the fluorescent nanoparticles. After a period of incubation and a washing step, the level of cytokines can be determined by quantifying the intensity of fluorescence from nanoparticle-labeled detection antibodies on the 3D fiber surface. This approach is different from the evanescent wave-based signal quantification in the traditional optical fiber sensors.[11] In this work, this variant of spatially resolved ELISA was successfully used for the detection of spatially localized cytokine IL-6 with the low limit of detection of 1 pg mL^{-1}, a sample volume of 1 μL, and the linear range of 1−400 pg mL^{-1}. The detection system also demonstrated high spatial resolution on the order of 200−450 μm for detecting localized IL-6 secreted by liposaccharide stimulated BV2 cells. The ability to reintroduce a new capture device into the catheter makes our design attractive for clinical applications, and this approach has the potential for the development of the point-of-care cytokine detection devices for neuroscience and other biomedical research.

EXPERIMENTAL SECTION

Chemicals. Aminopropyltriethoxysilane (APTES), concentrated sulfuric acid, hydrogen peroxide (30%), toluene, ethanol, 6-mercaptohexanoic acid, bovine serum albumin (BSA), 1-ethyl-3-(3-(dimethylamino)propyl)carbodiimide hydrochloride (EDC), *N*-hydroxysuccinimide (NHS), 2-(*N*-morpholino) ethanesulfonic acid (MES), and lipopolysaccharide were purchased from Sigma-Aldrich. Mouse interleukin-6 (IL-6), anti-mouse IL-6 polyclonal antibody (capture antibody), anti-mouse IL-6 monoclonal antibody (detection antibody), and donkey anti-Goat IgG NorthernLights NL493-conjugated antibody were purchased from R&D Systems. Carboxy-

DOI: 10.1021/acssensors.6b00619
ACS Sens. 2017, 2, 218−226

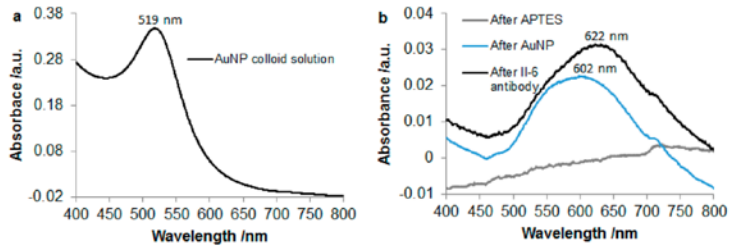

Figure 1. UV−vis absorbance of (a) gold colloid solution and (b) glass surface after stepwise modification with APTES, AuNP, and IL-6 capture antibody.

lated superparamagnetic iron oxide particles (SPIO, 1% solid, 10 mg mL^{-1}, ~0.9 μm, labeled with Dragon Green fluorophores (excitation 480 nm, emission 520 nm)) were obtained from Bangs Laboratories, USA. The optical fiber is a standard telecommunication silica fiber 62.5-μm-diameter core/125 μm acrylate cladding (LNF(TM) product from Pirelli, now Prysmian). The circular glass coverslips (diameter of 12 mm, thickness of 0.13 mm) were purchased from Fisher Scientific, Australia. Aqueous solutions were prepared using Milli-Q water. The phosphate buffer solution used in this work contained 0.1 M sodium phosphate, 0.15 M sodium chloride, adjusted to pH 7.2 with NaOH or HCl solution.

Protocol for Drilling Holes in Catheter by a Laser. The protocol for drilling holes by laser has been detailed in earlier literature.[33] The laser machining system is a Microstruct-C from 3D MicroMac, Germany with the 266 nm picosecond laser (Lumera/Coherent SuperRapid HE). A scanner with an F = 56 mm optics to drill an array of 50 of 100 μm holes was used and holes were drilled with 1 μJ pulses at 20 kHz pulse repetition frequency (80 holes along 1 cm length of fiber with 2 holes at each circumference).

Fabrication of the Sensing Interface. As shown in Scheme 1, the sensing interface was fabricated in several steps. First, the de-cladded optical fiber (or the glass coverslip used in preliminary characterizations) was immersed in a piranha solution (H_2SO_4 95% and H_2O_2 30% mixed at a volume ratio of 4:1) for 12 h in order to clean the glass and to form hydroxyl groups on its surface. After rinsing with deionized H_2O and ethanol and drying under N_2 stream, the cleaned optical fiber/coverslip was immersed in aminopropyltriethoxysilane (5% v/v) in toluene for 6 h to form an amine-terminated self-assembled monolayer. The fiber/coverslip was then rinsed with toluene and ethanol to remove the unbound monomers from the surface. The aminopropyltriethoxysilane-modified optical fiber was subsequently immersed into a 1 mL of AuNP (10 nm) solution for 5 h. Upon removal, the fiber/coverslip was copiously rinsed with deionized H_2O and finally blown dry with N_2. The AuNP modified optical fiber/coverslip thus prepared was then incubated in 0.1 mM 6-mercaptohexanoic acid solution overnight, and finally washed three times, in ethanol and deionized H_2O, respectively. To activate the carboxylic acid on the optical fiber/coverslip, the prepared fiber was incubated in the 25 mM MES buffer (pH 6.0) solution containing EDC (10 mg mL^{-1})/NHS (10 mg mL^{-1}) for 30 min. Then the fiber/coverslip was washed in the MES buffer twice. Finally, the fabricated optical fiber/coverslip was immersed in the anti-IL-6 capture antibody solution (50 μg mL^{-1}) in the MES buffer (pH = 6.0) at room temperature for 3 h and washed twice in deionized H_2O. Subsequently, the fiber/coverslip surface was blocked in a 0.25% BSA solution for 3 h to complete the preparation of the sensing interface. In order to confirm the presence of the capture antibody, the sensing interface was incubated with the anti-IL-6 secondary antibody (labeled with green fluorophores) solution (1:100) in PBS for 2 h. Then the interface was washed three times by PBS and deionized H_2O, respectively, and finally dried and imaged by confocal microscopy.

Cytokine Measurement. After modification of the optical fiber/coverslip surface with the anti-IL-6 capture antibodies, the optical fiber/coverslip was incubated in PBS solution or serum containing IL-6 in different concentrations for 2 h. Then the fiber/coverslip was washed with a wash buffer (PBS, 0.1% Tween-20) and dried by N_2 stream. Finally the optical fiber/coverslip was exposed to Dragon Green magnetic nanoparticles loaded with IL-6 detection antibody (DG_SPIO_IL-6_Ab; see the details of making DG_SPIO_IL-6_Ab in the Supporting Information) for 1 h by washing with wash buffer (PBS, 0.1% Tween-20) and deionized H_2O before fluorescence measurements described below.

Confocal Laser Scanning Microscopy Imaging and Fluorescent Signal Quantification. The fluorescence spectra for the fiber/coverslip based cytokine assay were collected at excitation wavelengths of 493 nm for green dye (NL493) with the emission range of 510−650 nm, and 480 nm for Dragon Green with the emission range of 500−650 nm using a Fluorolog Tau3 system (JY Horiba, Edison, NJ) in 10 mm quartz cuvettes at room temperature. The spectral band passes were 0.5 nm in both excitation and emission. The PMT voltage was adjusted to 950 V. The optical fiber samples were imaged using a SP2 (Leica) confocal microscope with objective HC PL FLUOTAR, magnification 10×, NA 0.3, *xy*-resolution 651 nm, pinhole 1× Airy disc, and field of view 1500 × 1500 μm^2. The *z*-stack of 10 *z*-planes over 125 μm height were collected, with the separation of around 12.5 μm between planes. All ten images were then processed, to calculate the maximum pixel value from these 10 planes. This maximum pixel value was then assigned as the pixel value in the combined image (Z-projection in ImageJ). For every concentration of IL-6, two different locations were imaged so that 3 mm fiber length in total was imaged for each cytokine measurement. The intensity of the green dots representing the Dragon Green fluorescent labels was quantified by integrating over a spatial window of 450 μm using ImageJ and Matlab software. In this way the spatial resolution of 450 μm was realized.

RESULTS AND DISCUSSION

Evaluation of the IL-6 Immunosensor Performance on the Glass Surface. The sensing interface in Scheme 1 was first produced on a glass coverslip instead of the optical fiber for ease of characterization. The self-assembled AuNPs deposited on a glass coverslip were characterized by UV−vis spectrophotometry (Figure 1). The spectrum of the AuNP colloid solution has a characteristic plasmon peak at 519 nm. This peak is absent for the glass surface after modification of APTES; however, a similar feature at 602 nm appears after modification of glass with AuNP, which confirms the successful attachment of AuNP. This modified spectral characteristics suggests that the Au colloids self-assembled on glass are close enough to affect the coupling of plasmons of individual particles resulting in an increased absorbance at wavelengths >600 nm when compared to that of the original AuNP in solution.[34] The plasmon peak showed a further redshift (622 nm) after the attachment of IL-6 capture antibody due to the change of the surrounding environment of AuNPs.[35] Fluorimetry was used to monitor surface modifications of the glass surface after the attachment of detection antibodies (Figure S1). The back-

DOI: 10.1021/acssensors.6b00619
ACS Sens. 2017, 2, 218−226

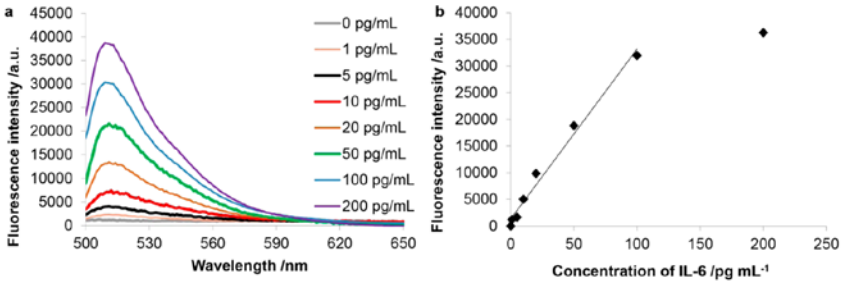

Figure 2. (a) Relationship between fluorescence intensity and the concentration of IL-6. (b) Calibration curve of IL-6 based on the sensing interface fabricated on a glass coverslip.(Fig.2b is a directly fluorescence signal value reading from Fig.2a)

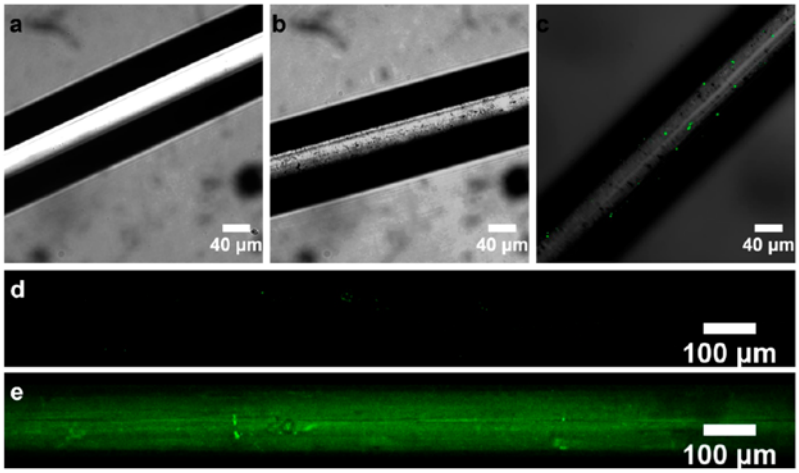

Figure 3. Confocal images for the stepwise modification of optical fiber: (a) original optical fiber, (b) AuNP modified optical fiber, and (c) IL-6 capture antibody modified optical fiber for determination of IL-6 after incubation with DG_SPIO_IL-6_Ab; (d) fiber surface without modification of IL-6 capture antibody; and (e) IL-6 capture antibody modified optical fiber after exposure to green dye (NL493) labeled secondary antibody, respectively.

ground fluorescence signal for the blank glass surface was observed around 530 and 600 nm, respectively; it disappeared after modification of the glass surface with APTES, due to the formation of a layer of amine groups on the surface. After further stepwise modification of the glass surface with 6-mercaptohexanoic acid, AuNP, incubation with the anti-IL-6 capture antibody followed by the incubation with IL-6 (100 pg mL^{-1}) and the fluorescent detection antibody (DG_SPIO_IL-6_Ab), the characteristic fluorescence peak of the Dragon Green beads appeared at about 518 nm, indicating a successful attachment of the detection antibody. Thus, this fabricated system is capable of detection of IL-6.

The sensing interface fabricated on the glass coverslip was used to detect IL-6 at different concentrations. Figure 2a shows the relationship between fluorescence intensity and the concentration of IL-6, and the fluorescence signal of the detection antibodies conjugated to Dragon Green beads increased linearly with the concentration of IL-6. The calibration curve of this sensing interface for IL-6 is plotted in Figure 2b. The lowest detectable concentration was 1 pg mL^{-1} with the linear range of 1−100 pg mL^{-1} which is within the physiological concentration range of IL-6 in the body.[4] Thus, this assay can be used to quantify the IL-6 concentration in vitro. This immunosensor scheme has been further applied to the optical fiber, as described in the following sections.

Performance of the Fabricated Sensor on Optical Fiber Surface. In order to realize the localized detection of cytokines, in the next stage the ELISA surface detailed previously was fabricated on an optical fiber, to be able to carry out a cytokine assay for the detection of Il-6. A stepwise modification of optical fiber was carried out, as previously described and the resulting fiber surface was characterized by confocal microscopy (Figure 3). The original de-cladded optical fiber showed a smooth and clean surface. After the fabrication of AuNPs on the fiber surface, some small black dots could be observed, suggesting the presence of AuNPs clusters resulting in an increased surface area for binding the IL-6 capture antibody. The SEM image of AuNP was included in Figure S2, further suggesting the presence of AuNP with the size of about 10 nm. No significant change could be seen in the confocal images after the attachment of capture antibody on the fiber surface. After the incubation of the sensing interface with the analyte IL-6 and the IL-6 detection antibodies (DG_SPIO_IL-6_Ab), very bright green dots were observed (Figure 3c), suggesting that the DG_SPIO_IL-6_Abs were attached to the sensing interface to form a sandwich structure with the IL-6 and IL-6 capture antibodies. The intensity of this green fluorescence

DOI: 10.1021/acssensors.6b00619
ACS Sens. 2017, 2, 218−226

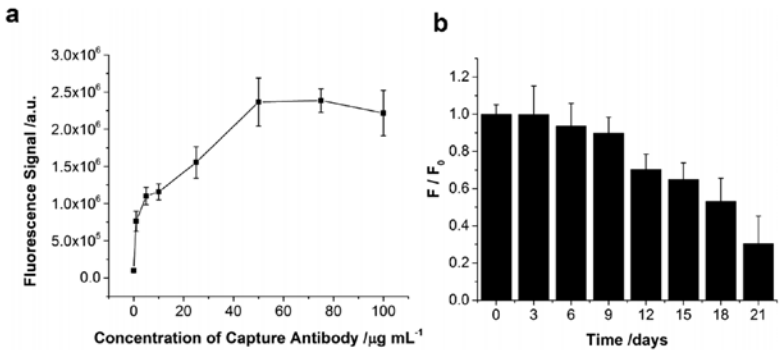

Figure 4. (a) Change in fluorescence signal of green dye with increasing concentration of IL-6 capture antibody. (b) Stability of the capture antibody modified sensing interface. F_0 and F are the fluorescence signals from the secondary antibody for the freshly prepared fiber and the same fiber after being stored in PBS for different periods of time.

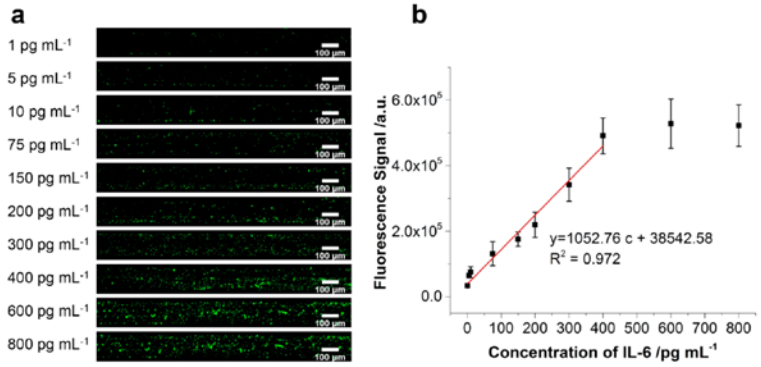

Figure 5. (a) Z-stack maximum intensity projection images of the optical fiber after its exposure to different concentration of IL-6 followed by the incubation of DG_SPIO_IL-6_Ab (27.5 μg mL^{-1}). (b) Calibration curve of IL-6 based on the fluorescence signal and IL-6 concentration obtained from (a).

could be used to quantify the analyte. To further confirm the presence of capture antibody, the green dye (NL493) labeled secondary antibody was applied on the capture antibody modified sensing interface and the fiber surface without the attachment of IL-6 capture antibody. Negligible levels of fluorescence on the fiber surface were detected after the incubation with a green dye-labeled secondary antibody (Figure 3e). However, the sensing interface demonstrated bright green fluorescence (Figure 3d), indicating the presence of the green dye-labeled secondary antibody and the capture antibody with a homogeneous distribution.

To maximize the amount of IL-6 capture antibody on the sensing interface required for high sensitivity, its concentration was optimized by quantifying the fluorescence intensity of the green dye-labeled secondary antibody (Figure 4a). The fluorescence signal on the 3D optical fiber was quantified using ImageJ and MatLab software. This signal increased with the concentration of IL-6 capture antibody used for fabrication of the sensing interface, and a maximum fluorescence signal was obtained when the concentration of capture antibody was 50 μg mL^{-1}. In addition, the stability of the capture antibody was investigated by leaving the fabricated sensing interface in PBS for extended periods of time followed by monitoring the concentration of IL-6 capture antibody using the green dye labeled secondary antibody (Figure 4b). The fluorescence signal was stable for the first 9 days, indicating that the capture antibody was still attached on the fiber surface. The fluorescence signal then continued to decrease to less 50% of the original intensity after 20 days, which might be due to limited stability of C−Au bonds between alkanethiols and AuNPs[36] resulting in a progressive release of the capture antibodies from the glass surface.

Detection of IL-6 Using the Fabricated Cytokine Immunosensing Device. After verifying the performance of the cytokine capture surface on glass slides we fabricated an identical capture surface on a glass fiber 125 μm in diameter. In order to quantify the fluorescence signal reporting on the presence of analyte molecules captured on fiber surface we developed a tailored approach. Drawing on the capability of laser scanning confocal microscope to reject out-of-focus signal and its depth of field that is much smaller than the fiber diameter, we recorded multiple images at different axial planes (Z-stack), around 12.5 μm apart, in order to image the total visible fiber area. This Z-stack was further processed to select the maximum pixel value from each image. This maximum value was then assigned to the corresponding pixel (maximum Z-projection in Image-J). This final composite image produced from a Z-stack was taken as a representation of the total fluorescence signal of a section of the fiber and it was used for further quantification of the signal. These data are shown in Figure 5a.

DOI: 10.1021/acssensors.6b00619
ACS Sens. 2017, 2, 218−226

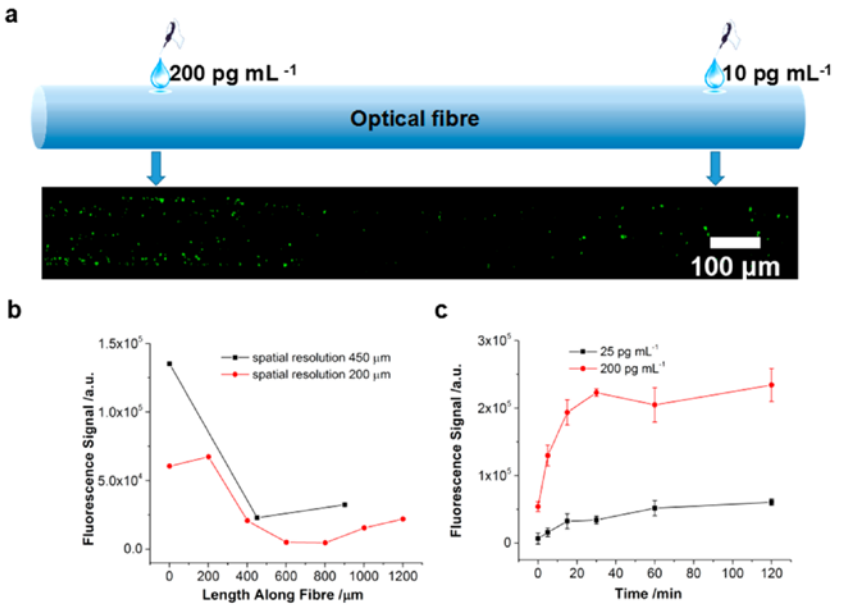

Figure 6. (a) Results of spatially localized cytokine detection experiments using our device. We simultaneously placed 1 μL of serum containing 10 and 200 pg mL^{-1} IL-6 on the fabricated sensing interface, respectively, followed by incubation with detection antibody and signal quantification. (b) Relationship between fluorescence signal in the 200 and 450 μm windows along the imaged length of the fiber. (c) Relationship between the fluorescence signal and the response time of the immunosensing device for the determination of IL-6 with the concentrations of 25 and 200 pg mL^{-1}.

The nonspecific protein adsorption of this sensing device was investigated using BSA as the blocking reagent (Figure S3). In the absence of BSA blocking, a significant nonspecific DG_SPIO_IL-6_Ab absorption was observed on the capture antibody-modified interface after the exposure to the detection antibody solution, likely due to physical adsorption of DG_SPIO_IL-6_Ab on surface defects. However, when the capture antibody-modified sensing interface was blocked with 0.25% BSA, only a few green dots were observed in the confocal image, suggesting negligible nonspecific absorption (5 orders of magnitude lower than the signal for 100 pg mL^{-1} IL-6). Such low nonspecific adsorption is required to achieve high detection specificity of IL-6. The capture antibody-modified sensing interface (with 0.25% BSA blocking) was further used for detection of IL-6 in the PBS solution. As shown in the Z-stack maximum intensity projection images (Figure 5a), the Dragon Green intensity increased with increasing IL-6 concentration, indicating that IL-6 could be quantified by integrating Dragon Green fluorescence by Image-J and Matlab software. A linear relationship between the fluorescence intensity and the concentration of IL-6 in the range 1−400 pg mL^{-1} was obtained (Figure 5b), which is within the physiologically relevant range.[4] The lowest detectable concentration of IL-6 was 1 pg mL^{-1}, which is similar to that of an electrochemical immunosensor based on ferrocene-loaded porous polyelectrolyte nanoparticles as labels (1 pg mL^{-1}).[37] The lowest detection limit is lower than the value reported in a recently developed liquid-gated field-effect transistor sensor based on horizontally aligned single-walled carbon nanotubes for detection of IL-6 (1.37 pg mL^{-1}),[38] and it is 1 order of magnitude lower than a fluorescence-based immunoassay (20 pg mL^{-1}).[39] The application of AuNPs on the sensing interface for loading large amounts of capture antibodies and the brightness of the nanoparticles labeled with detection antibody have contributed to high sensitivity achieved in this work. The reproducibility of the fabricated cytokine assay was evaluated by fabricating 10 separate pieces of optical fibers used for the detection of 60 pg mL^{-1} IL-6 (Figure S4). The relative standard deviation of these ten immunosensors was ±3.6%, indicating that the fabricated assay was closely reproducible in our test conditions.

The feasibility of the fabricated cytokine assay for the spatially localized detection of IL-6 was studied by placing single drops (~1 μL) of the serum sample containing 10 pg mL^{-1} and 200 pg mL^{-1} IL-6 onto various locations of the fabricated optical fiber surfaces (Figure 6), followed by incubation with the detection antibody. Subsequently, the optical fiber exposed to two different concentrations of IL-6 in two close locations was imaged (3 mm length in total) and signal quantification carried out. The intensity of the green dots representing the Dragon Green fluorescent labels were quantified by integrating over a spatial window of specific width (typically 100−500 μm) using ImageJ and Matlab software. This spatial window was chosen to ensure enough Dragon Green beads are imaged for the fluorescence quantification, even for the lowest cytokine concentration. The width of the spatial window is one of the factors determining the achievable spatial resolution. We found that the fluorescence in the fiber area exposed to 200 pg mL^{-1} IL-6 was significantly higher (5 times) than the fluorescence produced with 10 pg mL^{-1} IL-6, suggesting that the fabricated sensing interface was capable of differentiating IL-6 at different concentrations from the sample volume of 1 μL. Thus, the cytokine immunosensing device developed here requires minimal sample consumption and offers excellent assay performance, making it highly suitable for analyzing biomarkers

DOI: 10.1021/acssensors.6b00619
ACS Sens. 2017, 2, 218−226

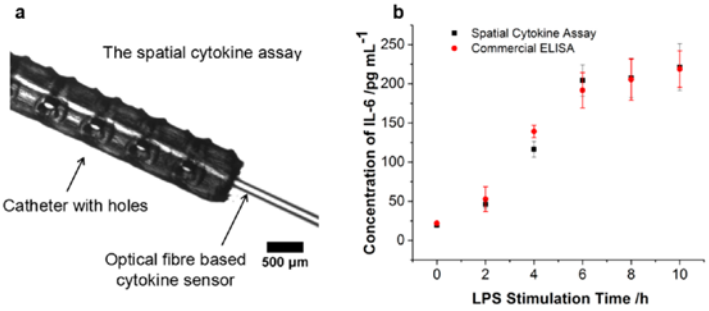

Figure 7. (a) Image of the optical fiber based cytokine assay (with catheter on) under bright field microscopy. (b) IL-6 secretion profile of BV2 cells after LPS stimulation for the commercial ELISA and the herein fabricated spatial fiber based cytokine assay.

and cytokines in precious biological samples. Moreover, our fiber has the capability of spatially resolving detection of localized IL-6 with resolution on the order of 200 to 450 μm. To our knowledge, so far only the Olink Bioscience's Proseek protein assay enables sensitive detection and quantification of proteins in a 1 μL sample volume,[40] but it does not offer spatial resolution. We also determined the response time of the immunosensing device for the detections of IL-6 at the concentrations of 25 and 200 pg mL^{-1}, respectively. The fluorescence signal of the SPIO-Ab (Figure 6c) increased dramatically with increasing incubation time for IL-6 (200 pg mL^{-1}) and it saturated around 30 min. In the case of lower concentration of IL-6 (25 pg mL^{-1}), the fluorescence signal increased about 1 order of magnitude more slowly than that for the high concentration of IL-6 (200 pg mL^{-1}). This more rapid transition toward the equilibrium is as expected by the basic laws of chemical kinetics.[41] We emphasize that for the concentration of 200 pg mL^{-1}, a measurable signal increase was observed already after 5 min incubation in the cytokine-containing medium.

Finally, the optical fiber sensor with the catheter on was applied for the detection of IL-6 secreted by live BV2 cells (Figure 7). Figure 7a shows the device which we used for the measurements in the medium. The concentration of IL-6 secreted into the medium increased with the LPS stimulation time and the maximum concentration was obtained after 6 h LPS stimulation. A similar IL-6 secretion pattern for BV2 cells was obtained by conventional ELISA but the lowest detection limit of our fiber device (1 pg mL^{-1}) was 1 order of magnitude lower than that in the conventional ELISA Kit from R&D System for IL-6 (10 pg mL^{-1}). Critically, in these experiments no media need to be removed from the culture; instead, repeated sampling can be achieved by replacing the fiber. Therefore, the cytokine assay device presented here is capable of monitoring cytokines ex vivo.

CONCLUSIONS

We fabricated and characterized a sensitive cytokine assay based on the optical fiber, which could be used for monitoring the localized cytokine concentration ex vivo. A spatially resolved ELISA sandwich assay was built on the optical fiber surface so that the fiber could be inserted into a perforated catheter. After exposure of the device to the cytokine-containing solution for a period of time, the optical fiber forming a cytokine test strip was removed from the catheter which could be inserted into the body. The fiber was then exposed to the solution of the detection antibody conjugated to fluorescent Dragon Green beads and washed, followed by quantification of cytokines based on the intensity of fluorescence by laser scanning microscopy. This variant of spatial ELISA was successfully used for the detection of cytokine IL-6 with the low limit of detection of 1 pg mL^{-1} and sample volume of 1 μL, and it showed high specificity to IL-6. The sensor interface was stable for up to 9 days in PBS solution, and it was capable of detecting localized IL-6 secreted by BV2 cells with liposaccharide stimulation. This technology provides a new strategy for monitoring spatially varying concentration of cell secreting products, and it has the potential to be developed as a point-of-care device for multiple health conditions.

ASSOCIATED CONTENT

Supporting Information

The Supporting Information is available free of charge on the ACS Publications website at DOI: 10.1021/acssensors.6b00619.

Supplementary figures for fluorescence spectra of the glass surface modified with different components, the SEM image of optical fiber modified with AuNPs, antifouling property of the sensing interface, reproducibility of the fabricated cytokine test strip. Experimental section describing the preparation of Dragon Green magnetic nanoparticles loaded with IL-6 detection antibodies and details for cell culture and ELISA measurement. (PDF)

AUTHOR INFORMATION

Corresponding Author

*E-mail: guozhen.liu@mq.edu.au. Tel: +61-2-98509547.

ORCID

Guozhen Liu: 0000-0002-0556-6404

Notes

The authors declare no competing financial interest.

ACKNOWLEDGMENTS

This work was financially supported by the funding from the ARC Centre of Excellence for Nanoscale Biophotonics CE140100003, MQRDG, the National Natural Science Foundation of China (Grant 21575045), and the self-determined research funds of CCNU (CCNU15A02015). K. Zhang acknowledges the iMQRES scholarship. Laser drilling was carried out at the OptoFab Node of the Australian National Fabrication Facility, utilising NCRIS and NSW Government Funding.

DOI: 10.1021/acssensors.6b00619
ACS Sens. 2017, 2, 218−226

REFERENCES

(1) Nicola, N. A. *Guidebook to cytokines and their receptors*; A Sambrook & Tooze Publication at Oxford University Press: Oxford, 1994.

(2) Xie, W. R.; Deng, H.; Li, H.; Bowen, T. L.; Strong, J. A.; Zhang, J. M. Robust increase of cutaneous sensitivity, cytokine production and sympathetic sprouting in rats with localized inflammatory irritation of the spinal ganglia. *Neuroscience* **2006**, *142* (3), 809−822.

(3) Zhang, J.; An, J. Cytokines, inflammation and pain. *Int. Anesthesiol. Clin.* **2007**, *45* (2), 27−37.

(4) Liu, G. Z.; Qi, M.; Hutchinson, M. R.; Yang, G. F.; Goldys, E. M. Recent advances in cytokine detection by immunosensing. *Biosens. Bioelectron.* **2016**, *79*, 810−821.

(5) Stow, J. L.; Low, P. C.; Offenhäuser, C.; Sangermani, D. Cytokine secretion in macrophages and other cells: pathways and mediators. *Immunobiology* **2009**, *214* (7), 601−612.

(6) Kulbe, H.; Chakravarty, P.; Leinster, D. A.; Charles, K. A.; Kwong, J.; Thompson, R. G.; Coward, J. I.; Schioppa, T.; Robinson, S. C.; Gallagher, W. M.; et al. A dynamic inflammatory cytokine network in the human ovarian cancer microenvironment. *Cancer Res.* **2012**, *72* (1), 66−75.

(7) Leng, S. X.; McElhaney, J. E.; Walston, J. D.; Xie, D.; Fedarko, N. S.; Kuchel, G. A. ELISA and multiplex technologies for cytokine measurement in inflammation and aging research. *J. Gerontol., Ser. A* **2008**, *63* (8), 879−884.

(8) Tisoncik, J. R.; Korth, M. J.; Simmons, C. P.; Farrar, J.; Martin, T. R.; Katze, M. G. Into the eye of the cytokine storm. *Microbiol. Mol. Biol. Rev.* **2012**, *76* (1), 16−32.

(9) Chen, P.; Chung, M. T.; McHugh, W.; Nidetz, R.; Li, Y.; Fu, J.; Cornell, T. T.; Shanley, T. P.; Kurabayashi, K. Multiplex Serum Cytokine Immunoassay Using Nanoplasmonic Biosensor Microarrays. *ACS Nano* **2015**, *9* (4), 4173−4181.

(10) Hou, Y.; Li, T.; Huang, H.; Quan, H.; Miao, X.; Yang, M. Electrochemical immunosensor for the detection of tumor necrosis factor α based on hydrogel prepared from ferrocene modified amino acid. *Sens. Actuators, B* **2013**, *182*, 605−609.

(11) Huang, Y. C.; Chiang, C. Y.; Li, C. H.; Chang, T. C.; Chiang, C. S.; Chau, L. K.; Huang, K. W.; Wu, C. W.; Wang, S. C.; Lyu, S. R. Quantification of tumor necrosis factor-α and matrix metalloproteinases-3 in synovial fluid by a fiber-optic particle plasmon resonance sensor. *Analyst* **2013**, *138* (16), 4599−4606.

(12) Jeong, H. H.; Erdene, N.; Park, J. H.; Jeong, D. H.; Lee, H. Y.; Lee, S. K. Real-time label-free immunoassay of interferon-gamma and prostate-specific antigen using a fiber-optic localized surface plasmon resonance sensor. *Biosens. Bioelectron.* **2013**, *39* (1), 346−351.

(13) Liu, Y.; Kwa, T.; Revzin, A. Simultaneous detection of cell-secreted TNF-α and IFN-γ using micropatterned aptamer-modified electrodes. *Biomaterials* **2012**, *33* (30), 7347−7355.

(14) Liu, Y.; Matharu, Z.; Rahimian, A.; Revzin, A. Detecting multiple cell-secreted cytokines from the same aptamer-functionalized electrode. *Biosens. Bioelectron.* **2015**, *64*, 43−50.

(15) Liu, Y.; Yan, J.; Howland, M. C.; Kwa, T.; Revzin, A. Micropatterned aptasensors for continuous monitoring of cytokine release from human leukocytes. *Anal. Chem.* **2011**, *83* (21), 8286−8292.

(16) Martinez-Perdiguero, J.; Retolaza, A.; Bujanda, L.; Merino, S. Surface plasmon resonance immunoassay for the detection of the TNFα biomarker in human serum. *Talanta* **2014**, *119*, 492−497.

(17) Miller, E. M.; Mcdade, T. W. A highly sensitive immunoassay for interleukin-6 in dried blood spots. *Am. J. Human Biol.* **2012**, *24* (6), 863−865.

(18) Palandra, J.; Finelli, A.; Zhu, M.; Masferrer, J.; Neubert, H. Highly specific and sensitive measurements of human and monkey interleukin 21 using sequential protein and tryptic peptide immunoaffinity LC-MS/MS. *Anal. Chem.* **2013**, *85* (11), 5522−5529.

(19) Pui, T. S.; Kongsuphol, P.; Arya, S. K.; Bansal, T. Detection of tumor necrosis factor (TNF-α) in cell culture medium with label free electrochemical impedance spectroscopy. *Sens. Actuators, B* **2013**, *181*, 494−500.

(20) Šípová, H.; Ševců, V.; Kuchař, M.; Ahmad, J.; Mikulecký, P.; Osička, R.; Malý, P.; Homola, J. Surface plasmon resonance biosensor based on engineered proteins for direct detection of interferon-gamma in diluted blood plasma. *Sens. Actuators, B* **2012**, *174*, 306−311.

(21) Stenken, J. A.; Poschenrieder, A. J. Bioanalytical chemistry of cytokines−A review. *Anal. Chim. Acta* **2015**, *853*, 95−115.

(22) Valentina, M.; Jan, F.; Peder, N. L.; Bo, Z.; Hongjie, D.; Pernille, K. Cytokine detection and simultaneous assessment of rheumatoid factor interference in human serum and synovial fluid using high-sensitivity protein arrays on plasmonic gold chips. *BMC Biotechnol.* **2015**, *15* (1), 73.

(23) Cohen, N.; Sabhachandani, P.; Golberg, A.; Konry, T. Approaching near real-time biosensing: Microfluidic microsphere based biosensor for real-time analyte detection. *Biosens. Bioelectron.* **2015**, *66*, 454−460.

(24) Oh, B. R.; Huang, N. T.; Chen, W.; Seo, J. H.; Chen, P.; Cornell, T. T.; Shanley, T. P.; Fu, J.; Kurabayashi, K. Integrated nanoplasmonic sensing for cellular functional immunoanalysis using human blood. *ACS Nano* **2014**, *8* (3), 2667−2676.

(25) Culshaw, B. Fiber-optic sensors: applications and advances. *Opt. Photonics News* **2005**, *16* (11), 24−29.

(26) Rajan, G. *Optical Fiber Sensors: Advanced Techniques and Applications*; CRC press, 2015; Vol. *36*.

(27) Caucheteur, C.; Guo, T.; Albert, J. Review of plasmonic fiber optic biochemical sensors: improving the limit of detection. *Anal. Bioanal. Chem.* **2015**, *407* (14), 3883−3897.

(28) Blicharz, T. M.; Siqueira, W. L.; Helmerhorst, E. J.; Oppenheim, F. G.; Wexler, P. J.; Little, F. F.; Walt, D. R. Fiber-optic microsphere-based antibody array for the analysis of inflammatory cytokines in saliva. *Anal. Chem.* **2009**, *81* (6), 2106−2114.

(29) Kapoor, R.; Wang, C.-W. Highly specific detection of interleukin-6 (IL-6) protein using combination tapered fiber-optic biosensor dip-probe. *Biosens. Bioelectron.* **2009**, *24* (8), 2696−2701.

(30) Wang, C. W.; Manne, U.; Reddy, V. B.; Oelschlager, D. K.; Katkoori, V. R.; Grizzle, W. E.; Kapoor, R. Development of combination tapered fiber-optic biosensor dip probe for quantitative estimation of interleukin-6 in serum samples. *J. Biomed. Opt.* **2010**, *15* (6), 067005−1−067005−7.

(31) Battaglia, T. M.; Masson, J.-F.; Sierks, M. R.; Beaudoin, S. P.; Rogers, J.; Foster, K. N.; Holloway, G. A.; Booksh, K. S. Quantification of cytokines involved in wound healing using surface plasmon resonance. *Anal. Chem.* **2005**, *77* (21), 7016−7023.

(32) Usuba, R.; Yokokawa, M.; Ackermann, T. N.; Llobera, A.; Fukunaga, K.; Murata, S.; Ohkohchi, N.; Suzuki, H. Photonic Lab-on-a-Chip for Rapid Cytokine Detection. *ACS Sens.* **2016**, *1* (8), 979−986.

(33) Illy, E. K.; Brown, D. J.; Withford, M. J.; Piper, J. A. Optimization of trepanning strategies for micromachining of polymers with high-pulse-rate UV lasers, In *Advanced High-Power Lasers and Applications*; International Society for Optics and Photonics, 2000; pp 608−616.

(34) Schmitt, J.; Mächtle, P.; Eck, D.; Möhwald, H.; Helm, C. Preparation and optical properties of colloidal gold monolayers. *Langmuir* **1999**, *15* (9), 3256−3266.

(35) Kumar, S.; Aaron, J.; Sokolov, K. Directional conjugation of antibodies to nanoparticles for synthesis of multiplexed optical contrast agents with both delivery and targeting moieties. *Nat. Protoc.* **2008**, *3* (2), 314−320.

(36) Liu, G. Z.; Luais, E.; Gooding, J. J. The fabrication of stable gold nanoparticle-modified interfaces for electrochemistry. *Langmuir* **2011**, *27* (7), 4176−4183.

(37) Li, T.; Yang, M. Electrochemical sensor utilizing ferrocene loaded porous polyelectrolyte nanoparticles as label for the detection of protein biomarker IL-6. *Sens. Actuators, B* **2011**, *158* (1), 361−365.

(38) Chen, H.; Choo, T. K.; Huang, J.; Wang, Y.; Liu, Y.; Platt, M.; Palaniappan, A.; Liedberg, B.; Tok, A. I. Y. Label-free electronic detection of interleukin-6 using horizontally aligned carbon nanotubes. *Mater. Des.* **2016**, *90*, 852−857.

DOI: 10.1021/acssensors.6b00619
ACS Sens. 2017, 2, 218−226

(39) Hun, X.; Zhang, Z. Functionalized fluorescent core-shell nanoparticles used as a fluorescent labels in fluoroimmunoassay for IL-6. *Biosens. Bioelectron.* **2007**, *22* (11), 2743−2748.
(40) Hjelm, F.; Tran, B.; Fredriksson, S. Sensitive detection of cytokines in 1-[mu] l serum samples using Proseek [reg]. *Nat. Methods* **2011**, *8* (9), iii−iv.
(41) Reverberi, R.; Reverberi, L. Factors affecting the antigen-antibody reaction. *Blood Transfusion* **2007**, *5* (4), 227.

DOI: 10.1021/acssensors.6b00619
ACS Sens. 2017, 2, 218−226

Supporting Information

Sensitive Cytokine Assay Based on Optical Fiber Allowing Localized and Spatially Resolved Detection of Interleukin-6

Guozhen Liu,[a,b] Kaixin Zhang,[a] Annemarie Nadort,[a] Mark R. Hutchinson,[c] Ewa M. Goldys[a]*

[a]ARC Centre of Excellence in Nanoscale Biophotonics (CNBP), Macquarie University, North Ryde 2109, Australia

[b]Key Laboratory of Pesticide and Chemical Biology of Ministry of Education, College of Chemistry, Central China Normal University, Wuhan 430079, P. R. China

[c]ARC Centre of Excellence in Nanoscale Biophotonics (CNBP), The University of Adelaide, Australia

This supporting information contains supporting figures on fluorescence spectra of the glass surface modified with different components, the SEM image of optical fibre modified with AuNPs, anti-fouling property of the sensing interface, reproducibility of the fabricated cytokine test strip. The experimental section describing the preparation of Dragon Green magnetic nanoparticles loaded with IL-6 detection antibodies and details for cell culture and ELISA measurement are also provided.

EXPERIMENTAL SECTION

Preparation of Dragon Green magnetic nanoparticles loaded with IL-6 detection antibodies. Carboxylated superparamagnetic iron oxide particles incorporating the Dragon Green fluorophore (1 mg) were dispersed in 1 mL of 25 mM MES buffer at pH 6.0. This dispersion was then mixed with 10 mg EDC (1-ethyl-3-[3 dimethylaminopropyl]carbodiimide hydrochloride, Thermo Scientific) and 10 mg NHS (N-hydroxysuccinimide) and vortexed at room temperature for 30 min. The protein, 20 µL anti-IL-6 monoclonal antibody (0.5 mg mL^{-1} in 1 × PBS) was added to the solution immediately, and stirred on a nonmagnetic mixing device for 2 h at room temperature. The resulting antibody-nanoparticle conjugates were magnetically separated by placing a magnet under the bottom of the reaction vessel, and the supernatant was discarded. Finally, the antibody modified SPIO (DG SPIO_IL-6_Ab) were separated and washed with a wash buffer (PBS, 0.1% Tween-20) once and subsequently blocked in 1ml PBS containing 0.25% BSA and 0.1% Tween-20 for 1 hour. The obtained DG SPIO_IL-6_Ab nanoparticles were redispersed in 0.5 mL PBS and stored at 4 ^{o}C. The ratio of antibodies to nanoparticles used here equates to 10 µg antibody per 1 mg nanoparticles.

Cell culture and ELISA measurement. Mouse BV2 cells were cultured in a T75 cm^2 flask containing Dulbecco's Modified Eagle's medium (DMEM) supplement with 10% FBS, 100 U mL^{-1} of penicillin, 0.1 mg mL^{-1} of streptomycin. The cells were cultured to about 80-90% confluence before harvesting. During harvesting, the cells were washed twice with DPBS followed by trypsinization using 2 mL of trypsin to detach the cells from the flask. The trypsin was neutralized by adding 4 mL of fresh supplemented medium, and the harvested cells suspended in the DMEM medium were transferred into a centrifuge tube and centrifuged at 200 rcf for 6 min. The supernatant was discarded and the cells were resuspended in a fresh medium. The prepared immunosensor and BD OptEIA^{Tm} Mouse IL-6

ELISA kit (BD Bioscience) were used to measure the concentration of IL-6 secreted by BV-2 cells into the medium after lipopolysaccharide (LPS, 100 ng mL^{-1}) stimulation. For preparation of the IL-6 samples, the cells with the density of 1 x 10^6 /mL were suspended in 1 mL of warm medium containing 0.11 µg mL^{-1} LPS from Escherichia coli 026:B6 to secrete IL-6. The supernatant (1 mL) with secretions were collected at different LPS stimulation time (0 h, 2 h, 4 h, 6 h, 8 h, and 10 h) in triplicate, respectively. The supernatants from cells were collected The Nunc MaxiSorp 96 well plate and Galaxy plate reader was used for ELISA. Results are reported as means ± standard deviation.

RESULTS

Fluorescence characterisation after attachment of fluorescence detection antibody to the glass sensing interface

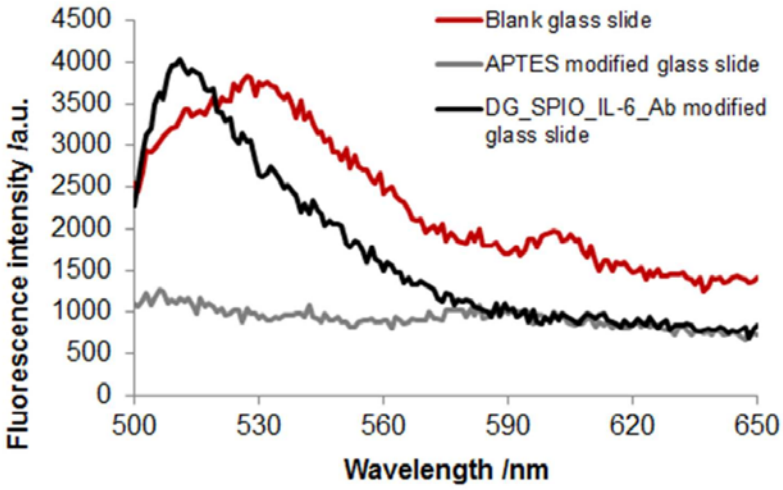

Figure S1. Fluorescence spectra of the glass cover slip after stepwise modification of different components on the sensing interface.

Characterisation of the gold nanoparticles modified fibre surface

The gold nanoparticles modified fibre surface was characterised by SEM as shown in Figure S2.

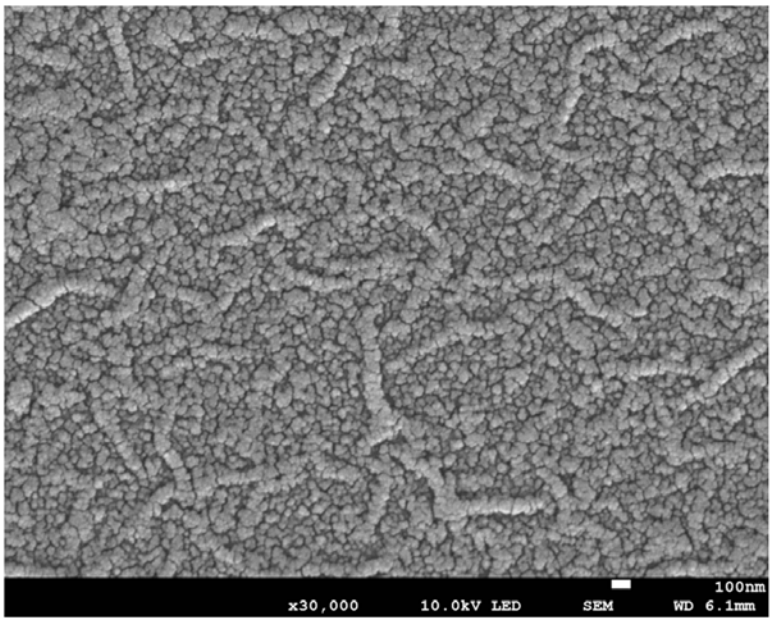

Figure S2. The SEM image of optical fibre after modification of AuNPs.

Anti-fouling property of the sensing interface

The non-specific absorption is an important factor having a significant effect on the sensitivity of the fibre sensor. In order to bring down the nonspecific binding, the blocking reagent BSA was applied onto the sensing interface. As shown in Figure S3, in the absence of BSA blocking, a significant non-specific DG SPIO IL-6_Ab absorption was observed on the capture antibody-modified interface after exposure to the DG SPIO IL-6_Ab solution, likely to be due to physical adsorption on surface defects. However, when the capture antibody-modified sensing interface was blocked with BSA, only a few green dots were observed in the confocal image, suggesting negligible non-specific absorption (5 orders of magnitude lower than the signal for 100 pg mL^{-1} IL6). Such low non-specific adsorption is required to maximize the detection specificity of IL-6.

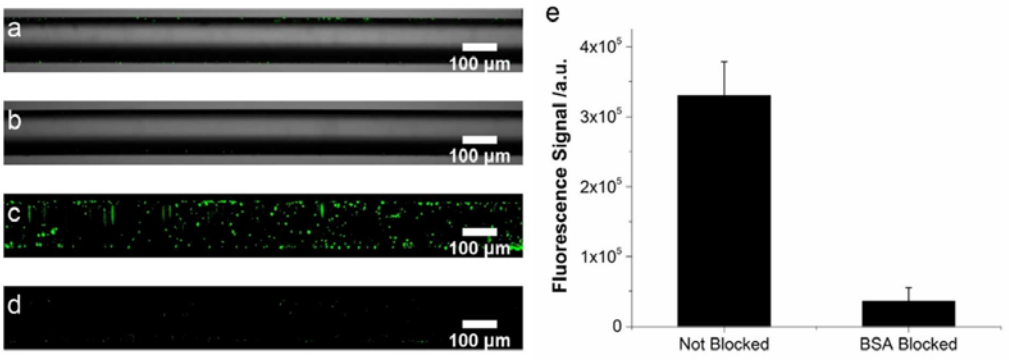

Figure S3. Confocal images of capture antibody modified fibres (a) before and (b) after BSA blocking. (c) Z-stack maximum intensity projection images of (a). (d) Z-stack maximum intensity projection images of (b). (e) Normalized fluorescence signals before and after BSA blocking in (c) and (d).

Reproducibility of the fabricated cytokine test strip

The reproducibility of the fabricated cytokine test strip was evaluated by fabricating 10 optical fibres used for the detection of 60 pg mL^{-1} IL-6 (Figure S4). The relative standard deviation of these ten immunosensors was ±3.6%, indicating that the fabricated assay was closely reproducible in tested conditions.

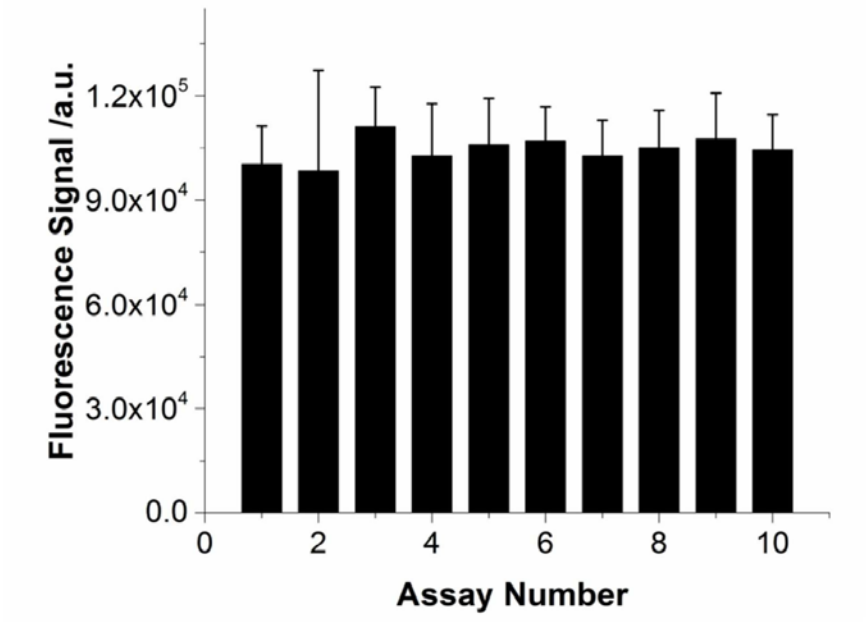

Figure S4 The reproducibility of ten fabricated cytokine test strips for detection of 60 pg mL^{-1} IL-6.

2.3 Appendix

Fluorescence visualization of the fiber sensing surface

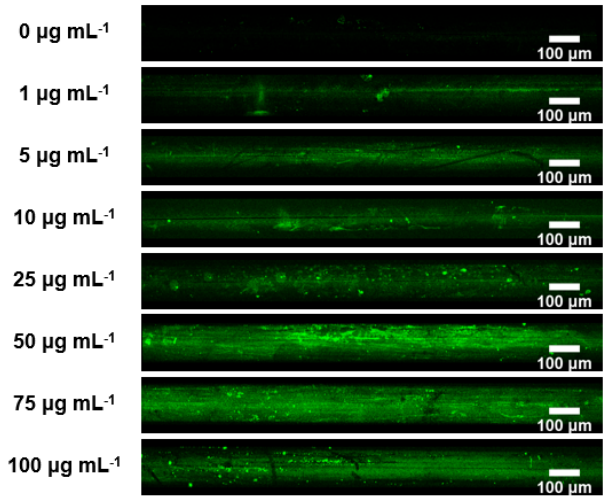

Figure 2-1 Confocal microscope images of the fiber surface reacting with different concentration of IL-6 capture antibody following stained by the fluorescent secondary antibody (donkey anti-Goat IgG NorthernLights NL493-conjugated antibody).

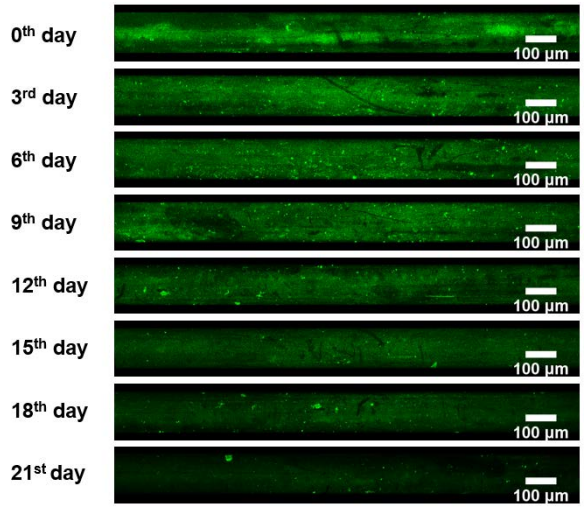

Figure 2-2 Confocal microscope images of the fiber sensing surface incubated in PBS for extended periods of time followed by monitoring the presentence of IL-6 capture antibody using the green dye-labeled secondary antibody (donkey anti-Goat IgG NorthernLights NL493-conjugated antibody).

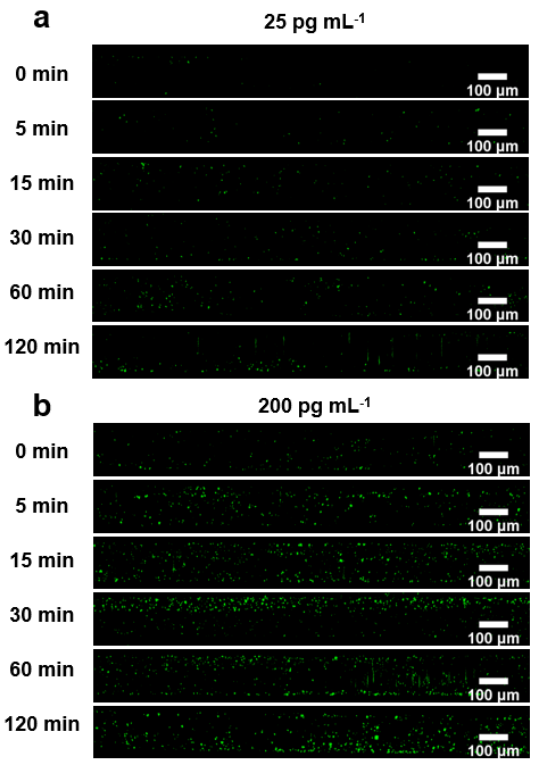

Figure 2-3 Optimization of incubation time: Z-stack images of the fiber in detection of 25 and 200 pg mL^{-1} IL-6 with different incubation time after exposure in the DG_SPIO_IL-6_Ab conjugates solution.

Comparison of the present method (method I) with other two methods on fabrication of the fiber sensor.

2.3.1 The preparation of the fiber sensing surface with the other two methods.

Method II: Diazonium-modified capture antibody for fabrication of the sensing surface

Firstly, the AuNP modified fiber surface was obtained by using the same protocol detailed in the manuscript. 10 mg of 4-carboxyphenyl diazonium tertrafluoroborate, 10 mg EDC and 10 mg NHS were mixed in 1 mL of water followed by 10 min incubation, then EDC/NHS activated 4-carboxyphenyl diazonium tertrafluoroborate was obtained. Next, 10 µL EDC/NHS activated 4-carboxyphenyl diazonium tertrafluoroborate was added to 200 µL 5 µg mL^{-1} IL-6 capture antibody solution in carbonate buffer (pH 11) and was allowed to incubate for 2 hours at room temperature. As EDC/NHS activated 4-carboxyphenyl diazonium tertrafluoroborate can react with the amine group existing on the capture antibody so the diazonium-modified capture antibody can be obtained in this way. The obtained diazonium-functionalized capture antibody was washed and concentrated by a 100 KDa

centrifugate filter for further usage. Subsequently, AuNP coated fiber was immersed in the diazonium-functionalized capture antibody solution (50 μg mL^{-1}) for 2 h to form the sensing surface.

Method III: Self-assemble method on the fabrication of the sensing surface

Firstly, the AuNP modified fiber surface was obtained by using the same protocol detailed in the manuscript. Then the AuNP coated fiber was incubated in 50 μg mL^{-1} IL-6 capture antibody overnight. And the capture antibody can self-assemble on the fiber surface through the interactions between the AuNP and -NH_2 or -SH group existing on the antibody.

Comparison of the fiber sensing surface

The fiber sensing surface prepared by the three different methods were stained by donkey anti-Goat IgG NorthernLights NL493- conjugated antibody before they were checked by confocal microscope. As can be seen from figure 2-4, the fluorescence intensity of method I showed higher fluorescence value than the other two methods, this can be attributed to the fact that when 6-mercaptohexanoic acid self-assembled on the AuNP coated fiber surface, it can create a uniform surface and provide more binding sites for the following attachment of the capture antibody. It is of note that under optimal conditions, diazonium salts can also lead to uniform coatings, and the functional groups available can be tuned depending on the conditions to achieve the optimum number of binding sites, however before the capture antibody being immobilized on the fiber surface, the procedure for purifying the diazonium salts functionalized antibody need multiple washing and dialysis, which will lead to a loss of the antibody, and some antibodies will tend to denaturate, which result in a relative lower performance.

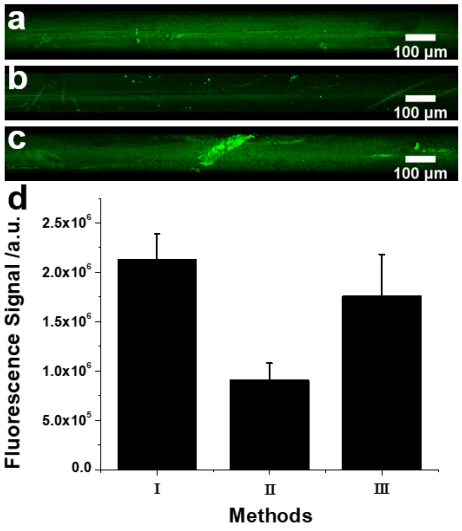

Figure 2-4 Confocal microscope images of fiber sensing surface prepared by method I (a), method II(b), and method III(c); (d) the corresponding fluorescence signal from the figure a, b and c.

Comparison of the performance of fiber sensing surface in detection of IL-6.

The performance of the fiber sensing surface was further compared by detection of a given concentration of IL-6 (400 pg mL^{-1}) in PBS containing 10 % FBS. After 2h incubation with the cytokine (which can help to keep the equilibrium between the fiber surface and the cytokine in the solution), fibers were then stained by DG_SPIO_IL-6 Ab conjugate. Figure 2-5 a, b and c showed the confocal images of the three types of fiber sensing surfaces in determination of 400 pg mL^{-1} IL-6 after incubating with DG_SPIO_IL-6 Ab conjugate solutions. Many green fluorescent particles could be observed around the method I prepared fiber, while less fluorescent particles appeared on the fiber being prepared by method II and III. It suggested that Method I prepared fiber had the best performance in the IL-6 detection, because the method I can help to make more capture antibody attached on the fiber surface resulting in a more sensitive performance in IL-6 detection. Furthermore, the fluorescence signal of the whole fiber surface was quantified by Z-stack imaging method (Figure 2-5 d, e and f). Images were collected and stacked by selecting the maximum pixel value from each image and the fluorescence signal was processed by Image J and Matlab software. A more obvious discrimination among the three fibers could be observed from the Z-stack images as the fluorescence signal of method I prepared fiber was 5.3×10^5 a.u. while method II and III got the value at 2.2×10^5 a.u. and 3.2×10^5 a.u., respectively.

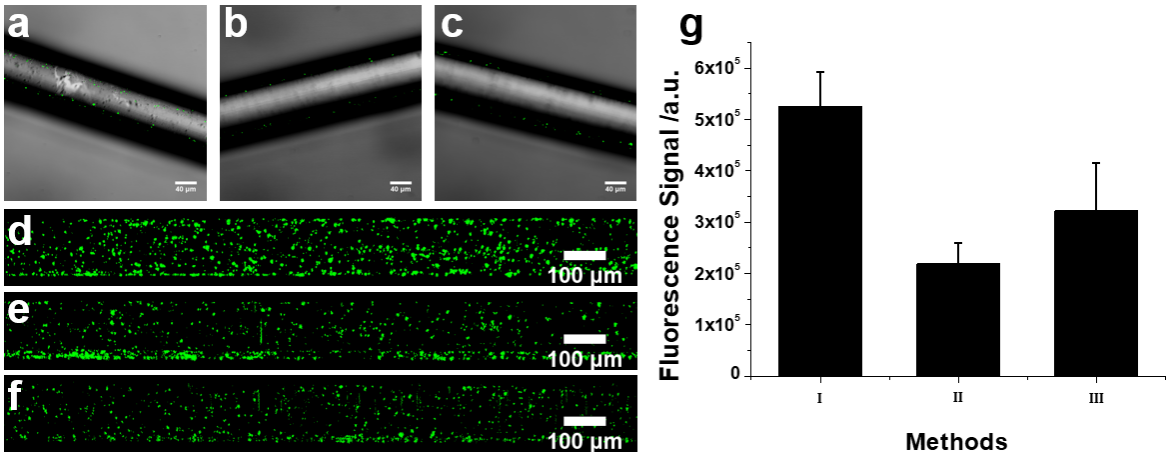

Figure 2-5 Combined confocal images (bright field and fluorescence field) of the method I (a), method II (b) and method III (c) prepared optical fiber for determination of 400 pg mL^{-1} after incubation with DG_SPIO_IL-6_Ab; Z-stack images of the the method I (d), method II (e) and method III (f) prepared optical fiber for determination of 400 pg mL^{-1} after incubation with DG_SPIO_IL-6_Ab. (g) the corresponding fluorescence signal from figure d, e and f.

Real sample analysis

In order to test the application of the proposed spatial fiber ELISA for real samples analysis, the fiber was also used to test the mouse IL-6 in cell culture medium by using the standard addition method. To protect the fiber from being destroyed, the fiber was placed in a cannula which has some hole on the cannula surface to keep the solute interaction. After the fiber finishing the capture of IL-6 in medium, then it was stained by DG_SPIO_IL-6_Ab, and fluorescence signal was collected by confocal microscope and the concentration of IL-6 was determined. The results are shown in Table 2-1, the IL-6 content determined was in agreement with the declared value, the recovery for standards added was 96.3% ~ 107.9% indicating that the fiber sensor was applicable for real sample detection.

Table 2-1. Determination of the recovery of IL-6 in cell culture medium by using the standard addition method.

	Added (pg)	Found (pg)	Recovery
1	200	215.7	107.9%
2	300	317.1	105.7%
3	400	385.3	96.3%

2.4 Summary

In this chapter, we fabricated and characterized a sensitive cytokine assay based on the optical fiber, which could be used for monitoring the localized cytokine concentration ex vivo. A spatially resolved ELISA sandwich assay was built on the optical fiber surface. After the immunocapture device was incubated with a cytokine solution to capture the analyte, the device was then exposed to the IL-6 detection antibody which was loaded on the fluorescently labeled magnetic nanoparticles, making it possible to quantify the cytokine concentration based on the intensity of fluorescence. This variant of spatial ELISA was successfully used for the detection of cytokine IL-6 with the low limit of detection of 1 pg mL^{-1} and sample volume of 1 μL, and it showed high specificity to IL-6. The sensor interface was stable for up to 9 days in PBS solution, and it was capable of detecting IL-6 secreted by BV2 cells with liposaccharide stimulation. This technology provides a new strategy for monitoring spatially varying concentration of cell secreting products, and it has the potential to be developed as a point-of care device for multiple health conditions.

3

Detection of Interleukin-1β on APTES -AuNP-MA Modified Glass Fiber

3.1 Introduction

Exaggerated inflammatory responses in the brain are thought to be a common core in the etiology of numerous psychiatric disorders such as depression, post-traumatic stress disorder (PTSD) and bipolar disorder. A major impediment for establishing a mechanistic link between neuroimmune signaling and disease-related neural circuit activity is the lack of tools that reliably monitor the release of signaling molecules (cytokine) by the brain's immune cells. For instance, due to their relatively high molecular weight, traditional real-time sampling methods in brain such as *in vivo* microdialysis provide a poor yield of extracellular cytokine levels.

In this chapter, we further extended the application of the way for fabrication immunosensor in chapter 1 and designed an optical fiber-based immunosensing device for repeated monitoring of spatially localized cytokine interleukin-1beta (IL-1β) release in the rat brain. This cytokine capture device comprises a de-cladded optical fiber labeled with a IL-1β capture antibody on the surface interface that can be inserted into a stainless steel implanted cannula with micrometer-sized holes drilled along its length to enable fluid exchange between the outside and inside of the cannula. Upon removal from the cannula, a new capture device can be reintroduced for repeated measurements. This technology represents an opportunity for unlocking the function of neuroimmune signalling, and has broad applicability for pre-clinical disease models assessing the impact of immune processes in brain function.

Zhang, K., Baratta, M.V., Liu, G., Frank, M.G., Leslie, N.R., Watkins, L.R., Maier, S.F., Hutchinson, M.R. and Goldys, E.M., 2018. A novel platform for in vivo detection of cytokine release within discrete brain regions. Brain, Behavior, and Immunity, 71, pp.18-22.

Summary of the Author contributions to paper 2 following the order of author.

Paper 2	K. Z	M.B	G. L	M. F	N. L	L. W	S. M	M. H	E. G
Experiment Design	•	•	•	•			•	•	•
Sample Preparation	•	•			•				
Data Collection	•	•			•				
Analysis	•	•							
Figures	•	•							
Manuscript	•	•		•		•	•	•	•

3.2 Full paper

ARTICLE IN PRESS

Brain, Behavior, and Immunity xxx (xxxx) xxx–xxx

Contents lists available at ScienceDirect

Brain, Behavior, and Immunity

journal homepage: www.elsevier.com/locate/ybrbi

Short Communication

A novel platform for *in vivo* detection of cytokine release within discrete brain regions

Kaixin Zhang[a,1], Michael V. Baratta[b,1], Guozhen Liu[a,c,d,*], Matthew G. Frank[b], Nathan R. Leslie[b], Linda R. Watkins[b], Steven F. Maier[b], Mark R. Hutchinson[e], Ewa M. Goldys[a,c,*]

[a] ARC Centre of Excellence in Nanoscale Biophotonics (CNBP), Macquarie University, Sydney, Australia
[b] Department of Psychology and Neuroscience, University of Colorado Boulder, Boulder, CO, USA
[c] Graduate School of Biomedical Engineering, The University of New South Wales, Sydney, Australia
[d] International Joint Research Center for Intelligent Biosensor Technology and Health, Central China Normal University, Wuhan, China
[e] ARC Centre of Excellence in Nanoscale Biophotonics (CNBP), The University of Adelaide, Adelaide, Australia

ARTICLE INFO

Keywords:
Cytokine
Immunosensing
Interleukin-1 beta
Hippocampus
Rat

ABSTRACT

Mounting evidence indicates that cytokines secreted by innate immune cells in the brain play a central role in regulating neural circuits that subserve mood, cognition, and sickness responses. A major impediment to the study of neuroimmune signaling in healthy and disease states is the absence of tools for *in vivo* detection of cytokine release in the brain. Here we describe the design and application of a cytokine detection device capable of serial monitoring of local cytokine release in discrete brain regions. The immunocapture device consisted of a modified optical fiber labeled with a capture antibody specific for the pro-inflammatory cytokine interleukin-1 beta (IL-1β). Using a sandwich immunoassay method, *in vitro* data demonstrate that the sensing interface of the modified optical fiber has a linear detection range of 3.9 pg mL^{-1}–500 pg mL^{-1} and spatial resolution on the order of 200–450 μm. Finally, we show that the immunocapture device can be introduced into a perforated guide cannula for repeated analyte measurements *in vivo*. An increase in fluorescence detection of spatially localized intrahippocampal IL-1β release was observed following a peripheral lipopolysaccharide challenge in Sprague-Dawley rats. This novel immunosensing technology represents an opportunity for unlocking the function of neuroimmune signaling.

1. Introduction

Biological communication in the central nervous system (CNS) involves complex and interconnected networks of cells that use a variety of chemical signals supporting information processing. Multiple lines of evidence indicate that immune responses generated in the CNS are mediated, in part, by pro-inflammatory cytokines that orchestrate aspects of sickness behavior such as shifts in motivational priorities, sensory processing, and cognitive performance (Larson, 2002; Maier, 2003; Rohan Walker and Yirmiya, 2016; Watkins et al., 1995). These molecular signals originate from resident innate immune cells in the CNS (e.g., microglia) that serve as the neuroimmune substrate for *de novo* synthesis and release of central cytokines, most notably the prototypic pro-inflammatory cytokine interleukin-1 beta (IL-1β) (Dinarello, 2011; Frank et al., 2007; Kreutzberg, 1996). However, our understanding of these neuroimmune signals in neuroinflammatory processes has been hampered, in large part, due to several limitations of current experimental approaches for the measurement of cytokines in the brain. The most common approaches, including immunohistochemical and ELISA based techniques, are restricted to quantifying total cytokine levels, but fail to capture interstitial cytokine levels or cytokine release in discrete brain regions.

Preclinical studies have traditionally relied on *in vivo* microdialysis for quantitative assessment of substances from the interstitial space in behaving animals (Chefer et al., 2009). This sampling technique requires implantation in brain of a dialysis probe with a semipermeable membrane that allows for repeated sampling of low molecular weight analytes. Expansion of this method for sampling other chemical signals such as cytokine proteins has posed several challenges such as reduced recovery across the size-limited dialysis membrane and the requirement

* Corresponding authors at: Graduate School of Biomedical Engineering, The University of New South Wales, Sydney, Australia.
E-mail addresses: kaixin.zhang@hdr.mq.edu.au (K. Zhang), michael.baratta@colorado.edu (M.V. Baratta), guozhen.liu@unsw.edu.au (G. Liu), matt.frank@colorado.edu (M.G. Frank), Nathan.Leslie@colorado.edu (N.R. Leslie), Linda.Watkins@colorado.edu (L.R. Watkins), Steve.Maier@colorado.edu (S.F. Maier), mark.hutchinson@adelaide.edu.au (M.R. Hutchinson), e.goldys@unsw.edu.au (E.M. Goldys).
[1] These authors contributed equally to this work.

https://doi.org/10.1016/j.bbi.2018.04.011
Received 17 January 2018; Received in revised form 2 April 2018; Accepted 16 April 2018

Please cite this article as: Zhang, K., Brain, Behavior, and Immunity (2018), https://doi.org/10.1016/j.bbi.2018.04.011

for a large sampling volume for cytokine detection given that concentrations in the extracellular milieu are low, typically in the pM range (Ao and Stenken, 2006; Liu et al., 2016; Qi et al., 2017; Schenk et al., 2001).

To address these limitations, we designed an optical fiber-based immunosensing device for repeated monitoring of spatially localized cytokine IL-1β release in the rodent brain. This cytokine capture device comprises a de-cladded optical fiber labeled with a IL-1β capture antibody on the surface interface that can be inserted into a stainless steel implanted cannula with micrometer-sized holes drilled along its length to enable fluid exchange between the outside and inside of the cannula. Upon removal from the cannula, a new capture device can be re-introduced for repeated measurements. The removed capture device carries the antibody-bound analyte, IL-1β, which can then be quantified *ex vivo* using a sandwich immunoassay method. Here we demonstrate detection of spatially localized cytokine IL-1β with a low limit of detection of 3.9 pg mL^{-1} and a high spatial resolution on the order of 200–450 μm. *In vivo* evaluation of the detection system demonstrated an increased fluorescence signal in capture devices inserted into the rat dorsal hippocampus following a peripheral challenge with lipopolysaccharide (LPS), a constituent of the cell wall of gram-negative bacteria. Thus, this immunosensing system holds great promise for selective, rapid and serial measurement of cytokine release in the CNS.

2. Material and methods

2.1. Subjects

Male Sprague–Dawley rats (225–250 g; Envigo, Indianapolis, IN, USA) were pair housed on a 12-h light–dark cycle (lights on at 0600 h). Food (standard laboratory chow) and water were available *ad libitum*. Rats were allowed to acclimate to colony conditions for at least one week prior to experimentation. All experiments were approved by the Institutional Animal Care and Use Committee of the University of Colorado Boulder in compliance with the National Institutes of Health *Guide for the Care and Use of Laboratory Animals*.

2.2. Chemicals and materials

Recombinant rat IL-1β protein, polyclonal goat anti-IL-1β IgG (capture antibody, Catalog: AF-501-NA, Lot: YR0913021) and monoclonal mouse anti-IL-1β IgG (detection antibody, Catalog: MAB501, Clone: 38139, Lot: ZG0908021) were obtained from R&D Systems. Toluene, phosphate buffered saline (PBS), sulfuric acid (95.0–98.0%), hydrogen peroxide (30%), (3-aminopropyl)triethoxysilane (APTES), 6-mercaptohexanoic acid (MA), gold nanoparticles (AuNP; 10 nm diameter, OD 1, in 0.1 mM PBS), N-hydroxysuccinimide (NHS), 1-ethyl-3-(3-dimethylaminopropyl) carbodiimide hydrochloride (EDC), 2-(N-morpholino) ethanesulfonic acid (MES, pH 6.0), and bovine serum albumin (BSA) were obtained from Sigma-Aldrich. Fluorescent carboxylated magnetic microspheres with 1% solid content were from Bangs Laboratories.

2.3. Fabrication of the fiber sensing interface

The fabrication of the fiber sensing interface was conducted as in our previous report (Liu et al., 2017). To prepare for the fiber sensing interface, the decladded fiber (125 μm diameter core multimode optical fiber; Prysmian) was initially immersed in piranha solution (H_2SO_4 95% and H_2O_2 30% mixed at a volume ratio of 7:3) for 12 h to clean the glass and to form hydroxyl groups on its surface. Upon removal the fiber was washed with Milli-Q water and ethanol and then dried under a N_2 stream. Fibers were then immersed in APTES (5% v/v) in toluene for 6 h to form amine-terminated polymer layers. The unbound monomers were removed from the fiber surface by toluene. Subsequently, the APTES-modified optical fiber was incubated in a 1 mL AuNP (10 nm) solution for 3 h to form the AuNP modified fiber. After several water rinses, the AuNP modified optical fiber was immersed into 0.1 mM MA solution overnight, and finally washed three times with Milli-Q water. Subsequently, the MA-modified fiber surface was incubated in a 25 mM MES buffer (pH 6.0) solution with EDC (10 mg mL^{-1})/NHS (10 mg mL^{-1}) for 30 min. The fiber was then washed in the MES buffer twice and incubated with the anti-IL-1β capture antibody (50 μg mL^{-1}) in MES buffer at room temperature (RT) for 3 h. The capture antibody modified fiber surface was subsequently blocked in 0.5% BSA solution for 3 h at RT to complete the preparation of the sensing interface. The prepared fiber sensing interface was then stored in blocking buffer before usage.

2.4. Preparation of SPIO-IL-1β detection antibody conjugates

Fluorescent carboxylated superparamagnetic iron oxide (SPIO) beads were vortexed thoroughly to ensure homogeneous suspension of the beads. SPIO beads (50 μL) were introduced into a 1.5 mL microcentrifuge vial followed by two washes with 1 mL of MES buffer, and then collected with a magnetic separator. To activate the carboxylic acid groups on SPIO, SPIO beads were resuspended in 500 μL freshly prepared EDC (10 mg mL^{-1} in MES buffer)/NHS (10 mg mL^{-1} in MES buffer) solution, vortexed, and incubated by mixing on a rotary wheel for 30 min at RT. The SPIO were then washed three times with 1 mL MES buffer with a magnetic separator to remove excess EDC/NHS coupling reagents. Finally, 10 μg IL-1β detection antibody (diluted in 100 μL MES buffer) was added to the tube to be coupled with the SPIO. The mixture was incubated for 3 h at RT with constant rotation. Finally, these microsphere-antibody conjugates (SPIO-IL-1β) were collected by the magnetic separator and washed twice with MES buffer and twice with washing buffer (PBS, 0.05% Tween20), and then dispersed in 0.5 mL 0.1 M PBS for further use. For measuring IL-1β *in vitro*, the immunolabeled fiber was incubated in serum containing IL-1β in varying concentrations for 1 h (Fig. 1). The fiber was then washed with PBS five times to remove unbound IL-1β. Finally the optical fiber was exposed to a SPIO-IL-1β detection antibody solution for 1 h followed by PBS washes before fluorescence measurement.

2.5. Imaging

Scanning electron microscope (SEM) images were obtained at a JEOL JSM-7100F SEM operating at 10 kV. All z-stack images of fiber samples were acquired by a SP2 (Leica) confocal microscope with a 10X objective (excitation/emission at 480 and 520 nm). The fluorescence signal was collected by a z-stack method under the confocal microscope, as detailed in our previous manuscript (Liu et al., 2017). Ten z-planes (125-μm total height), with an approximate 12.5 μm separation between each plane were collected. Total sensing fiber length (1.5 mm) was imaged for cytokine measurement and the fluorescence signal was quantified by integrating over a certain spatial (450 μm) window using ImageJ and Matlab software. To demonstrate spatial selectivity and concentration-dependent response following local administration of IL-1β (Fig. 1F), we placed droplets of two different concentration of IL-1β (15 and 400 pg mL^{-1}) on the fiber surface. The entire fiber was imaged and the fluorescence signal was quantified with two spatial resolution windows (200 μm and 450 μm) along the fiber length.

2.6. Perforation and implantation of guide cannula

Stainless-steel guide cannulae cut 4 mm below pedestal (Plastics One Inc.) were perforated by a laser system to create windows such that the fiber based sensing interface could access the extracellular space once introduced into the cannula. The inner diameter of the cannula (24 gauge) was sufficiently larger than that of the immunocapture fiber so that the immunosensing interface (i.e. gold na-noparticle/capture antibody coating) is not damaged upon insertion.

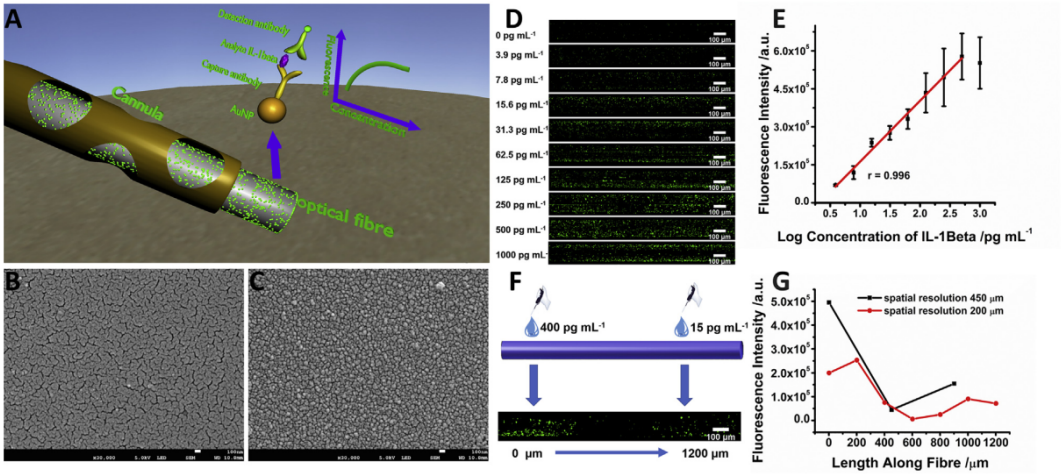

Fig. 1. *In vitro* characterization and optimization of the spatial cytokine detection system. (A) Schematic of the procedural steps for establishing the optical fiber sensing interface for interleukin-1 beta (IL-1β) detection. (B) Scanning Electron Microscopy images of the clean immunosensing fiber surface before and (C) after coating with gold nanoparticles. (D) Confocal z-stack maximum intensity projection images of the optical fiber following exposure to different concentrations of IL-1β. (E) Calibration curve of IL-1β based on the mean fluorescence signal of protein concentrations listed in (D), the number of replicates is three for every concentration. Error bars indicate standard error of the mean (SEM). (F) IL-1β sensing fibers demonstrate spatial and concentration selectivity to local administration of IL-1β (400 pg mL^{-1} and 15 pg mL^{-1}) on the fiber surface. (G) The fluorescence signal along the fiber length with the spatial resolution 200 µm and 450 µm, respectively. The data point at zero length on this figure indicates the total signal integrated from 0 to 200 µm or 450 µm along the fiber.

Cannula were treated with 85% orthophosphoric acid to etch any laser affected metal oxides and to passivate the stainless steel. They were then thoroughly rinsed and ultrasonic cleaned before implantation.

Stereotactic surgeries were carried out under isoflurane (5% induction, 2% maintenance in 2.5 L/min O_2; Piramal Critical Care) anesthesia. Rats were implanted with a single perforated cannula targeted to the dorsal hippocampus (A/P: -3.5; M/L: 2.0; D/V: −3.0 mm from skull surface) and secured to the skull with stainless steel screws and dental cement. A dummy cannula was inserted into the cannula and held in place with a fitted dust cap (Plastics One). Following surgery, subjects were placed on a heating pad and kept in a recovery box until ambulatory before returning to the colony. Rats were given four weeks to recover from surgery before experimentation.

2.7. In vivo detection of hippocampal extracellular IL-1β protein

IL-1β sensing fibers were inserted into the guide cannula for baseline sample collection prior to LPS or Vehicle treatment. Two baseline samples were collected at 20 min intervals and following another 20 min interval subjects were challenged with either 100 µg kg^{-1} LPS (i.p., dissolved in pyrogen-free, sterile 0.9% saline; Sigma) or Vehicle. Two more 20-min samples were collected 1 and 4 h post challenge. Fiber insertion and measurements were taken serially, one fiber per time point per subject. Subjects were freely-moving in their home cage following LPS or Vehicle administration and during cytokine detection. Body weight was collected prior to experimentation and 24 h following LPS or Vehicle administration.

2.8. Statistics

All data are expressed as mean ± SEM. Statistical analyses consisted of two-tailed unpaired t tests. Threshold for statistical significance was set at $\alpha = 0.05$.

3. Results

3.1. Characterization of the IL-1β sensing interface

A schematic for the design of the IL-1β immunosensing fiber is shown in Fig. 1A. The IL-1β capture device was produced on a decladded optical fiber surface that was modified with self-assembling AuNPs linked to the IL-1β capture antibody. SEM was used to investigate the ultrastructure features of the IL-1β sensing interface before and after coating with AuNPs (Fig. 1B, C). Prior to modification with AuNPs, the optical fiber showed a relative plain surface with some impurities. After attachment of AuNPs to the fiber surface, the impurities were covered by a layer of AuNPs resulting a homogeneous surface with big surface area, which is favorable for the attachment of the maximum amount of capture antibody.

Following modification of the optical fiber surface with anti-IL-1β capture antibodies, the time window for IL-1β binding equilibrium to be reached with the fiber was investigated and the equilibrium time was in the range of 15–30 min (Fig. S1). Subsequently, the fiber with anti-IL-1β capture antibodies was incubated in 10 different concentrations of IL-1β in PBS containing 10% fetal bovine serum over the equilibrium time, then stained with SPIO-IL-1β Ab conjugates to form the sandwich immunocomplex. Fluorescence signal intensity of each fiber was imaged by the z-stack method under the confocal microscope (Fig. 1D). Quantification of confocal images revealed that the fiber fluorescence intensity increased with the concentration of IL-1β. A linear relationship between fluorescence intensity and log concentration of IL-1β was obtained in the range of 3.9 pg mL^{-1} to 500 pg mL^{-1} with the correlation coefficient of 0.996, as plotted in the Fig. 1E. The limit of detection (at signal to noise ratio of 3.0) could be up to 1.2 pg mL^{-1}, which is lower than the clinical concentration of IL-1β (around 4 pg mL^{-1}) (Biancotto et al., 2013) suggesting that the fiber based sensing interface could be used as a sensitive immunosensor for *in vitro* IL-1β detection.

Additionally, the IL-1β immunosensing fiber demonstrated spatial selectivity and concentration-dependent response following local administration of IL-1β. To establish this, a volume of 1 µL of two different

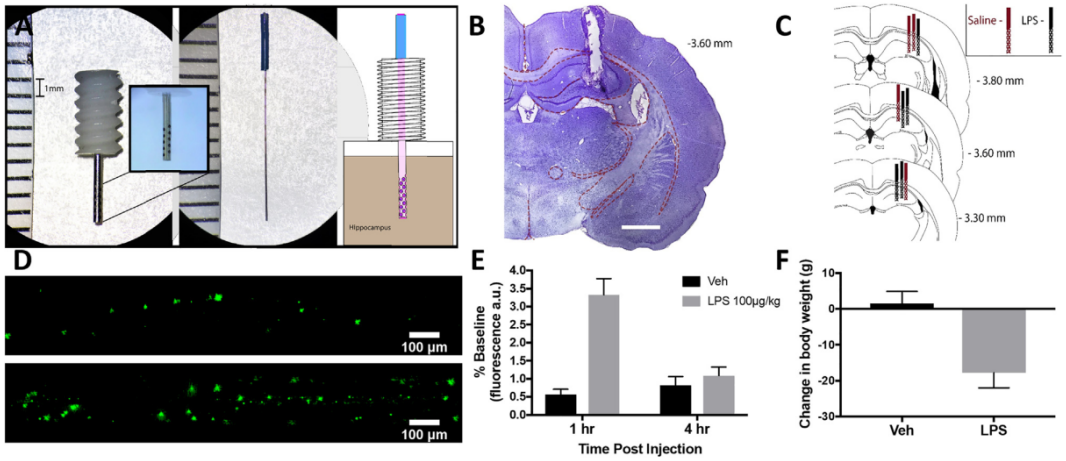

Fig. 2. *In vivo* detection of hippocampal IL-1β release following peripheral lipopolysaccharide (LPS) administration. (A) Design of the IL-1β sensing fiber with perforated stainless steel guide cannula. (B) Representative photomicrographs illustrating placement of cannula in the dorsal hippocampus. (C) Schematic representation of perforated guide cannula placements for all subjects in dorsal hippocampus. Numerals indicate in mm distance from bregma. (D) Confocal z-stack maximum intensity projection images of optical fibers taken before (top) and 1 hr after LPS administration (bottom). (E) Mean (± SEM) fluorescent signal expressed as the percentage of baseline of optical fibers following LPS or Vehicle treatment (n = 4–5 subjects/group; 1 fiber/subject at each time point). Mean baseline was determined by averaging fluorescence arbitrary units (a.u.) from two separate samples prior to injection. Percent baseline was calculated by dividing the fluorescent signal at a particular time post injection (1 h or 4 h) with the mean baseline. (F) Mean (± SEM) 24-h change in body weight following LPS or Vehicle administration.

concentrations of IL-1β (15 and 400 pg mL^{-1}) was pipetted onto two spatially separated locations of the sensing surface. Following staining with the SPIO-IL-1β antibody conjugate, z-stack confocal images were taken of the two different spotting areas on the fiber surface. Green fluorescent dots could be observed in both areas, with significantly greater fluorescent intensity in the area of 400 pg mL^{-1} (Fig. 1F). The fluorescence intensity of the 400 pg mL^{-1} area was approximately 3 times greater than that of 15 pg mL^{-1} area ($p < 0.05$, Fig. 1G) demonstrating that the immunosensing fiber has the capacity to spatially discriminate between different concentrations of IL-1β.

To evaluate specificity of antibody-antigen interactions, the immunosensing fiber was incubated with several potentially interfering compounds including IL-6, TNF-α, IFN-γ under the same conditions. The IL-1β 200 pg mL^{-1} standard was mixed with these potentially interfering substances (one at a time, at concentration 1000 pg mL^{-1}). There was no significant fluorescence change in the presence of the interfering substances ($p > 0.05$). The variation of the fluorescence intensity caused by the additional interfering cytokines was < 5% of the IL-1β 200 pg mL^{-1} standard alone, indicating high specificity of the immunosensor. For evaluation of the reproducibility of the fiber sensor, 20 fiber samples from 4 separate batches (5 fibers per batch) were applied for the detection of 25 pg mL^{-1} IL-1β in PBS containing 10% fetal bovine serum. The coefficient of variation of intra-assay can be calculated to 7.3% (in batch difference) and 12.5% (batch-to-batch difference), suggesting an acceptable precision and reproducibility of the measurements made using the fiber sensor.

3.2. *In vivo* application of the fabricated fiber sensor

It is well established that a peripheral immune challenge induces an increase in pro-inflammatory cytokine mRNA and protein in the hippocampus, when quantified using gross tissue samples. It is also clear that the hippocampus plays a critical role in mediating the impact of inflammation on cognitive function. However, the release of cytokines and the repeated sampling within a single animal has not been established. Therefore, we tested whether the IL-1β immunosensing device would capture intra-hippocampal IL-1β release following peripheral administration of LPS, a component of the outer membrane of gram-negative bacteria. Rats were implanted in the dorsal hippocampus with a stainless-steel cannula perforated with small windows drilled along its length to enable fluid exchange between the outside and inside of the cannula. A schematic of the design along with cannula placement within the dorsal hippocampus is shown in Fig. 2.

Prior work has demonstrated that intracranial cannula implantation can activate local glia such that a subsequent neuroinflammatory stimulus produces a potentiated pro-inflammatory response. However, the priming of brain glia by cannula implantation has been shown to dissipate by four weeks (Holguin et al., 2007). Therefore, experimentation was initiated four weeks after implantation. Two baseline samples (20 min each) were taken by inserting the IL-1β immunosensing device into the perforated cannula. Animals then received 100 µg/kg LPS (i.p.) or equal volume of 0.9% endotoxin-free saline. Two additional fiber samples (20 min each) were collected 1 and 4 h post injection. Subsequent immunoprocessing of the IL-1β sensing fibers revealed that LPS compared to saline treatment led to increased fluorescent intensity 1 h post injection, returning to baseline values by 4 h ($p < 0.01$, $n = 4–5$/group, Fig. 2E). Additionally, 24 h after injection body weights were significantly reduced in LPS but not saline-treated subjects ($p < 0.01$, Fig. 2F). Furthermore, if we assume a negligible effect of the hippocampal components, the approximate concentration based on the *in vitro* calibration (Fig. 1E) detection of IL-1β could be obtained and the values are shown in Fig. S2.

4. Conclusion

Studies of neuroinflammatory processes typically evaluate total cytokine levels within brain regions using either ELISA or immunohistochemical approaches, which precludes determination of cytokine release into the interstitial space in discrete brain regions. In addition, these approaches are limited to a single measurement in time, thus requiring a between subjects design to capture cytokine changes across time after an immune challenge. The present study characterizes an innovative approach, which addresses both of these methodological limitations inherent to ELISA and immunohistochemical approaches.

As with other invasive methods, the issue of compromising the blood-brain barrier due to cannula implantation makes it difficult to discern immune signals derived from brain-resident immune cells and those generated by peripheral immune cells. In the present manuscript we mitigate this issue by waiting 4 weeks post cannulation until LPS administration and compared to other sampling methods, we used a cannula with an inner diameter that is far smaller than that of a typical microdialysis probe. Both features should minimize the contribution of LPS-induced blood borne IL-1β to the overall detection. Moreover, the present approach shows CNS specificity of the signal that is not influenced by blood borne factors as peripheral blood IL-1β level will be still rising at 4 h time points after challenge with a similar LPS dose (Cusumano et al., 1997).

Here, an IL-1β immunosensor based on the sandwich immunocomplex performed on an optical fiber surface enables the selective and sensitive *in vitro* determination of IL-1β. The modified fiber was found to have a limit of detection of $1.2\,\mathrm{pg\,mL^{-1}}$ and it showed the ability to localize detection of IL-1β *in vitro* (Fig. 1). In addition, the optical fiber sensor with implanted perforated cannula demonstrated good performance in the *in vivo* determination of IL-1β in rat dorsal hippocampus following systemic administration of LPS (Fig. 2). Critically, in this experiment repeated sampling was achieved by replacing the fiber at an experimenter-defined time interval in which we demonstrate that the hippocampal IL-1β response was significantly elevated at 1 h but not 4 h following LPS administration. Prior work has shown that LPS-stimulated hippocampal IL-1β levels persist beyond 1 h (e.g., Nguyen et al., 1998), but these studies exclusively focus on total IL-1β protein, which includes both intracellular *and* extracellular levels. Future studies should examine the relationship between IL-1β total production and the relative fraction that is released. Given the role of neuroimmune communication in the etiology of numerous psychiatric disorders (Jones and Thomsen, 2013), this technology provides a novel strategy for monitoring the release of cytokine proteins from innate immune cells in discrete neural circuits, and it has the potential to elucidate pathological dynamics underlying neuropsychiatric disease.

Author disclosure statement

The authors declare no conflicts of interest.

Acknowledgments

The authors would also like to thank Dr. James Orth, the University of Colorado Boulder Light Microscopy Core Facility, and the OptoFab Node of the Australian National Fabrication Facility for their support. This work was supported by the ARC Centre of Excellence for Nanoscale Biophotonics (Grant CE140100003), ARC Future Fellowship, Macquarie University Research Development Grant, National Natural Science Foundation of China (Grant 21575045), iMQRES scholarship (KZ), and the American Australian Association Fellowship (MVB).

Appendix A. Supplementary data

Supplementary data associated with this article can be found, in the online version, at https://doi.org/10.1016/j.bbi.2018.04.011.

References

Ao, X., Stenken, J.A., 2006. Microdialysis sampling of cytokines. Methods 38, 331–341.
Biancotto, A., Wank, A., Perl, S., Cook, W., Olnes, M.J., Dagur, P.K., Fuchs, J.C., Langweiler, M., Wang, E., McCoy, J.P., 2013. Baseline levels and temporal stability of 27 multiplexed serum cytokine concentrations in healthy subjects. PLoS ONE 8, e76091.
Chefer, V.I., Thompson, A.C., Zapata, A., Shippenberg, T.S., 2009. Overview of brain microdialysis. Curr. Protoc. Neurosci. Chap. 7 (Unit7), 1.
Cusumano, V., Mancuso, G., Genovese, F., Cuzzola, M., Carbone, M., Cook, J.A., Cochran, J.B., Teti, G., 1997. Neonatal hypersusceptibility to endotoxin correlates with increased tumor necrosis factor production in mice. J. Infect. Dis. 176, 168–176.
Dinarello, C.A., 2011. A clinical perspective of IL-1beta as the gatekeeper of inflammation. Eur. J. Immunol. 41, 1203–1217.
Frank, M.G., Baratta, M.V., Sprunger, D.B., Watkins, L.R., Maier, S.F., 2007. Microglia serve as a neuroimmune substrate for stress-induced potentiation of CNS pro-inflammatory cytokine responses. Brain Behav. Immun. 21, 47–59.
Holguin, A., Frank, M.G., Biedenkapp, J.C., Nelson, K., Lippert, D., Watkins, L.R., Rudy, J.W., Maier, S.F., 2007. Characterization of the temporo-spatial effects of chronic bilateral intrahippocampal cannulae on interleukin-1beta. J. Neurosci. Methods 161, 265–272.
Jones, K.A., Thomsen, C., 2013. The role of the innate immune system in psychiatric disorders. Mol. Cell. Neurosci. 53, 52–62.
Kreutzberg, G.W., 1996. Microglia: a sensor for pathological events in the CNS. Trends Neurosci. 19, 312–318.
Larson, S.J., 2002. Behavioral and motivational effects of immune-system activation. J. Gen. Psychol. 129, 401–414.
Liu, G., Qi, M., Hutchinson, M.R., Yang, G., Goldys, E.M., 2016. Recent advances in cytokine detection by immunosensing. Biosens. Bioelectron. 79, 810–821.
Liu, G., Zhang, K., Nadort, A., Hutchinson, M.R., Goldys, E.M., 2017. Sensitive cytokine assay based on optical fiber allowing localized and spatially resolved detection of interleukin-6. ACS Sens 2, 218–226.
Maier, S.F., 2003. Bi-directional immune-brain communication: Implications for understanding stress, pain, and cognition. Brain Behav. Immun. 17, 69–85.
Nguyen, K.T., Deak, T., Owens, S.M., Kohno, T., Fleshner, M., Watkins, L.R., Maier, S.F., 1998. Exposure to acute stress induces brain interleukin-1beta protein in the rat. J. Neurosci. 18, 2239–2246.
Qi, M., Huang, J., Wei, H., Cao, C., Feng, S., Guo, Q., Goldys, E.M., Li, R., Liu, G., 2017. graphene oxide thin film with dual function integrated into a nanosandwich device for in vivo monitoring of interleukin-6. ACS Appl. Mater. Interfaces 9, 41659–41668.
Rohan Walker, F., Yirmiya, R., 2016. Microglia, physiology and behavior: a brief commentary. Brain Behav. Immun. 55, 1–5.
Schenk, T., Irth, H., Marko-Varga, G., Edholm, L.E., Tjaden, U.R., van der Greef, J., 2001. Potential of on-line micro-LC immunochemical detection in the bioanalysis of cytokines. J. Pharm. Biomed. Anal. 26, 975–985.
Watkins, L.R., Maier, S.F., Goehler, L.E., 1995. Immune activation: the role of pro-inflammatory cytokines in inflammation, illness responses and pathological pain states. Pain 63, 289–302.

Supplementary material

Title: A novel platform for *in vivo* detection of cytokine release within discrete brain regions

Authors: Kaixin Zhang[a,1], Michael V. Baratta[b,1], Guozhen Liu[a,c,d*], Matthew G. Frank[b], Nathan R. Leslie[b], Linda R. Watkins[b], Steven F. Maier[b], Mark R. Hutchinson[e], and Ewa M. Goldys[a,c*]

Author Affiliations: [a]ARC Centre of Excellence in Nanoscale Biophotonics (CNBP), Macquarie University, Sydney, Australia; [b]Department of Psychology and Neuroscience, University of Colorado Boulder, Boulder, Colorado, USA; [c] Graduate School of Biomedical Engineering, The University of New South Wales, Sydney, Australia; [d]International Joint Research Center for Intelligent Biosensor Technology and Health, Central China Normal University, Wuhan, China; [e]ARC Centre of Excellence in Nanoscale Biophotonics (CNBP), The University of Adelaide, Adelaide, Australia

[1]These authors contributed equally to this work.

Email addresses: kaixin.zhang@hdr.mq.edu.au (KZ); michael.baratta@colorado.edu (MVB); guozhen.liu@unsw.edu.au (GL); matt.frank@colorado.edu (MGF); Nathan.Leslie@colorado.edu (NRL); Linda.Watkins@colorado.edu (LRW); Steve.Maier@colorado.edu (SFM); mark.hutchinson@adelaide.edu.au (MRH); e.goldys@unsw.edu.au (EMG)

***Corresponding Authors:** Guozhen Liu, Ewa M. Goldys; Graduate School of Biomedical Engineering, The University of New South Wales, Sydney, Australia **email:** guozhen.liu@unsw.edu.au; e.goldys@unsw.edu.au

Optimization of the time for IL-1β binding equilibrium with the fiber sensing surface

The time window for IL-1β binding equilibrium to be reached with the fiber was investigated by using the functionalized fiber in the detection of a certain concentration of IL-1β solution (10 pg mL^{-1}) with different incubation time *in vitro*. The results are shown below in Figure S1. As the time varied from 0 to 60 min, the fluorescence intensity increased and reached the maximum at 30 min, indicating that the time window needed to reach a reproducible binding equilibrium with the fiber should be in the range of 15-30 min. In addition, to further validate the reproducible binding equilibrium time window, we used 6 separate sensing fibers to detect the certain concentration of IL-1β solution (10 pg mL^{-1}) with a 30 min incubation time, the relative standard deviation of the detection result was 6.3% indicating the reproducible binding equilibrium time window for the fiber sensing surface.

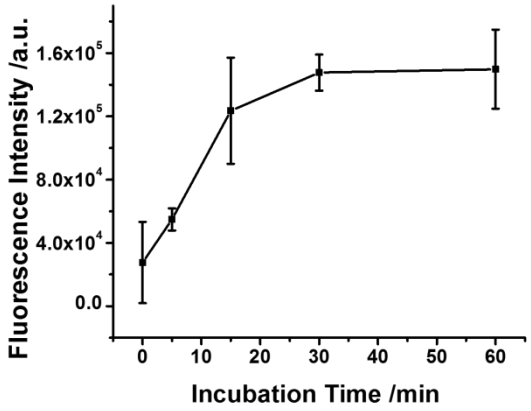

Figure S1. Optimization of the time window for IL-1β binding equilibrium with the fiber sensing surface. Error bars indicate standard error of the mean of three replicates for each incubation time point.

Calculation of the concentration of IL-1β in dorsal hippocampus.

If we assume a negligible effect of the hippocampal components, the approximate concentration based on the *in vitro* calibration (see Figure 1E) detection of IL-1β could be obtained. Using this approach, the baseline level of the IL-1β was calculated to 5.0 ± 2.1 pg mL^{-1}, and the values following LPS or Vehicle treatment are shown below in Figure S2.

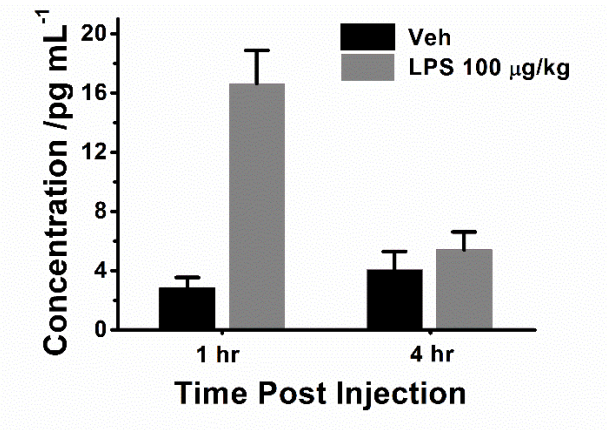

Figure S2. Mean (± SEM) concentrations of IL-1β following LPS or Vehicle treatment.

3.3 Appendix

Perforation of the stainless-steel guide cannula.

Stainless-steel guide cannulas were drilled by a laser system. The laser machining facility used for drilling the cannulas consists of a 266 nm Q-switched laser source and 4-axis motion control (XYZ and U (lathe) axes). The laser source is based on a Lightwave Electronics Q-201, producing 532 nm pulses of 15 ns duration and up to 2 mJ pulse energy. To produce a finer laser spot and allow better management of thermal processes while laser drilling, the laser is externally frequency doubled with a single pass in a BBO crystal yielding a few percent efficient conversion to 266 nm. This is then separated from the 532 nm with a Pellin Brocca prism, and a mechanical shutter is used to control the laser onto the work area. The beam is brought to focus on the work piece through a 3x Micro-Spot UV objective available from Thorlabs (LMU-3x-266). The stages and motion control are Aerotech ATS-100 stages (200mm travel) with a U500 controller for XYZ and an ART310 rotation axis used a lathe axis to rotate/index the cannulas. An imaging system behind the final turning mirror before the objective lens, allows for in-situ (top-down) viewing of the laser drilling, and precise setting of the focal height using the Z-axis stage. The cannulas were held in a small chuck on the face of the U-axis (lathe) (Figure. 3-1), and drilled with 100 mW average power at a 500 Hz repetition frequency, thus approximately 200 μJ pulse energy and estimated fluence (by pulse) of 250 J cm^{-2}. The holes were drilled through the cannula by slow trepanning using the XY stages (25 mm/min federate and 25 passes require to cleanly drill through), the cannula could then be indexed and translated through 90 degrees using the U-axis to further drilling through the orthogonal direction. The cannulas were post-processed by several hours soaking in 85% orthophosphoric acid to etch any laser affected metal oxides and passivate the steel. They were then thoroughly rinsed and ultrasonic cleaned.

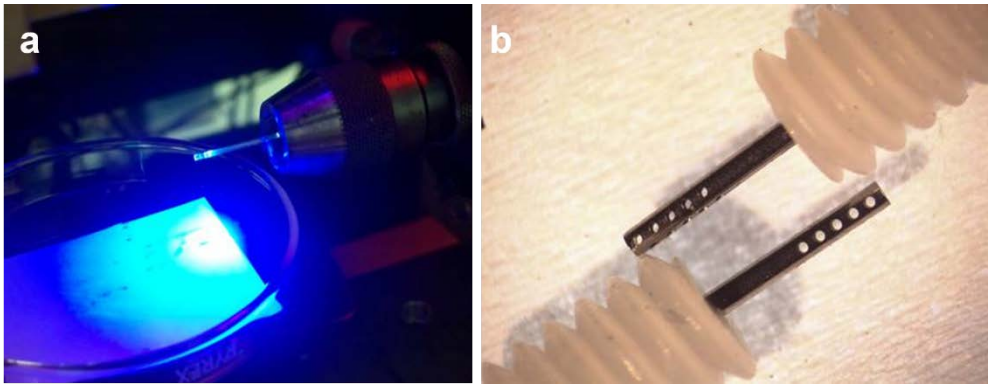

Figure 3-1 (a) Lathe-type arrangement used for laser drilling cannulas held in a small chuck, 266 nm laser beam incident from above. (b) Laser drilled stainless-steel guide cannulas after post-processing.

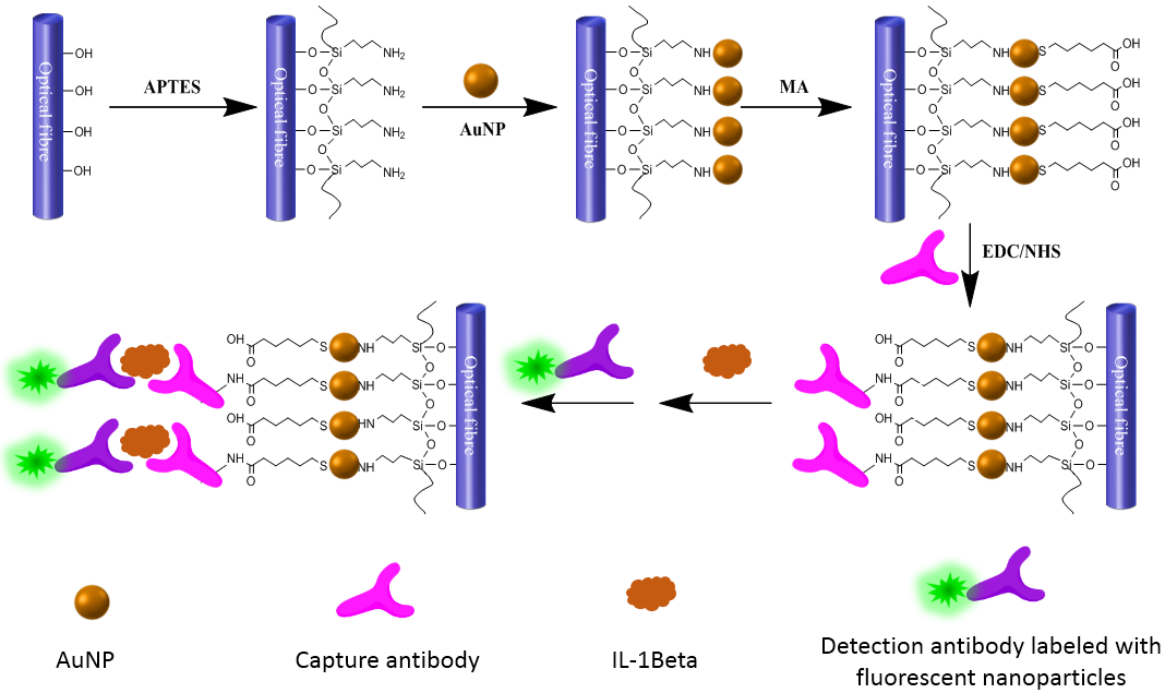

Scheme 3-1 the procedure of the fabrication of the fiber sensor

Characterization of the fabrication of fiber sensing interface

The successful attachment of the AuNP on the fiber surface could also be confirmed by the UV-Vis spectra (Figure 3-2a). It was observed that the AuNP colloid showed a characteristic plasmon peak at 522 nm. The absorbance was absent from the UV-Vis spectrum of the APTES coated fiber. While after the APTES functionalized fiber reacting with the AuNP, a broadened and redshifted peak appeared at 650 nm. The appearance of the broaden peak could be attributed to the fact that AuNP can self-assembled on the APTES functionalized fiber surface and the tightly attached AuNP aggregate together resulting in the longitudinal plasmon resonance. The attachment of the capture antibody was characterized by the fluorescent secondary antibody. The fiber before/after binding with the capture antibody was stained by Donkey Anti-Goat IgG NorthernLights™ NL493-conjugated Antibody (NL003). Fluorescent visitation images of the fiber had displayed that there was only minimal fluorescence signal observed before the fiber binding with the capture antibody (Figure 3-2b). The observed fluorescence signal could be attributed to the nonspecific absorption of the fiber surface. A high fluorescent signal appeared when the fiber incubated with the capture antibody (Figure 3-2c) followed staining by NL003, which suggested that the capture antibody had been successfully attached on the fiber surface through EDC/NHS coupling and thus the sensing interface had formed.

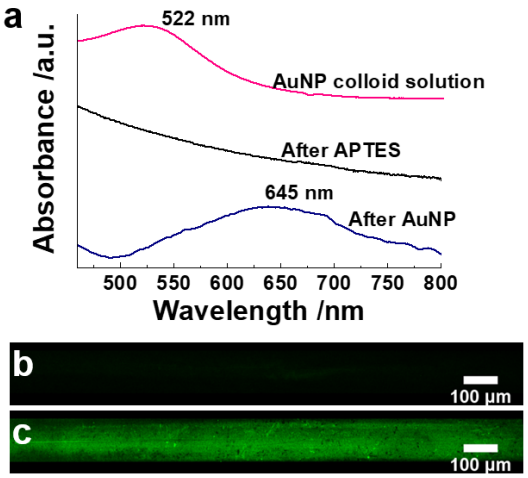

Figure 3-2 (a) UV-vis absorption spectra of AuNP colloid solution and the fiber after being stepwise treated by APTES and AuNP; Fluorescent visulation of the fiber before(c)/after(d) reacting with the capture antibody followed being stained by the fluorescent secondary antibody (Donkey Anti-Goat IgG NorthernLights™ NL493-conjugated Antibody (NL003))

Optimization of the sensing interface

To maximize the density of the capture antibody on the fiber surface, the concentration of the capture antibody was optimized through quantifying the fluorescence intensity of the fluorescent secondary antibody (Donkey Anti-Goat IgG NorthernLights™ NL493-conjugated Antibody (NL003)). Figure 3-3a displayed the fluorescence intensity increased with the increasing of the concentration of the capture antibody. The signal plateaued around 50 μg mL^{-1}, and slightly fluctuated when the concentration of the capture antibody further increased, which indicated that the surface of the fiber reached the saturation of the capture antibody at the concentration of 50 μg mL^{-1}. Thus 50 μg mL^{-1} was deemed as the optimal concentration when the capture antibody was modified on the fiber surface. Furthermore, the density of the capture antibody was calculated. 1 μL different concentration of standard fluorescent secondary antibody was transferred on the confocal microscope dish, and the fluorescence intensity was collected and quantified. Suppose the mole ratio of combination between the capture antibody and fluorescent secondary antibody was 1:1, the density of the capture antibody on the fiber surface could be calculated to 0.28 μg mL^{-1}.

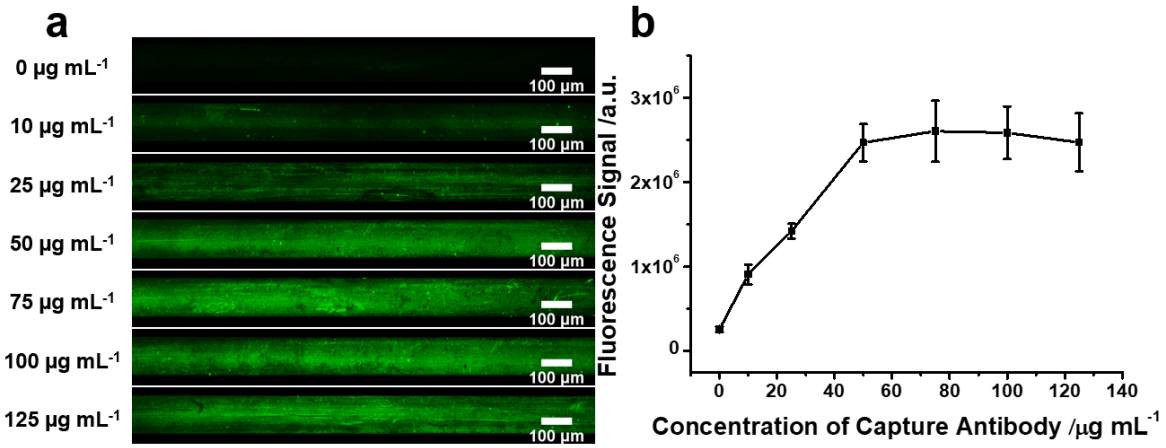

Figure 3-3 (a) Fluorescent visulization of the fiber after(d) reacting with various concentrations of the capture antibody followed being stained by the fluorescent secondary antibody (Donkey Anti-Goat IgG NorthernLights™ NL493-conjugated Antibody (NL003); (b) The corresponding fluorescence signal in Figure (a).

In addition, the stability of the sensing interface was also studied (Figure 3-4). Fiber was stored in PBS and then stained by the fluorescent secondary antibody. Fluorescence signal of the fiber was measured by confocal microscope every three days. It was found that the fluorescence signal decreased with the storage time increasing and the fluorescence intensity could keep over 90% of the freshly prepared fiber sensing surface within the control limits for 9 days.

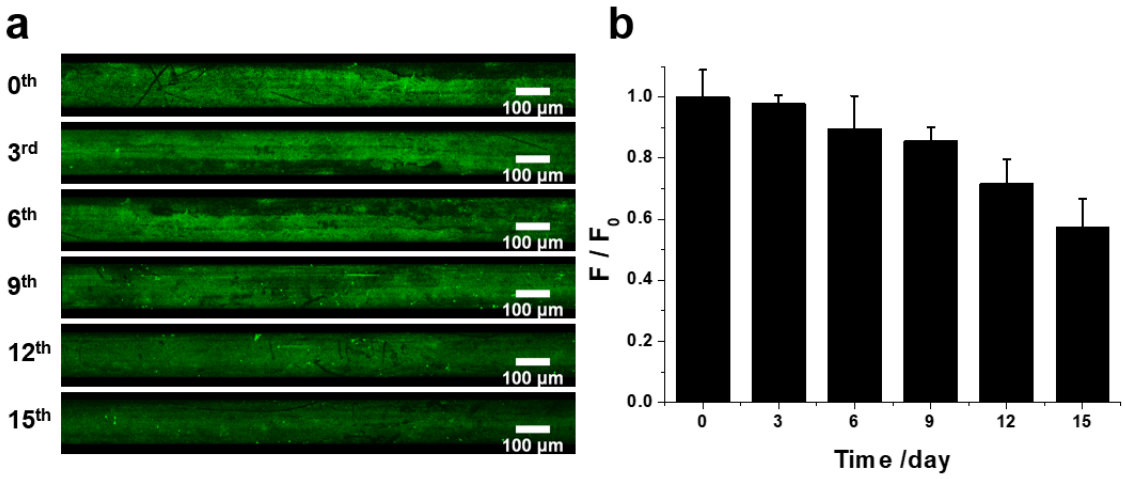

Figure 3-4 (a) Fluorescent of the fiber surface with capture antibody in PBS with various storage times followed being stained by the fluorescent secondary antibody (Donkey Anti-Goat IgG NorthernLights™ NL493-conjugated Antibody (NL003). (b) Stability of the capture antibody modified sensing interface monitored by using F/F_0. F_0 and F are the fluorescence signals from the secondary antibody for the freshly prepared fiber and the same fiber after being stored in PBS for different periods of time.

To reduce the non-specific adsorption of the fiber sensing interface, the blocking reagent BSA was used to block the fiber. The comparison of the performance between the blocked and not blocked fiber was shown in Figure 3-5. When the fibers were focused on the middle under the confocal microscope, some green fluorescent dots appeared on both sides of the not blocked fiber indicating the nonspecific adsorption of the sensing surface. While after being blocked by BSA, less green fluorescent dots were observed, suggesting that the defects on the sensing surface could be covered by BSA molecules resulting in the elimination of non-specific protein adsorption. Moreover, to have a whole view of the fiber surface, Z-stack images of the fiber were collected and quantified by Image J and MATLAB software. A more obvious discrimination could be observed between the fiber being treated

before and after BSA blocking. The non-specific fluorescence intensity decreased from 8.6 $\times 10^4$ a.u. to 1.1 $\times$ 10^4 a.u. indicating the efficiency of BSA in the elimination of protein adsorption.

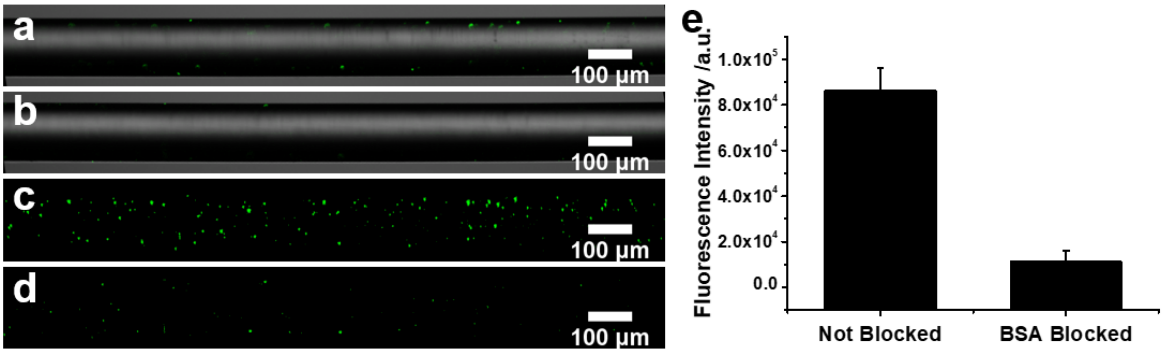

Figure 3-5 (a,b) The confocal microscope images of the fiber sensing surface before (a)/after (b) being treated by BSA followed incubating with SPIO-IL-1beta conjugates; (c, d) Z-stack images of the fiber without(c)/with(d) BSA blocking; (e) fluorescence intensity of (c) and (d).

3.4 Summary

An IL-1β immunosensor based on the sandwich immunocomplex performed on an optical fiber surface enables the selective and sensitive in vitro determination of IL-1β with a limit of detection at 1.2 pg mL^{-1}. In addition, the optical fiber sensor with implanted perforated cannula demonstrated good performance in the *in vivo* determination of IL-1β in rat dorsal hippocampus following systemic administration of LPS. Critically, in this experiment repeated sampling was achieved by replacing the fiber at an experimenter-defined time interval in which we demonstrate that the hippocampal IL-1β response was significantly elevated at 1 h but not 4 h following LPS administration. Prior work has shown that LPS-stimulated hippocampal IL-1β levels persist beyond 1 h but these studies exclusively focus on total IL-1β protein, which includes both intracellular and extracellular levels. Future studies should examine the relationship between IL-1β total production and the relative fraction that is released. Given the role of neuroimmune communication in the etiology of numerous psychiatric disorders, this technology provides a novel strategy for monitoring the release of cytokine proteins from innate immune cells in discrete neural circuits, and it has the potential to elucidate pathological dynamics underlying neuropsychiatric disease.

4

Detection of Interleukin-6 on Biotin-Avidin System Modified Glass Fiber

4.1 Introduction

In chapter 1 and 2, we have demonstrated a cytokine detection immunosensor based on APTES-AuNP-MA modified silica optical fiber for the monitoring of locally variable cytokine concentrations using a sandwich immunoassay scheme. However, the stability of the sensing surface can only be stable for around 9 days in PBS which might be due to limited stability of N−Au or S-Au bonds between APTES/alkanethiols and AuNPs resulting in a progressive release of the capture antibodies from the glass surface. (The low stability (around 9 days) of the fiber sensing surface prepared by APTES-AuNP-MA method in chapter 1 and 2 is not due to the denaturation of the antibody, as we stored the antibody coated fiber in PBS at 4 °C, the contained BSA (0.5%) in PBS can keep the antibody stabilized for above 1 months (MATER METHODS 2012;2:120)). And also, there is room for improvement in the sensitivity of the immunosensor by promoting the performance of the sensing surface. Therefore, to achieve a more robust cytokine immunosensor, we introduced another antibody immobilization method to fabricate the cytokine immunosensor.

In this chapter, biotin-avidin coupling strategy was used to attach the capture antibody which helps to enhance the robustness and binding sites of the sensing interface and the subsequent sensitivity. We demonstrated the localised and spatially resolved detection of IL-6 secreted in serum. The stability of the sensing surface can up to around 4 weeks. And nanoparticle labelling developed here provided a combination of low limit of detection (0.1 pg mL^{-1}) and low the sample volume requirement of 1 µL. This device also has potential to be used as a cytokine test strip for localised detection of cytokines *in vivo*.

Zhang, K., Liu, G. and Goldys, E.M., 2018. Robust immunosensing system based on biotin-streptavidin coupling for spatially localized femtogram mL^{-1} level detection of interleukin-6. Biosensors and Bioelectronics, 102, pp.80-86.

Summary of the author contributions to paper 3 following the order of author.

Paper 3	K. Z	G. L	E. G
Experiment Design	•		
Sample Preparation	•		
Data Collection	•		
Analysis	•		
Figures	•		
Manuscript	•	•	•

4.2 Full paper

Biosensors and Bioelectronics 102 (2018) 80–86

Contents lists available at ScienceDirect

Biosensors and Bioelectronics

journal homepage: www.elsevier.com/locate/bios

Robust immunosensing system based on biotin-streptavidin coupling for spatially localized femtogram mL^{-1} level detection of interleukin-6

Kaixin Zhang[a], Guozhen Liu[a,b,*], Ewa M. Goldys[a,**]

[a] ARC Centre of Excellence for Nanoscale Biophotonics (CNBP), Macquarie University, North Ryde 2109, Australia
[b] Key Laboratory of Pesticide and Chemical Biology of Ministry of Education, College of Chemistry, Central China Normal University, Wuhan 430079, PR China

ARTICLE INFO

Keywords:
Optical fibre
Cytokine assay
Biotin-streptavidin
Interleukin-6
Immunosensor

ABSTRACT

Detection of a very low amount of cytokines such as interleukin-6 (IL-6) in clinical fluids is important in biomedical research and clinical applications. Here, we demonstrate spatially-localized ultrasensitive (femtogram mL^{-1}) level detection of IL-6 in serum and in cell culture media. Our approach is based on a sandwich immunosensor fabricated on the surface of an optical fibre. Firstly, the biotinylated IL-6 capture antibody was immobilized on the fibre surface by biotin-streptavidin coupling. Then the fabricated fibre was used for capturing IL-6 followed by exposure to detection antibody which was labeled with the fluorescent magnetic nanoparticles to report the signal. A linear relationship between IL-6 concentration and the fluorescence signal was obtained in the range from 0.4 pg mL^{-1} to 400 pg mL^{-1} of IL-6, with the limit of detection down to 0.1 pg mL^{-1}. In addition, this optical fibre sensor was successfully applied for the localized detection of IL-6 with the spatial resolution of 200 μm and a sample volume of 1 μL. Finally, the performance of the fibre sensor was demonstrated by detection of IL-6 secreted by BV-2 cells with comparable performance of the conventional enzyme-linked immunosorbent assay (ELISA).

1. Introduction

Cytokines, are hormone like polypeptides with a wide variety of molecular weight ranges from approximately 6 to 70 kDa. They are secreted by many different cells of the immune system (neutrophils, macrophages, monocytes, T-cells, and B-cells) to regulate both local and systemic inflammatory responses (Aksu and Çıkım, 2016; Alvarado et al., 2016; Angiolilli et al., 2016; Buzza et al., 2017; Liu et al., 2016a). Interleukin-6 (IL-6), acting as a both pro-inflammatory and anti-inflammatory cytokine, plays a key role in the inflammatory response. Many diseases such as osteoarthrosis, asthma, psoriasis, cardiovascular disease, diabetes and inflammatory bowel disease are closely associated with IL-6, which can cause an increase in the IL-6 level in serum. The abnormal concentration of IL-6 is, in turn, closely associated with mortality (Hsu et al., 2016). Therefore, it is essential to develop and optimize new technologies for quantitative detection of IL-6 for research and clinical applications.

Immunoassay techniques based on highly specific molecular recognition of antigen epitops by antibodies are among the leading methods for detection of IL-6 including those using capillary electrophoresis (Phillips and Smith, 2003), electrochemical (Deng et al., 2011; Malhotra et al., 2010; Peng et al., 2011; Wang et al., 2014), and optical immunosensors (Kapoor and Wang, 2009; Wong et al., 2009). For example, Phillips *et al.* fabricated an antibody-based capillary electrophoresis system coupled with an on-line laser-induced fluorescence detector capable of measuring IL-6 in cell culture media cell numbers as low as 100 cells (Phillips and Smith, 2003) . Wang et al. developed an IL-6 electrochemical immunosensor, with a dynamic working range of 1–40 pg mL^{-1} with a low detection limit of 0.3 pg mL^{-1}(Wang et al., 2014). Kapoor et al. reported a biosensor capable of specific detection of IL-6 (0.12 ng mL^{-1}) in the presence of much higher concentration of a non-specific protein with a tapered fibre-optic biosensor dip-probe (Kapoor and Wang, 2009). Commercial enzyme-linked immunosorbent assay (ELISA) are also widely available for quantification of cytokines. They are characterized by the relatively long assay times (5 h) and relative large sample volumes (in the order of 100 μL). The sensitivity of current ELISA assays for detection of IL-6 is around 1 pg mL^{-1}(R & D IL-6 Quantikine ELISA Kit). However, it does not has the capability to detect spatially localized cytokines. Additionally, the problems of reducing the sample volume and increasing sensitivity and stability of the sensing system still remain unsolved.

The sensitivity of an immunosensor depends on the density of the

* Corresponding authors at: ARC Centre of Excellence for Nanoscale Biophotonics (CNBP), Macquarie University, North Ryde 2109, Australia.
** Corresponding author.
E-mail addresses: guozhen.liu@mq.edu.au (G. Liu), ewa.goldys@mq.edu.au (E.M. Goldys).

http://dx.doi.org/10.1016/j.bios.2017.11.023
Received 9 August 2017; Received in revised form 3 November 2017; Accepted 4 November 2017
Available online 06 November 2017
0956-5663/

binding sites of the capture surface and biological activity of the biomolecules anchored on the surface. The stability of the sensing interface relies on the binding affinity of the biomolecules on the sensing surface (Liang et al., 2008). Therefore, appropriate surface chemistry has a significant effect on the performance of the sensing surface. Immobilization of receptor biomolecules onto surfaces can be carried out using covalent and non-covalent methods (Prieto-Simon et al., 2008; Samanta and Sarkar, 2011). Stable immobilization formed by chemical activation of the inorganic surface can be achieved by covalently binding the receptors via chemical groups such as carboxyl (Herrwerth et al., 2003; Hosseini et al., 2014), aldehydes (Zang et al., 2016), maleimides (Song et al., 2009), or epoxides (Nguyen et al., 2015). However, the immobilization efficiency of the covalent method is not satisfactory. Even for the most common method by using N-hydroxysuccinimide (NHS) esters to form stable amide bonds between the antibody and amine groups functionalized substrate, only a modest immobilization yields (50–60%) can be achieved (Wong et al., 2009). On the other hand, physical non-covalent adsorption is widely used in immobilization biomolecules on surfaces due to its simplicity and cost-effectiveness. However, the formed sensing surfaces are often not stable, as the weakly bound receptors may be exchanged for molecules with a higher affinity (Ball et al., 1994; Cao, 2006; Oliveira et al., 2015). Therefore, it is desired to find a simple method to form a stable sensing surface with antibody in high density. The biotin-streptavidin system is characterized by a very strong non-covalent biological interaction with a dissociation constant of 10^{15} M (Green, 1975; Holmberg et al., 2005). This high affinity ensures high coupling efficiency between the biotin/biotin-derivatives and streptavidin. These biotin-streptavidin complexes, once immobilized, are not disturbed by extreme changes in pH, temperature, organic solvents and other denaturing agents (Schetters, 1999). Therefore, surface immobilized-streptavidin offers a suitable platform for building optimized immunosensors.

Herein we report a sensitive immunoassay on the optical fibre surface for accurate quantification of IL-6 in serum samples. The capture antibody was immobilized on the fibre surface via biotin-streptavidin coupling strategy. Biotin was directly attached to the fibre surface by reacting sulfo-NHS-biotin with the aminopropyltriethoxysilane (APTES) coated fibre. Then a streptavidin layer contains two biotin-binding sites facing the optical fibre and two terminated binding sites which are available to bind capture molecules, the biotinylated capture antibody. After capturing IL-6, the sensing interface was exposed to the detection antibody which was labeled with fluorescent magnetic nanoparticles. Because the dye in the fluorescent magnetic nanoparticles are incorporated throughout, the fluorescence output antibody/antigen bond is significantly greater than that obtained from fluorophore conjugates. We have compared the ability to immobilize the capture antibody on the fibre surface between the biotin-streptavidin system (BAS) and the method through covalent reaction with 6-mercaptohexanoic acid (MA) reported in our previous work (Liu et al., 2016b). The herein fabricated fibre immunosensor showed high sensitivity in detection of IL-6 at the fg mL^{-1} level. The analytical performance of the immunosensor was evaluated by detection of IL-6 in BV-2 cell culture medium and spatially localized detection capability with a sample volume as low as 1 μL.

2. Experimental section

2.1. Chemicals and materials

Recombinant mouse IL-6 protein, mouse IL-6 biotinylated antibody (capture antibody), mouse IL-6 antibody monoclonal rat IgG1 (detection antibody), mouse IL-6 quantikine ELISA Kit and donkey anti-goat IgG northernLights™ NL493-conjugated antibody (NL003) were obtained from R & D Systems. EZ-Link™ NHS-biotin was obtained from Thermo Fisher Scientific. (1-ethyl-3-(3-dimethylaminopropyl)carbodiimide hydrochloride (EDC), N-hydroxysuccinimide (NHS), concentrated sulfuric acid, hydrogen peroxide (30%), aminopropyltriethoxysilane (APTES), toluene, ethanol, 2-(N-morpholino)ethanesulfonic acid (MES), phosphate buffered saline, Tween 20, streptavidin, Fluorescein isothiocyanate (FITC)-avidin and bovine serum albumin (BSA) were purchased from Sigma-Aldrich. Carboxylated superparamagnetic iron oxide particles (SPIO, 1% solid, ~0.9 μm, labeled with P(S/6%DVB/V-COOH), excitation 480 nm, emission 520 nm) were purchased from Bangs Laboratories, Inc. Inc (Product NO : MC03F/11060), USA. MC03F/11060 is a polystyrene based superparamagnetic particle with iron-oxide enclosed within the particle (some iron-oxide may be partially exposed or on the particle surface) and surface acid groups (carboxyl). All these chemicals were used as received without further purification and Milli-Q water was used throughout the experiments. The phosphate buffer solution (PBS) used in this work contained 0.01 M phosphate buffer, 0.0027 M potassium chloride and 0.137 M sodium chloride, pH 7.4, at 25 °C. MES buffer contained 25 mM 2-(N-morpholino)ethanesulfonic acid, adjusted to pH 6.0 with NaOH solution. The optical fibre was a standard telecommunication silica fibre 62.5 μm diameter core /125 μm acrylate cladding (LNF(TM) product from Prysmian).

2.2. Preparation of SPIO-IL-6 detection antibody conjugates

A single 1.5 mL tube containing 50 μL carboxylated superparamagnetic iron oxide particles (SPIO) (10 mg mL^{-1}, 1%) were vortexed, and washed twice with 1 mL 25 mM pH 6.0 MES buffer, and then SPIO beads were collected with a magnetic separator. After removal of residual buffer, the magnetic beads were activated by adding 500 μL of the freshly prepared NHS solution (10 mg mL^{-1} in pH 6.0 MES buffer) and 500 μL freshly prepared EDC solution (10 mg mL^{-1} in pH 6.0 MES buffer). This mixture was vortexed and placed on a non-magnetic orbital shaker at 300 rpm for 30 min. The beads were then washed twice with 1 mL MES buffer with a magnetic separator to remove excess crosslinking reagents. To the tube 2 μg IL-6 detection antibody (diluted in 50 μL pH 6.0 MES buffer) were added to couple with the beads via the available amino groups with shaking at 300 rpm for 2 h. After that, these fluorescent beads antibody conjugates (SPIO-IL-6 Ab) were washed twice with MES buffer and twice with washing buffer (PBS, 0.05%Tween20), and finally dispersed in 0.5 mL PBS pH 7.2 at 4 °C for further use.

2.3. Fabrication of the fibre sensor

The fibre sensor was fabricated in a sequence of following steps. Firstly, the fibre coatings were removed by a piranha solution (H_2SO_4 95% and H_2O_2 30% mixed at a volume ratio of 7:3). The de-cladded optical fibre was treated with a piranha solution for 12 h to form hydroxyl groups on the surface. After washing by Milli-Q water and drying under N_2 stream, the cleaned fibre with –OH terminated surface, was immersed in aminopropyltriethoxysilane (APTES, 5% v/v) in toluene for 6 h to form an amine-terminated self-assembled monolayer. The unbound monomers were washed away from the fibre surface by toluene and ethanol, respectively. The amine group-modified optical fibre was subsequently incubated with freshly prepared sulfo-NHS-biotin solution for 30 min in PBS at room temperature. The presence of the biotin on the fibre surface was characterized by using FITC-avidin with the aid of the confocal microscope. After three times washing, biotin functionalized fibre was immersed in 50 μg mL^{-1} streptavidin solution for another 40 min incubation and finally washed three times with the washing buffer (PBS, 0.05% Tween20). To attach the capture antibody on the fibre surface, biotinylated capture antibody dispersed in PBS (16 μg mL^{-1}) was employed to interact with the streptavidin coated fibre for 1 h at room temperature. Next, the capture antibody modified fibre sensing surface was incubated with 0.5% BSA in PBS for 1 h at room temperature to eliminate nonspecific adsorption. For the measurement of IL-6, the optical fibre was incubated in the assay buffer

(PBS + 10%FBS) with a varying concentration of IL-6 for 1 h. Then the fibre was washed with washing buffer six times and PBS one time to remove unbounded IL-6 molecules. Finally, the optical fibre was exposed to SPIO-IL-6 Ab solution for 1 h following washed with washing buffer and PBS before imaging by confocal microscopy.

2.4. Quantification of the fluorescence signal

The fibre samples were imaged by a SP2 (Leica) confocal microscope with objective HC PL FLUOTAR, magnification 10×, NA 0.3, xy-resolution 651 nm, pinhole 1× Airy disc and field of view 1500 × 1500 μm^2. To record the fluorescence signal of the whole fibre surface, the Z-stack method was employed over the fibre (125 μm height). 10 Z-planes with around 12.5 μm separation height between planes were collected. Then the maximum pixel value of these 10 planes was calculated and assigned as the pixel value in the combined image (Z-project in ImageJ). For each concentration of IL-6, 1.5 mm fibre length in total was imaged for each cytokine measurement. The intensity of green dots representing the fluorescent P(S/6%DVB/V-COOH) labels was quantified by integrating over a spatial window of 450 μm using Image J and Matlab software. Thus, a spatial imagining resolution of 450 μm was obtained in this way.

3. Results and discussion

3.1. Optimization of the sensing interface

Sulfo-NHS-biotin reacted with the APTES coated fibre by forming amide bonds. The successful attachment of biotin on the fibre surface was characterized by FITC-avidin and the concentration of sulfo-NHS-biotin was optimized by quantifying the fluorescence intensity of FITC-avidin. As seen in Fig. 1a, nearly no fluorescence signal was observed on the APTES functionalized fibre after reacting with FITC-avidin. After the attachment of sulfo-NHS-biotin followed by FITC-avidin, the fluorescence signal appeared and it increased with the concentration of sulfo-NHS-biotin in the concentration range up to 0.0625 mg mL^{-1}(Fig. 1b). The increase of the fluorescence signal suggested that the sulfo-NHS-biotin has successfully reacted with the primary amino groups on the fibre surface to form a biotin terminated fibre surface. With further increase of the sulfo-NHS-biotin concentration, the value of fluorescence signal changed only slightly, suggesting that primary amino groups on the fibre surface have completely reacted with sulfo-NHS-biotin. Thus, 0.0625 mg mL^{-1} was used as the optimum concentration of sulfo-NHS-biotin.

In the next step, streptavidin was attached to the biotinylated fibre surface followed by the attachment of biotinylated anti IL-6 antibody. In order to maximize the amount of the capture antibody on the sensing interface, the concentration of capture antibody (biotinylated anti IL-6 antibody) attached on the optical fibre was optimized by quantifying the fluorescence intensity of NL493-conjugated secondary antibody (Fig. 1c). It was observed that the fluorescence intensity increased with the concentration of capture antibody, and it reached the maximum value at 16 μg mL^{-1} indicating the saturation of the capture antibody on the fibre surface. In addition, the stability of the sensing interface was investigated (Fig. 1d). The prepared fibres were stored at 4°Cin PBS and the fluorescence signal was measured every 7 days. The fluorescence intensity remained over 90% of the fresh prepared surface within the control limits for at least 35 days (no longer times were tested). These data confirm that the fibre sensing interface thus prepared is very stable, due to strong affinity interaction between the streptavidin and biotin/biotin derivatives (Diamandis and Christopoulos, 1991; Dundas et al., 2013).

To demonstrate the efficiency of the BAS method introduced here for the detection of IL-6, the ability of this surface to immobilize the

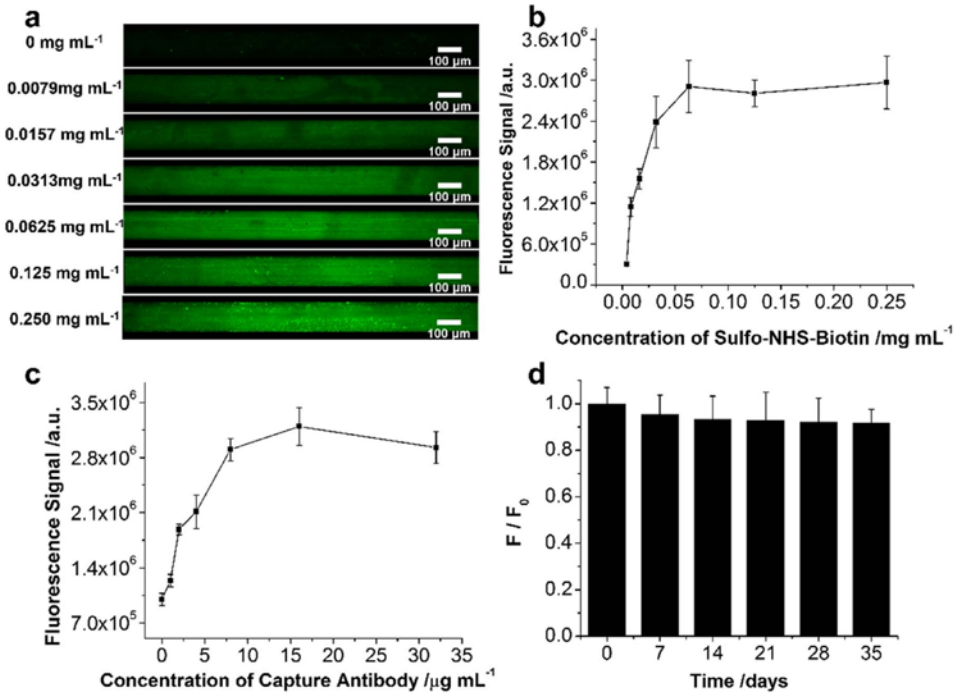

Fig. 1. (a) Fluorescence microscope images of the fibre incubated with different concentration of sulfo-NHS-biotin after being stained by FITC-avidin; (b) The corresponding fluorescence intensity of the fibre calculated from the images in (a); (c) Optimization of the concentration of capture antibody; (d) Stability of the capture antibody on the sensing interface.

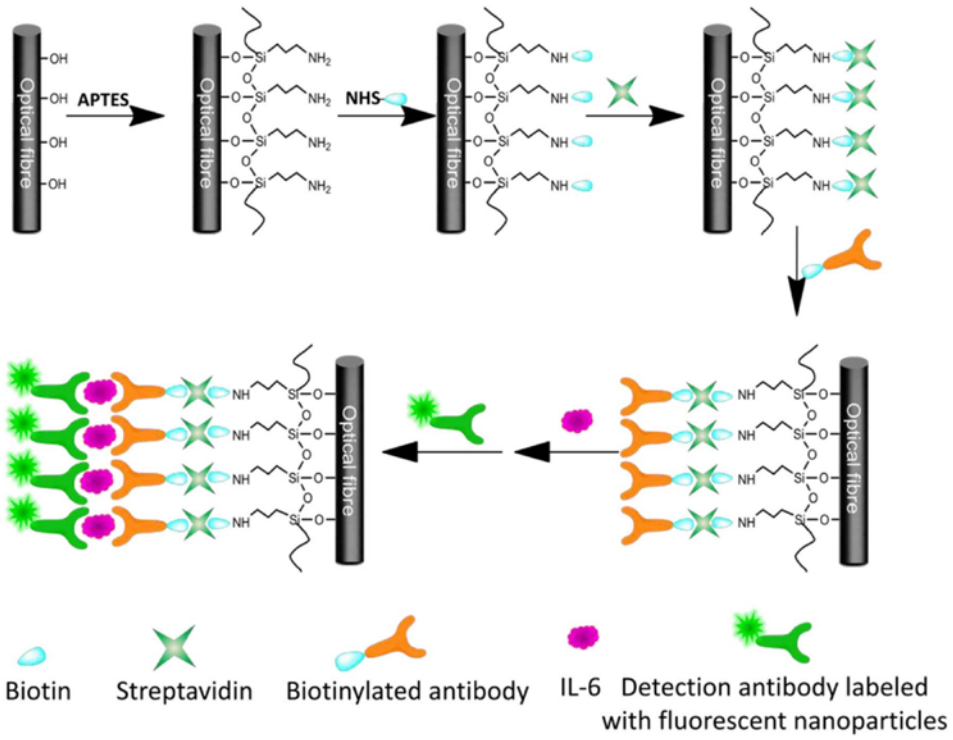

Scheme 1. The procedure of the preparation of the immunosensor based on the optical fibre for detection of the localized analyte IL-6.

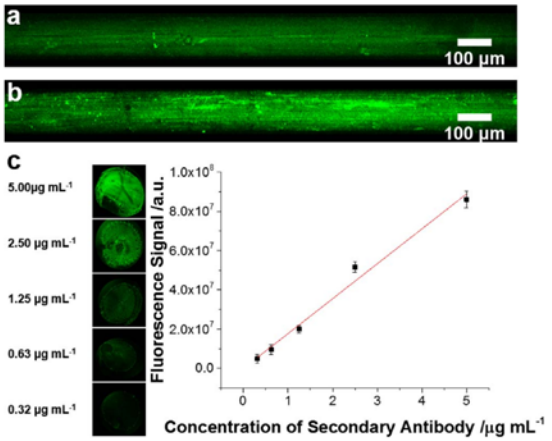

Fig. 2. (a, b) Fluorescence microscope images of the fibre prepared by 6-mercaptohexanoic acid (MA) (a) method and biotin-streptavidin system (BAS) (b) after stained by fluorescent secondary antibody; (c) the calibration curve of the fluorescence intensity versus the concentration of the secondary antibody.

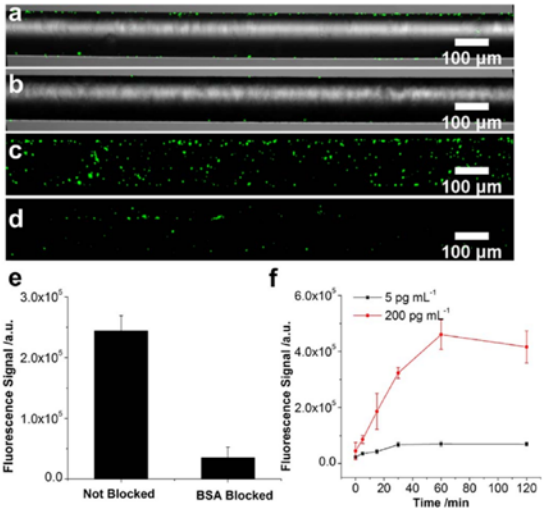

Fig. 3. The effect of the fibre blocked by BSA: combined confocal images (bright field and fluorescence field) of the not blocked(a)/blocked(b) fibre after exposed in the SPIO-IL-6 Ab conjugates solution; Z-stack images of the fibre not blocked(c)/blocked(d) by BSA after exposed in the SPIO-IL-6 Ab conjugates solution; e) the corresponding fluorescence intensity of the Z-stack images obtained from c and d; (f) Optimization of incubation time with two different concentration of IL-6 (200 pg mL^{-1} and 5 pg mL^{-1}) respectively.

capture antibody was compared with that of the fibre surface using 6-Mercaptohexanoic acid (MA) as cross-linker as reported in our previous work (Liu et al., 2016b). The procedure for preparation of the fibre sensing surface by the MA method was detailed in Supplementary Scheme 1. After staining by NL493-conjugated secondary antibody, the fluorescence intensity of the two types fabricated fibres modified with the capture antibody was compared. It could be seen from Fig. 2 that the fibre prepared by BAS method (Fig. 2b) showed a brighter fluorescence signal (1.5 times higher fluorescence intensity) than that

prepared by MA method (Fig. 2a), which suggested that BAS method had a higher immobilization efficiency than MA method. Moreover, the antibody density on the fibre surface could be quantified through the fluorescence intensity versus the quantity of the secondary antibody. The volume of 1 μL NL493-conjugated secondary antibody with different concentration was spotted on the confocal dish, respectively. And a green fluorescent subround area can be obtained for each concentration on the confocal dish. Then the fluorescence signal was collected and calculated. The related calibration curve between concentration and fluorescence was shown in Fig. 2c and the slope of the calibration curve was 1.78×10^7 a.u. ng^{-1}. Assuming the capture antibody and secondary antibody reacted in 1:1 mol ratio, and the density of the antibody on the fibre surface prepared by BAS and MA method could be calculated to be 0.38 ± 0.03 μg cm^{-2} and 0.25 ± 0.02 μg cm^{-2}, respectively. The higher immobilization efficiency of the BAS method could be attributed to the fact that the biotin layer introduced a streptavidin layer with two active sites facing outward, resulting in an enhanced binding capacity for the biotinylated capture antibody. Moreover, the stable biotin-streptavidin complex further ensured the effective immobilization of the biotinylated capture antibody (Smith et al., 2005). While for the method by using MA as cross-linker, EDC/NHS reacting with MA leads to a NHS-ester intermediate layer that was amine-reactive allowing for amide bond formation with primary amines existed in antibody. However the activation yield of the NHS-ester was limited (around 50%) (Moraillon et al., 2008), and also there was a competition between amidation and hydrolysis when NHS-ester reacted with the antibody. As a result, the MA method showed relative lower immobilization efficiency than that of BAS method.

To form the sensing interface having the capability of resisting nonspecific protein adsorption. The blocking reagent BSA was applied on this sensing interface. Fig. 3a and b showed the confocal images of the BSA treated and no BSA treated fibres sensing interface after incubating with SPIO-IL-6 Ab conjugates solutions. Many green fluorescent particles could be observed around the non BSA treated fibre, while significantly less fluorescent particles appeared on the fibre being blocked by BSA. It suggested that BSA molecules filled in the defects on the sensing interface resulting in high resistance ability to non-specific adsorption. Furthermore, the fluorescence signal of the whole fibre surface was quantified by Z-stack imaging method (Fig. 3c and d). Images were collected and stacked by selecting the maximum pixel value from each image and the fluorescence signal was processed by Image J and Matlab software. A more obvious discrimination between the two fibres could be observed from the Z-stack images. After the fibre surface was treated by BSA, the fluorescence signal of non-specific absorption decreased from 2.4×10^5 a.u. to 3.5×10^4 a. u. (Fig. 3e) suggesting the efficient of BSA in resisting protein adsorption. In addition, we have optimized the incubation time of the antibody-antigen binding in this immunoassay. Fig. 3f showed the fluorescence signal of the fibre incubated in 200 pg mL^{-1} and 5 pg mL^{-1} IL-6 solution changed with the incubation time, respectively. For the fibre incubated in 200 pg mL^{-1} IL-6 solution, the fluorescence intensity increased significantly with incubation time varying from 0 to 30 min and then reached maximum value at about 60 min. A similar trend was also observed when fibre exposed to 5 pg mL^{-1} IL-6. These suggested that the binding reaction nearly finished when the incubation time was 60 min.

3.2. Detection of IL-6 by using the fabricated cytokine immunosensing device

Under the optimized condition, the performance of the fabricated immunosensing system for detection of IL-6 was investigated (Fig. 4). High fluorescence was observed when the immunosensing interfaces were incubated with IL-6 in higher concentration. As shown in Fig. 4b, the fluorescence intensity increased linearly with incremental concentration of IL-6 in the range from 0.4 to 400 pg mL^{-1}. The corresponding linear regression equation was represented as $F = 1887.29c + 65{,}754.69$ with a correlation coefficient of 0.99. The detection limit of this fibre sensor was calculated by the following equation (Shrivastava and Gupta, 2011): $C = 3S_b/k$, where k represents the slope of the calibration plot, and S_b represents the standard deviation of the replicate blank measurements. The detection limit of this fibre sensor could be up to 0.1 pg mL^{-1}, which was 10 times lower than that in our pervious study (Liu et al., 2016b). This confirmed that BAS immobilizing more capture antibody on the fibre could enhance the sensitivity of the fibre sensor. Moreover, the comparison of this immunosensors with others for the determination of IL-6 was shown in table S1. The reproducibility of the fabricated fibre immunosensor was examined at a certain concentration of IL-6. Twenty five fibre samples from five batches with five fibre samples per batch were applied for the detection of 50 pg mL^{-1} IL-6 in PBS containing 10% FBS. The coefficient of variation of intra-assay and inter-assay can be calculated to 4.9% and 1.2%, respectively. Which suggested that the fabricated fibre immunosensor demonstrated good reproducibility. For evaluating the specificity of the fibre immunosenser, possible interferences for the detection of IL-6 was investigated by spiking various foreign cytokines at physiologically relevant concentrations into a fix concentration of IL-6. A tolerable relative error of 5% was considered acceptable. It was found that recombinant mouse IL-1β, TFN-α, IFN-γ, IL-2, IL-4, IL-8 and IL-10 had no interference with the target cytokine IL-6.

To demonstrate the capability of the fibre sensing interface to detect localized concentration of IL-6, 1 μL of 300 pg mL^{-1} and 20 pg mL^{-1} of IL-6 were dropped on the various locations of the fibre followed by incubation with SPIO-IL-6 Ab conjugates (Fig. 5a). It was observed that more green florescence beads on the both sides of fibre than that in the middle of the fibre. The fluorescence intensity of the fibre exposed in the area of 300 pg mL^{-1} IL-6 was more than 10 times higher than the area of 10 pg mL^{-1} IL-6. This indicated that the fibre could discriminate different concentration of IL-6 with the sample volume of 1 μL at different locations to make it possible for localized determination of IL-6. The achievable spatial resolution depended on the spatial window we used for imaging. It was observed that the fibre was able to detect the IL-6 with spatial resolution in order of 200–450 μm (Fig. 5b).

In order to test the application of the proposed fibre sensor for detection of IL-6 in cell culture medium, the fabricated fibre was used to test IL-6 secreted by BV-2 cells. BV-2 cells seeded in 96 micro-plate were stimulated by lipopolysaccharides (0.1 μg mL^{-1}). The supernatants with different stimulation time were collected and then they were analyzed by the herein fabricated fibre sensing interface. To protect the fibre from being destroyed, the fibre was placed in a cannula which had holes on the surface to maintain the solution interaction inside and outside of the cannula. After incubation of the fibre with the cell culture medium, the sensing interface was washed and stained by SPIO-IL-6 Ab conjugates. Finally, the concentration of IL-6 was quantified by fluorescence intensity in confocal microscope images. In parallel, the performance of the fibre immunobiosensor was compared with that of conventional IL-6 ELISA Kit. It was observed that the amount of the green fluorescent dots varies with different stimulation time of BV-2 cells secretions (Fig. S4). Moreover, the concentration of IL-6 in BV-2 cells secretions increased with the stimulation time and reached the maximum value at the stimulation time of 8 h (Fig. 5c). The IL-6 content determined was in agreement with that from the commercial ELISA, indicating that the fibre sensor was applicable for IL-6 detection in *ex vivo*.

4. Conclusions

In summary, an immunosensor based on optical fibre was fabricated for monitoring locally variable concentration of cytokine IL-6. This fibre sensor functioned on a technique of sandwich immunoassay and the signal was reported by fluorescence. A superior sensing surface

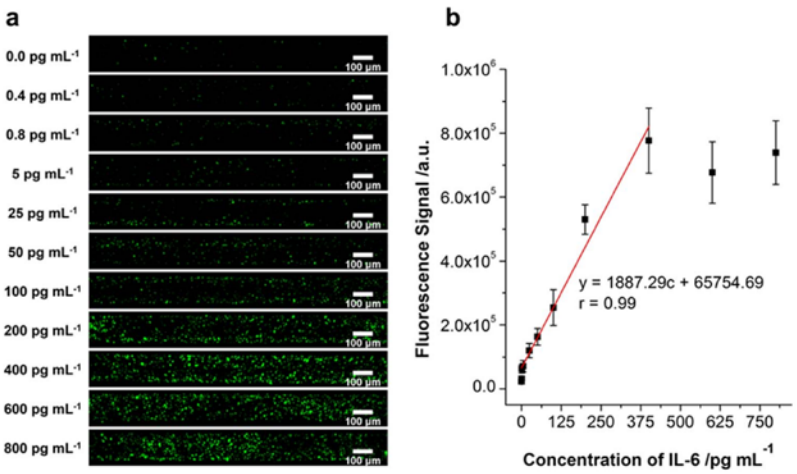

Fig. 4. (a) Fluorescence signal of the optical fibre after exposure to different concentration of IL-6 followed by the incubation with SPIO-IL-6 Ab conjugates; (b) The corresponding calibration curve of IL-6 based on the fluorescence signal and IL-6 concentration in PBS containing 10% FBS.

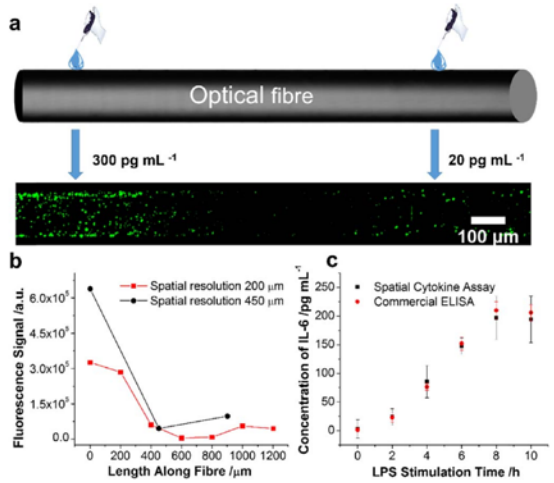

Fig. 5. (a) localized determination of IL-6 by dropping two different concentration of IL-6 on the fibre surface; (b)The changes of the fluorescence intensity along the length of fibre with the spatial resolution of 200 μm and 450 μm, respectively; (c) the comparsion of the IL-6 in BV-2 cells secretions detected by the fibre sensor and commercial ELISA kit.

coated with biotinylated capture antibody was fabricated according to biotin-streptavidin binding strategy. Moreover, compared with the antibody immobilization method through covalent reaction with 6-mercaptohexanoic acid reported in our previous work, the biotin-streptavidin system could boost the amount of capture antibody immobilized on the fibre surface, leading to increased sensitivity of the immunosensor to 0.1 pg mL^{-1}. The fabricated fibre showed satisfying performance in detection of IL-6 in BV-2 cell secretions and localization detection of IL-6 with the sample volume 1 μL IL-6 and spatial resolution of 200 μm. This immunosensor offers the potential to detect IL-6 in clinical samples and monitoring multiple health conditions.

Acknowledgements

This research was supported by funding from the ARC Centre of Excellence for Nanoscale Biophotonics CE140100003, ARC Future Fellowship, Macquarie University MQRDG, the National Natural Science Foundation of China (Grant 21575045), and the self-determined research funds of CCNU (CCNU15A02015). K. Zhang acknowledges the iMQRES scholarship.

Appendix A. Supplementary material

Supplementary data associated with this article can be found in the online version at http://dx.doi.org/10.1016/j.bios.2017.11.023.

References

Aksu, E., Çıkım, G., 2016. Int. J. Health Sci. Res. 6, 33–41.
Alvarado, A., Bernal, L., Ferreira, D., Paige, C., Romero-Sandoval, A., 2016. J. Pain. 17, S45–S46.
Angiolilli, C., Grabiec, A.M., Ferguson, B.S., Ospelt, C., Fernandez, B.M., van Es, I.E., van Baarsen, L.G., Gay, S., McKinsey, T.A., Tak, P.P., 2016. Ann. Rheum. Dis. 75, 430–438.
Ball, V., Huetz, P., Elaissari, A., Cazenave, J., Voegel, J., Schaaf, P., 1994. Proc. Natl. Acad. Sci. USA 91, 7330–7334.
Buzza, M.S., Johnson, T.A., Conway, G.D., Martin, E.W., Mukhopadhyay, S., Shea-Donohue, T., Antalis, T.M., 2017. J. Biol. Chem. 292, 10801–10812.
Cao, L., 2006. Carrier-bound Immobilized Enzymes: Principles, Application and Design. John Wiley & Sons.
Deng, C., Qu, F., Sun, H., Yang, M., 2011. Sens. Actuators B: Chem. 160, 471–474.
Diamandis, E.P., Christopoulos, T.K., 1991. Clin. Chem. 37, 625–636.
Dundas, C.M., Demonte, D., Park, S., 2013. Appl. Microbiol. Biotechnol. 97, 9343–9353.
Green, N.M., 1975. Adv. Protein Chem. 29, 85–133.
Herrwerth, S., Rosendahl, T., Feng, C., Fick, J., Eck, W., Himmelhaus, M., Dahint, R., Grunze, M., 2003. Langmuir 19, 1880–1887.
Holmberg, A., Blomstergren, A., Nord, O., Lukacs, M., Lundeberg, J., Uhlen, M., 2005. Electrophoresis 26, 501–510.
Hosseini, S., Ibrahim, F., Djordjevic, I., Rothan, H.A., Yusof, R., van der Marel, C., Benzina, A., Koole, L.H., 2014. Eur. Polym. J. 60, 14–21.
Hsu, D.C., Ma, Y.F., Hur, S., Li, D., Rupert, A., Scherzer, R., Kalapus, S., Deeks, S., Sereti, I., Hsue, P.Y., 2016. Aids 30, 2065–2074.
Kapoor, R., Wang, C.W., 2009. Biosens. Bioelectron. 24, 2696–2701.
Liang, K.-Z., Qi, J.S., Mu, W.-J., Chen, Z.G., 2008. J. Biochem. Biophys. Methods 70, 1156–1162.
Liu, G., Qi, M., Hutchinson, M.R., Yang, G., Goldys, E.M., 2016a. Biosens. Bioelectron. 79, 810–821.
Liu, G., Zhang, K., Nadort, A., Hutchinson, M.R., Goldys, E.M., 2016b. ACS Sens. 2, 218–226.
Malhotra, R., Patel, V., Vaqué, J.P., Gutkind, J.S., Rusling, J.F., 2010. Anal. Chem. 82, 3118–3123.
Moraillon, A., Gouget-Laemmel, A., Ozanam, F., Chazalviel, J.N., 2008. J. Phys. Chem. C 112, 7158–7167.
Nguyen, A.T., van Doorn, R., Baggerman, J., Paulusse, J.M., Klerks, M.M., Zuilhof, H., van Rijn, C.J., 2015. Adv. Mater. Interfaces 2, 1400292.
Oliveira, S.F., Bisker, G., Bakh, N.A., Gibbs, S.L., Landry, M.P., Strano, M.S., 2015. Carbon 95, 767–779.
Peng, J., Feng, L.N., Ren, Z.J., Jiang, L.P., Zhu, J.J., 2011. Small 7, 2921–2928.
Phillips, T.M., Smith, P., 2003. Biomed. Chromatogr. 17, 182–187.
Prieto-Simon, B., Campas, M., Marty, J.-L., 2008. Protein Pept. Lett. 15, 757–763.

Samanta, D., Sarkar, A., 2011. Chem. Soc. Rev. 40, 2567–2592.
Schetters, H., 1999. Biomol. Eng. 16, 73–78.
Shrivastava, A., Gupta, V., 2011. Chron. Young Sci. 2 (21-21).
Smith, C., Milea, J., Nguyen, G., 2005. Immobilisation of DNA on Chips II. Springer, Berlin Heidelberg, pp. 63–90.
Song, H.Y., Ngai, M.H., Song, Z.Y., MacAry, P.A., Hobley, J., Lear, M.J., 2009. Org. Biomol. Chem. 7, 3400–3406.
Wang, G., He, X., Chen, L., Zhu, Y., Zhang, X., 2014. Colloids Surf. B 116, 714–719.
Wong, L.S., Khan, F., Micklefield, J., 2009. Chem. Rev. 109, 4025–4053.
Zang, B., Ren, J., Xu, L., Jia, L., 2016. J. Chromatogr. B 1008, 132–138.

Supplementary Material

Robust immunosensing system based on biotin-streptavidin coupling for spatially localized femtogram/ml level detection of interleukin-6

Kaixin Zhang[a], *Guozhen Liu*[a, b*], *Ewa M. Goldys*[a*]

[a]ARC Centre of Excellence for Nanoscale Biophotonics (CNBP), Macquarie University, North Ryde 2109, Australia

[b]Key Laboratory of Pesticide and Chemical Biology of Ministry of Education, College of Chemistry, Central China Normal University, Wuhan 430079, P. R. China

*To whom correspondence should be addressed.

Email: guozhen.liu@mq.edu.au;

ewa.goldys@mq.edu.au.

Fabrication of the optical fibre based sensing surface by using MA as cross-linker

The fibre sensing surface formed by using 6-mercaptohexanoic acid (MA) as cross-linker was fabricated in several steps. Firstly, the fibre coatings was removed by piranha solution (H_2SO_4 95% and H_2O_2 30% mixed at a volume ratio of 7:3). Upon the de-cladded optical fibre was kept in piranha solution for 12 h to clean and form hydroxyl groups on its surface. Then the cleaned fibre, washed by Milli-Q water and dried under N_2 stream, was immersed in aminopropyltriethoxysilane (5% v/v) in toluene for 6 h to form an amine-terminated self-assembled monolayer. The unbound monomers were washed away from the fibre surface by toluene. Subsequently, the aminopropyltriethoxysilane-modified optical fibre was incubated in a 1 mL of AuNP (10 nm) solution for 3 h to form the AuNP modified fibre. After rinsed by water, AuNP modified optical fibre was then immersed into 0.1 mM 6-mercaptohexanoic acid solution overnight, and finally washed three times with deionized H_2O. To make the capture antibody attached on the fibre surface, the prepared fibre surface was activated by EDC (10 mg mL^{-1})/NHS (10 mg mL^{-1}) for 30 min in 25 mM MES buffer (pH 6.0) solution. Then the fibre was washed in the MES buffer twice and incubated with Mouse IL-6 polyclonal antibody Polyclonal Goat IgG (capture antibody) (50 μg mL^{-1}) in MES buffer (pH=6.0) at room temperature for 3 h. The fibre surface was subsequently blocked in 0.25% BSA solution for 3 h.

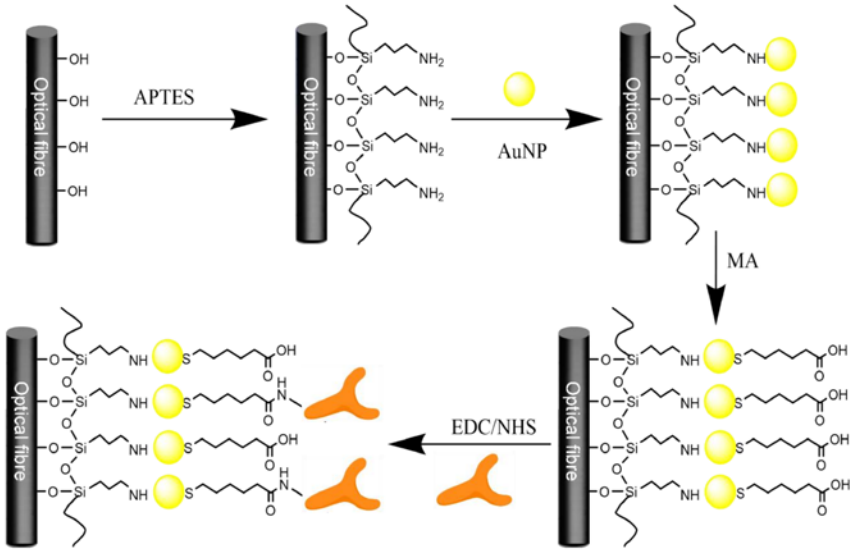

Scheme 1 The procedure of fabrication of the optic fibre based sensing surface by using MA as cross-linker

The successful conjugating between AuNPs and optical fibre was confirmed by the changes of the fibre colour. It can be seen from Fig. S1 that before the fibre conjugating with the AuNPs, the fibres were clear and transparent (Fig. S1a), while after the fibre conjugating with AuNPs, the colour of the fibre surface changed to purple (Fig. S1b), which suggested that the AuNPs had successfully conjugated with the fibre. Moreover, SEM image of the fibre after conjugating with AuNPs could further confirm the successfully self-assembling of the AuNPs on the aminopropyltriethoxysilane (APTES) functionalized fibre surface (Fig. S1c).

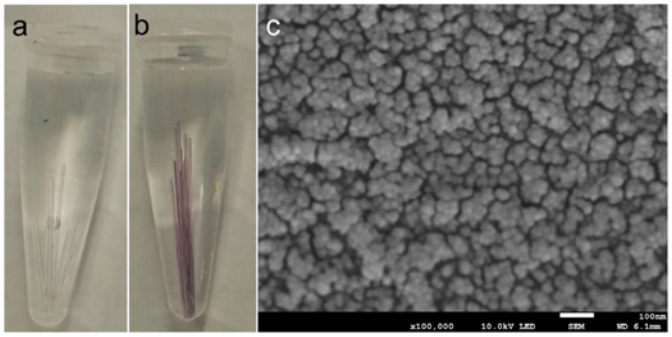

Fig. S1 photograph of the fibres before (a) and after (b) conjugating with the AuNPs. (c) SEM image of the fibre after conjugating with AuNPs

For the evaluation of the successful conjugation processes of antibody labelled with magnetic nanoparticles, Zeta-potential was applied to monitor the changes of the magnetic nanoparticles surface. It could be seen from Fig. S2 that the value of the Zeta Potential of the SPIO-IL-6Ab conjugates increased with the concentration of antibody increasing, then the value reached the maximum at the concentration of antibody at 35 μg mL-1. The changes of the Zeta Potential suggested that the antibody had been successfully conjugated to the surface of magnetic nanoparticles. With further increasing of the antibody concentration, only a slight change of the Zeta Potential was observed, which indicated that the surface of the magnetic nanoparticles got saturated with the antibody.

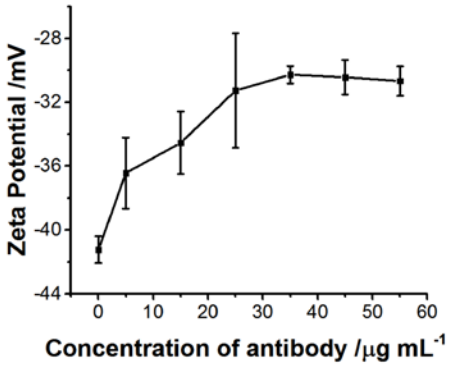

Fig. S2 Zeta Potential of the fluorescent beads antibody conjugates (SPIO-IL-6 Ab)

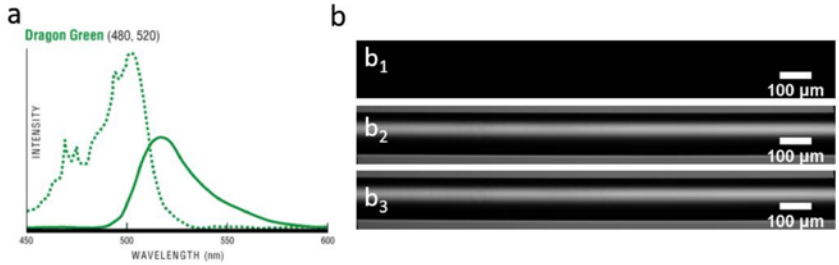

Fig. S3 (a)The fluorescent spectra of the fluorescent beads. (b)The fluorescent field (b_1), bright field (b_2) and combination of fluorescent field and bright field (b_3) of the clean fibre under the fluorescent microscope.

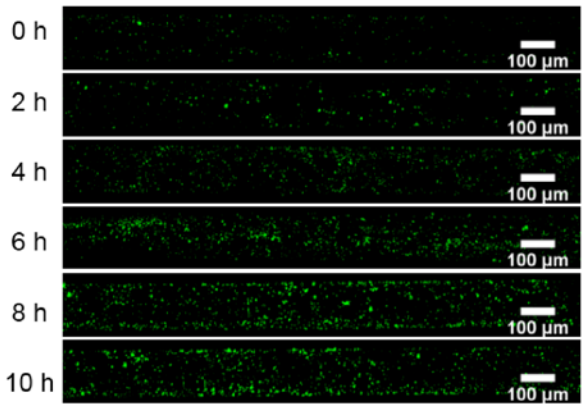

Fig. S4 Fluorescence microscope visualization of the fibre incubated with the BV-2 cells secretions with different stimulation time after exposure in SPIO-IL-6 Ab conjugates solution.

Table S1. Comparison of the immunosensors for the determination of IL-6.

Method	Minimum sample Volume	Linear range (pg mL^{-1})	Detection limit (pg mL^{-1})	Localized detection of IL-6	Reference
Electrochemical magnetoimmunosensor(Amperometry)	25 µL	1.75-500	0.39	No	(Ojeda et al. 2014)
Magnetic electrochemical immunosensor (DPSV)	25 µL	0.5-100000	0.1	No	(Peng et al. 2011)
Electrochemical immunosensor (SWV)	10 µL	5.0-50000	2	No	(Deng et al. 2011)
Electrochemical immunosensor (Amperometry)	10 µL	4.0-800	1	No	(Wang et al. 2010)
Electrochemical immunosensor (Amperometry)	10 µL	0.5-5	0.5	No	(Malhotra et al. 2010)
Fluorescence-based fibre-optic biosensors	Not available	120-12000	120	No	(Kapoor and Wang 2009)
Microarray fluorescence immunoassay	30 µL	100-10000	100	No	(Wu et al. 2008)
Conductometric immunosensor	50 µL	30-300	10	No	(Liang et al. 2006)
enzyme-linked immunospot assay	100 µL	39-2500	39	No	(Turner et al. 2004)
Fluorescence-based fibre immunosensor	1 µL	0.4-400	0.1	Yes	This work

DPSV differential pulse stripping voltammetry, *SWV* square-wave voltammetry

Deng, C., Qu, F., Sun, H., Yang, M., 2011. Sens. Actuators, B 160, 471-474.
Kapoor, R., Wang, C.-W., 2009. Biosens. Bioelectron. 24(8), 2696-2701.
Liang, K., Mu, W., Huang, M., Yu, Z., Lai, Q., 2006. Electroanalysis 18, 1505-1510.
Malhotra, R., Patel, V., Vaqué, J.P., Gutkind, J.S., Rusling, J.F., 2010. Anal. Chem. 82, 3118-3123.
Ojeda, I., Moreno-Guzmán, M., González-Cortés, A., Yáñez-Sedeño, P., Pingarrón, J., 2014. Anal. Bioanal.Chem. 406, 6363-6371.
Peng, J., Feng, L.N., Ren, Z.J., Jiang, L.P., Zhu, J.J., 2011. Small 7, 2921-2928.
Turner, C.K., Blieden, T.M., Smith, T.J., Feldon, S.E., Foster, D.C., Sime, P.J., Phipps, R.P., 2004. J. Immunol. Methods 291, 63-70.
Wang, G., Huang, H., Zhang, G., Zhang, X., Fang, B., Wang, L., 2010. Langmuir 27, 1224-1231.
Wu, H., Huo, Q., Varnum, S., Wang, J., Liu, G., Nie, Z., Liu, J., Lin, Y., 2008. Analyst 133, 1550-1555.

4.3 Appendix

Fluorescence visualization of the fiber sensing surface

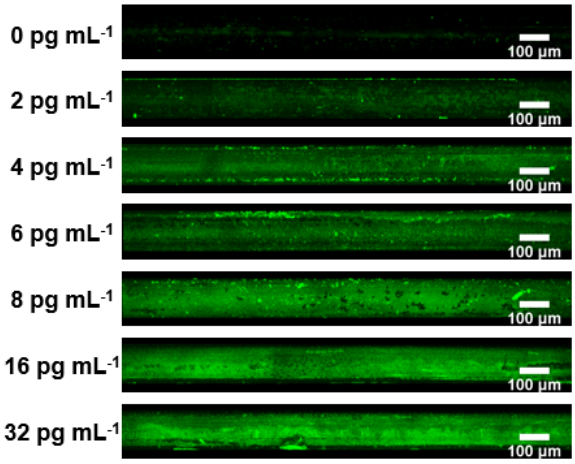

Figure 4-1 Confocal microscope images of the streptavidin-coated fiber surface reacting with different concentration of mouse IL-6 biotinylated antibody (capture antibody) following stained by the fluorescent secondary antibody (donkey anti-Goat IgG NorthernLights NL493- conjugated antibody).

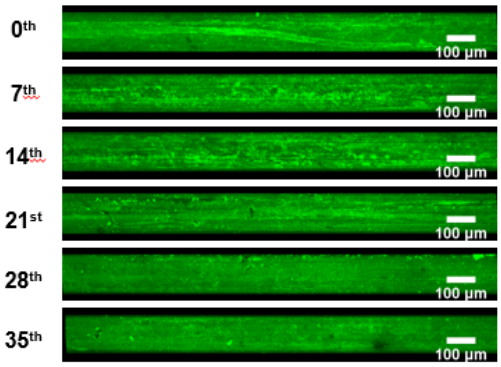

Figure 4-2 Confocal microscope images of the fiber sensing surface incubated in PBS for extended periods of time followed by monitoring the presence of IL-6 capture antibody using the green dye labeled secondary antibody (donkey anti-Goat IgG NorthernLights NL493- conjugated antibody).

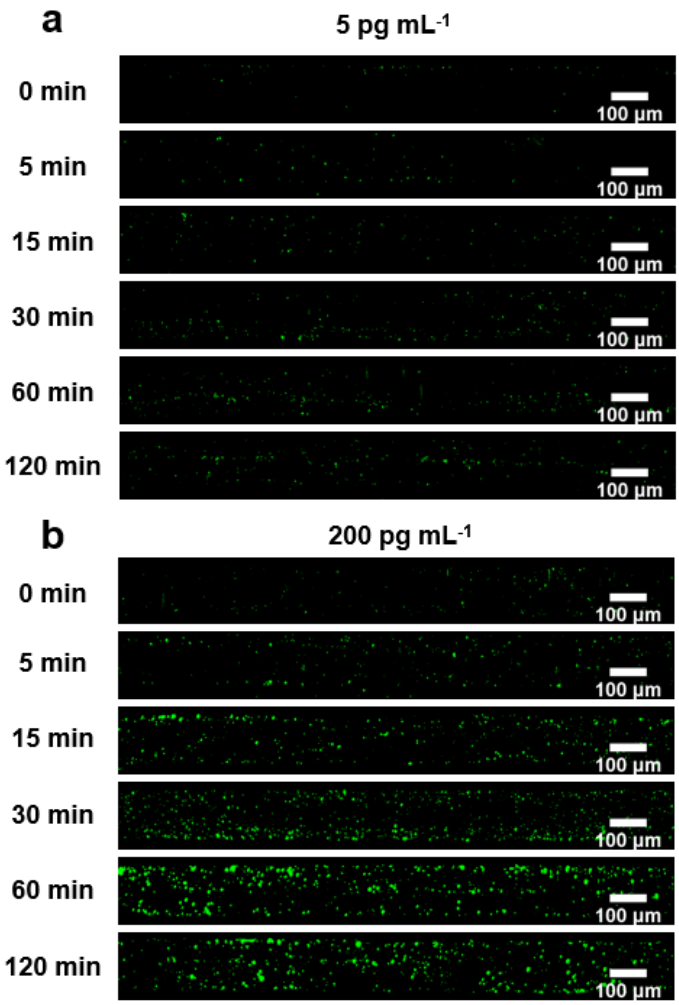

Figure 4-3 Optimization of incubation time: Z-stack images of the fiber in detection of 5 and 200 pg mL^{-1} IL-6 with different incubation time after exposure in the SPIO-IL-6 Ab conjugates solution.

Comparison of the performance of fiber sensing surface in detection of IL-6.

The performance of the fiber sensing surface prepared by biotin-streptavidin system (BAS) in this chapter was compared with the sensing surface prepared by 6-mercaptohexanoic acid (MA) as cross-linker (a) which detailed in chapter 2. The performance of the fiber prepared by the two methods was investigated by applying them in detecting a certain concentration of IL-6. Figure 4-4 a and b showed the Z-stack images of the fibers in determination of 400 pg mL^{-1} IL-6 after exposure to SPIO-IL-6 conjugates solutions. It can be seen that fiber prepared by BAS method can catch more fluorescent beads than that of MA method and the fluorescent intensity of BAS fiber also showed around 1.5 times higher than that of MA fiber indicating a higher affinity for the fiber prepared by BAS method, which will be favorable to extended detection limit for IL-6.

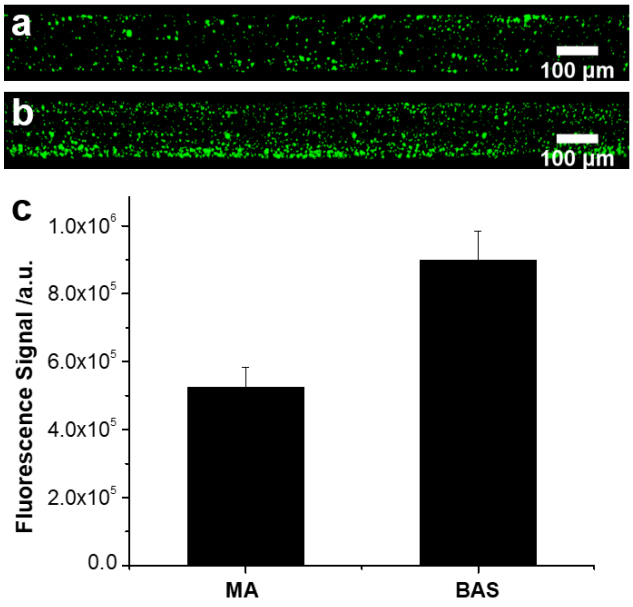

Figure 4-4 (a,b) Fluorescence microscope visualization of the fiber prepared by 6-mercaptohexanoic acid (MA)(a) method and biotin-streptavidin system (BAS)(b) in detection of 400 pg mL^{-1} IL-6 following exposure in SPIO-IL-6 Ab solution; (c) the corresponding fluorescence signal in figure a and b.

4.4 Summary

In this chapter, a superior sensing surface coated with biotinylated capture antibody was fabricated according to biotin-streptavidin binding strategy. Moreover, compared with the antibody immobilization method through covalent reaction with 6-mercaptohexanoic acid reported in chapter 1 and 2, the biotin-streptavidin system could boost the amount of capture antibody immobilized on the fibre surface, leading to increased limit of detection of the immunosensor to 0.1 pg mL^{-1} and the stability of the sensing surface was improved from 9 days to around 4 weeks. In addition, the fabricated fiber immunosensor showed satisfying performance in detection of IL-6 in BV-2 cell secretions and localization detection of IL-6 with the sample volume 1 μL and spatial resolution of 200 μm. This immunosensor offers the potential to detect IL-6 in clinical samples and monitoring multiple health condition as well.

5

Detection of Interleukin-1β on Biotin - Avidin System Modified Glass Fiber

5.1 Introduction

Spinal cord injury (SCI) is one of the major traumas of the central nervous system (CNS) leading to devastating neurological outcomes. The damages of CNS are usually related to the changes of the cytokine concentrations in the spinal cord, as elevated cytokine concentration in this local area can cause uncontrolled inflammatory response, and the upregulation of these cytokines, as well as the consequent cellular infiltration they cause, plays a crucial role in the determination of the extent of the secondary tissue damage and neural degeneration after SCI. Thus, localized measurements of the cytokine in the spinal cord would help to define the role of the cytokine in SCI and provide useful information for SCI diagnosis and therapy.

In this chapter, we have further extended the application of the fiber immunosensor by establishing a model in the rat spinal cord. Compared to chapter 4, from one hand, we have advanced the biotin-streptavidin coupling strategy for the immobilization of capture antibody on the sensing surface and characterised the properties of the sensing surface such as stability and reproducibility. On the other hand, we have established a model for the cytokine detection in the spinal cord by testing the application of the fiber immunosensor in the localized cytokine IL-1beta detection in the rat spinal cord.

Zhang, K., Arman, A., Anwer, A.G., Hutchinson, M.R. and Goldys, E.M., 2019. An optical fiber based immunosensor for localized detection of IL-1β in rat spinal cord. Sensors and Actuators B: Chemical, 282, pp.122-129.

Summary of the author contributions to paper 4 following the order of author.

paper 4	K. Z	A. Arman	A. Anwer	M. H	E. G
Experiment Design	•	•		•	•
Sample Preparation	•	•	•		
Data Collection	•	•	•		
Analysis	•				
Figures	•				
Manuscript	•	•		•	•

5.2 Full paper

Article Type: Full length Article

Title: An optical fiber based immunosensor for localized detection of IL-1β in rat spinal cord

Authors: Kaixin Zhang[1,2], Azim Arman[3,4], Ayad G Anwer[1,2], Mark R Hutchinson[3,4], Ewa M Goldys*[5]

Author Affiliations: [1]ARC Centre of Excellence in Nanoscale Biophotonics (CNBP), Macquarie University, Sydney, NSW 2109, Australia; [2]Department of Physics and Astronomy, Macquarie University, Sydney, NSW 2109, Australia; [3]ARC Centre of Excellence for Nanoscale BioPhotonics (CNBP), The University of Adelaide, Adelaide, SA 5005, Australia; [4]Institute for Photonics and Advanced Sensing (IPAS) and Adelaide Medical School, The University of Adelaide, Adelaide, SA 5005, Australia; [5]Graduate School of Biomedical Engineering, The University of New South Wales, Sydney, NSW 2052, Australia

***Corresponding Authors:** Ewa M. Goldys; Graduate School of Biomedical Engineering, The University of New South Wales, Sydney, NSW 2052, Australia

email: e.goldys@unsw.edu.au

Keyword: optical fiber, interleukin-1beta, in vivo, sensor, immunosensor,

Abstract

Sensitive and localized measurements of cytokines is important in biomedicine as cytokines are produced locally where needed to induce an immune reaction. Here, we present a novel immunosensor deposited on the optical fiber surface. The sensor is capable of localized detection of interleukin-1beta (IL-1β) in the rat spinal cord. In this immunosensor, a stable immunocapture surface was formed via a biotin-streptavidin coupling strategy and fluorescent carboxylated superparamagnetic iron oxide (SPIO)-IL-1β detection antibody conjugates were used for signal amplification. Under the optimal condition, the proposed immunosensor can be used for the estimation of IL-1β *in vitro* in the range from 3.13 $pg.mL^{-1}$ to 400 $pg.mL^{-1}$ with a detection limit of 1.12 $pg.mL^{-1}$. Furthermore, the performance of the fiber sensor was firstly assessed by *ex-vivo* monitoring the secretions of the rat macrophages stimulated by lipopolysaccharide (LPS), and the results demonstrated significant correlations with a commercial ELISA kit. Furthermore, the fiber sensor was successfully utilized to carry out a localized measurement of IL-1β in a spinal cord of an anesthetized rat. The result indicates that such fiber sensors can be used as an effective and sensitive tool for localised detection of IL-1β *in vivo*, in a range of research and clinical applications.

1. Introduction

Cytokines are small proteins secreted by different type cells in the course of cell signalling and communication. It is well known that these soluble proteins play a critical role in regulation of local and systemic inflammatory responses [1]. IL-1β is a powerful pro-inflammatory cytokine that is pivotal for host-defence responses to infection and injury [2-5]. Evidence has shown that inappropriate production and release of IL-1β accompanies a multitude of health conditions especially acute trauma [6, 7], rheumatoid arthritis [8, 9], exanthema [10], conjunctivitis [11], serositis [12], amongst many others. Therefore, a more thorough understanding of the release of IL-1β during inflammation would be valuable in disease diagnostics and therapy. As a result, reliable techniques for the measurements of IL-1β especially those with spatial resolution are required.

However, the detection of IL-1β is challenging because of its local dynamic secretion process and low abundance *in vivo* with physiological concentrations normally at pM range [5]. The leading standard method for IL-1β detection relies on the Enzyme-linked Immunosorbent Assay (ELISA), generally regarded as reliable and accurate. It shows high reproducibility and accuracy, but the requirement of the large volume sample (>100 µL) for the ELISA makes it inadequate to detect trace levels of IL-1β in complicated samples. To overcome this sensitivity issue, surface plasmon resonance [13, 14], advanced integrated circuit [15], microfluidic array [16,17], microarray [18], electrochemical [16, 19-21] and photonic crystal fiber-based [22] techniques have been introduced for the development of highly sensitive biosensors for the detection of cytokine. For example, a fiber-optic surface plasmon resonance sensor was developed for the detection of IL-1β with detection limits below 1 $ng.mL^{-1}$ in a spiked cell culture medium [14]. Krause et al. developed a

microfluidic array capable of detection of IL-1β at 10 fg.mL^{-1} in 5 µL serum sample [16]. Aydın et al. fabricated an impedimetric biosensor that was able to detect IL-1β at fg.mL^{-1} level in serum and saliva samples [19]. Although these biosensors enhance the IL-1β detection at very low concentrations, providing valuable options for the prediction of the first signs of inflammation, all of them are limited to *in vitro* analysis of samples, which involved in extraction of the biological fluid or cell culture medium. However, the IL-1β *in vivo* is usually produced locally (i.e. at the site of injury or disease), while cytokine measurements are usually carried out on accessible biological fluids away from these local sites of action. As a result, the measured concentration may be greatly reduced compared to the actual concentration which is present at the active site. Therefore, the development of a method with sufficient sensitivity that can directly measure the locally released IL-1β is highly desirable.

We recently developed a fiber immunosensing platform [23,24] that was able to demonstrate spatially localized measurements of cytokines along the fiber length based on the quantification of the fluorescent signal on the sensing interface. With capture antibodies immobilized on an optical fiber surface by the biotin-streptavidin coupling strategy, a sandwich mode of operation was used, where upon target capture, the fiber is exposed to the detection antibody labeled with a fluorescent nanoparticle. The bright fluorescent nanoparticle labeled detection antibody together with high immobilization efficiency of the capture antibody have enabled this platform to be effectively applied to ultrasensitive detection of the cytokine IL-6 *in vitro*.

In the present work, we adapt the biotin-streptavidin coupling strategy to achieve a highly sensitive capture surface capable of localized measurements of IL-

1β in the rat spinal cord. A biotin layer was introduced on the fiber surface by reacting the sulfosuccinimidyl-2-[biotinamido]ethyl-1,3-dithiopropionate (NHS-biotin) with the fiber covalently grafted with aminopropyltriethoxysilane (APTES). As one streptavidin molecule can bind up to four biotin molecules, it acts as a bridge to immobilize the biotin-labeled capture antibody on the fiber surface. The fiber sensing surface thus prepared was applied to capture IL-1β, and quantify its concentration based on the quantification of the fluorescent signal after incubation with fluorescent magnetic nanoparticles labelled detection antibody. In this work, compared to our previous study, we have advanced the biotin-streptavidin coupling strategy for the immobilization of capture antibody on the sensing surface and characterised the properties of the sensing surface such as stability and reproducibility. The application of the fiber immunosensor was first tested *ex-vivo* by analysing the secretions of rat macrophages stimulated by lipopolysaccharide (LPS). As this fabricated fiber sensor can be applied to spatially localized detection of IL-1β, which makes it possible to detect the variations in local concentration of the released cytokines. The fiber sensor was successfully utilized for the localized measurement of IL-1β in rat spinal cord suggesting that our system provides the capacity to repeatedly sample from the same animal, spatially and temporally resolved cytokine release. This capability is fundamentally important in research and clinical applications.

2. Experimental section

2.1. Chemicals and materials

Recombinant rat IL-1β/IL-1F2 Protein, rat IL-1β /IL-1F2 biotinylated antibody (capture antibody, Catalog: BAF501), rat IL-1 β /IL-1F2 antibody polyclonal goat IgG (detection antibody, Catalog: AF-501-NA), and Donkey anti-Goat IgG

NorthernLights™ NL493-conjugated antibody (secondary antibody, Catalog: NL003) were purchased from R&D Systems. NHS-biotin was obtained from Thermo Fisher Scientific Inc. Concentrated sulfuric acid (H_2SO_4) (95.0%~98.0%), hydrogen peroxidase (H_2O_2) (30%), aminopropyltriethoxysilane (APTES), toluene, N-hydroxysuccinimide (NHS), 1-ethyl-3-(3-dimethylaminopropyl) carbodiimide hydrochloride (EDC), 2-(N-morpholino) ethanesulfonic acid (MES), phosphate buffered saline tablet, Tween 20, and bovine serum albumin (BSA) were purchased from Sigma-Aldrich. Fluorescent carboxylated superparamagnetic iron oxide microspheres with 1% solid content (SPIO, ~0.90 µm, labelled with P(S/6%DVB/V-COOH) Mag (480, 520)) were obtained from Bangs Laboratories, USA. MES buffer contained 25 mM 2-(N-morpholino) ethanesulfonic acid, adjusted to pH 6.0 with NaOH solution. The phosphate buffer solution (PBS) used in this work was prepared by the phosphate buffered saline tablet containing 10 mM phosphate buffer, 2.7 mM potassium chloride and 137 mM sodium chloride, pH 7.4, at 25 ℃. The optical fiber is a standard telecommunication silica fiber (200 µm diameter core /320 µm acrylate coating) from Thorlabs Inc.

2.2 Subjects

Adult male Sprague-Dawley rats housed in 18°C ± 6 with 12:12 hours light: dark and with food and water provided ad libitum. All procedures were conducted under the University of Adelaide Animal Ethics approval number M-2015-257.

2.3 Cell line and conditions

Rat macrophages (RMcp) were provided by Cell Applications, Inc. The cell line was cultured as previously described in RPMI supplemented with 10% fetal bovine serum (FBS), at a 37°C, 5% CO_2 humidified incubator. For the collection of

conditioned medium, cells were initially seeded and grown in the 24-well plate with 60-70% confluency. After 12h' incubation, the medium was removed and then 2 mL fresh macrophage culture medium with 1 μg.mL^{-1} lipopolysaccharide (LPS) was added to each well for 3 h for priming. Then ATP was added (0.5 mM) and the cell culture medium was collected at 2h, 4h, 7h, 10h, 24 h. Cell debris were removed by a brief centrifugation and all the collected supernatants were frozen in -80 ºC prior to assay of IL-1β.

2.4 Preparation of SPIO-IL-1 β detection antibody conjugates (SPIO-IL-1β Ab)

The SPIO-IL-1β detection antibody conjugates were prepared by a two-step process. Firstly, 25 μL SPIO were washed with Milli-Q water and MES buffer respectively. Then the SPIO were activated by incubating with the carbodiimide activating reagents EDC/NHS (10 mg.mL^{-1}) for 30 min in MES buffer at room temperature. The activated SPIO were collected by a magnetic separator and the excess activating reagents were removed. Then the activated SPIO with a highly active ester (O-acylisourea) intermediate provided by EDC/NHS coupling reagent was reacted with a primary amine on the protein to form a stable peptide bond. The bioconjugation was achieved by incubating the detection antibody (50 μg.mL^{-1}) with the activated SPIO on a vortexer for 2 h to permit amide coupling. After the amide coupling, the achieved SPIO-1L-1β conjugates were washed and then incubated in blocking buffer (PBS, 0.5% BSA and 0.1% Tween 20) for 2 h to block the residual active site of the SPIO. The biocombination was assessed by Zeta potential (Figure S1). Finally, the SPIO-1L-1β conjugates were collected and redispersed for further use.

2.5 Fabrication of the fiber sensor

We used a standard glass telecommunication fiber with a 200 micrometer diameter core (Thorlabs Inc.) cut into ~ 10 cm sections. The fiber coatings were firstly removed by piranha solution (a mixture of H_2SO_4 and H_2O_2 with a volume ratio of 7:3). Then the fiber surface was hydroxylated (added OH groups) by incubating in the fresh piranha solution for another 12 h. After washed by Milli-Q water and ethanol, the sections of hydroxylated fiber were dried by the N_2 stream. Subsequently, they were placed in a 5% APTES toluene solution for 6 hours' incubation to form an amine-introduced surface. As shown in Scheme 1, to introduce biotin-streptavidin system on the surface, the layer of biotin was formed by using NHS-Biotin reacting with the amine group on the fiber surface. After that, the biotin-coated fiber was incubated in a streptavidin solution (50 μg mL^{-1}) for 40 min to form the streptavidin-coated fiber surface. Upon the removal of residual streptavidin, the fiber was placed in the rat IL-1β biotinylated antibody solution (15 μg.mL^{-1}) for 60 min to form the sensing surface. Finally, the fiber surface modified with the capture antibody was blocked by 0.5% BSA in PBS for 1 h at room temperature to reduce nonspecific adsorption (Figure S2). For the detection of IL-1β, the fiber functionalized with the capture antibody was used to incubate with the analyte in the assay solution with a varying concentration for 1 h. Then the fiber was washed and finally exposed to SPIO-IL-1β conjugates solution for 1 h to form the sandwich immunocomplex which can be imaged by a laser scanning microscopy. The procedure for laser microscopy images of the completed assay is described in reference [25]. The optical fiber samples with 1500 μm length for each were imaged using an SP2 (Leica) confocal microscope by a z-stack method with the separation of around 10 μm between planes. The fluorescence signal was quantified by integrating over a spatial window of 450 μm using ImageJ and Matlab software.

3. Results and discussion

3.1 Stepwise optimization of the fabrication of sensing surface

The fabrication procedure has been optimized to ensure the best performance for the fiber immunosensor. Firstly, the treatment time of the fiber in the APTES solution has been optimized. The fibers treated by APTES with different incubation time (from 0 to 10 hours) were reacted with NHS-biotin respectively, and then they were stained by streptavidin-FITC for the assessment of fluorescence. As seen in Figure 1a and b, the fluorescence signal increased gradually over the incubation time and reached the maximum value at 6 h, which suggested that the fiber surface could be completely covered by APTES after 6 h incubation. Therefore, 6 h was used as the optimal treatment time for the fiber functionalized by APTES. Subsequently, the optimal concentration of NHS-biotin and reaction time were also investigated by using streptavidin-FITC. Figure 1c displays the fluorescence signal changes with the NHS-biotin concentration variation, the maximum fluorescence signal value appeared at when the concentration of NHS-biotin was up to 0.0625 $mg.mL^{-1}$. For the reaction time of the NHS-Biotin, it could be seen from Figure 1d, that the fluorescence signal reached a plateau as the reaction time over 20 min. This indicates that, for the NHS-biotin concentration of 0.0625 $mg.mL^{-1}$, and a reaction time over 20 min, the amine group from APTES functionalized fiber was able to completely react with NHS-biotin. This procedure thus created a layer of biotin on the fiber surface. In the next step, streptavidin was added to the fiber surface. Streptavidin comprises four identical subunits so that a stacked composition of biotin/streptavidin/biotin can be used for antibody immobilization. This is because two of subunits facing the surface can bind the biotin layer, and the left two sites facing outward can capture biotinylated proteins. For the formation of

the streptavidin layer on the fiber surface, streptavidin-FITC conjugate was used to confirm the optimal concentration of streptavidin, Figure 1e and f showed that at the concentration of 50 $\mu g.mL^{-1}$ with over 25 min incubation, streptavidin could saturate the biotin-coated fiber surface. Therefore, 50 $\mu g.mL^{-1}$ streptavidin with over 25 min incubation was used in the fabrication of the fiber sensor.

Immobilization of antibodies on the fiber surface antibody is a crucial element on the performance of the immunosensor, so the attachment of the capture antibody was characterized by the fluorescent secondary antibody. It could be seen that there was only a weak fluorescence signal observed (Figure 2a) before the immobilization of the capture antibody, which was due to non-specific adsorption of the streptavidin-coated fiber. A very strong fluorescence signal appeared (Figure 2b) after the streptavidin-coated fiber incubated with the biotinylated capture antibody, suggesting that the capture antibody had been successfully attached on the fiber surface, thus the sensing interface was correctly formed. As high immobilization density on the substrate could enhance the sensitivity of the immunosensor, we optimized the immobilization of the capture antibody in terms of concentration (Figure 2c) and incubation time (Figure 2d). All the fibers incubated with capture antibody stained by the fluorescent secondary antibody were imaged under the confocal microscope. Figure 2c showed that increased capture antibody concentration induced an increase in the fluorescence signal, which then reached the maximum at 15 $\mu g.mL^{-1}$, while for the incubation time of capture antibody, a plateau was reached in 40 min suggesting the saturation of the capture antibody. Therefore, that the concentration of capture antibody at 15 $\mu g\ mL^{-1}$ with the incubation time of 40min or more, was chosen as the optimal condition for the preparation of the sensing surface. In addition, the density of the capture antibody was calculated through the fluorescent secondary antibody. A series of 1 µL

standard fluorescent secondary antibody with different concentration were spotted on the confocal microscope dish. Assuming the reaction between the capture antibody and secondary antibody was carried out at a mole ratio 1:1, the density of the capture antibody on the fiber surface could be calculated according to the slope of the fluorescence signal versus the concentration of the secondary antibody (Figure S3). As a result, the capture antibody density could be calculated to be 0.46 ± 0.15 $\mu g.cm^2$.

3.2. Properties of the of sensing surface

The performance of the fiber greatly relies on the properties of the sensing surface, so we have further explored the stability of the fiber sensing surface in terms of the effect of pH, temperature and storage time. All fabricated fiber samples were stained by the fluorescent secondary antibody after they were exposed to different pH, temperature and storage time. As seen in Figure 3a, when the fiber samples were exposed pH in range of 9 to 4, a negligible change had been observed indicating good stability of the sensing surface, but when the pH varied from 4 to 0, the fluorescence signal significant decreased, which could be attributed to the dissociation of the biotin-streptavidin complex at the extreme pH [26]. In addition, from Figure 3b, we could see that the temperature change from 4 ºC to 45 ºC had no effect on the sensing surface. To explore the effect of the storage time on the sensing surface, the freshly prepared fiber sample was stored in PBS at 4 ºC for periods of up to 20 days (Figure 3c), and the fluorescence signal of the fiber after staining by the secondary antibody was recorded every 5 days. The fluorescence signal retained above 90% of its original value indicating thus fabricated sensing interface had good storage stability. The good stability of the sensing interface could be attributed to strong interaction between the biotin and streptavidin resulting in the

high binding affinity of the biomolecules on the sensing surface. The reproducibility of the fabrication sensing surface was monitored by 10 freshly prepared fiber samples (Figure S4). It could be observed that the relative standard deviation of the fluorescence signal was 8.2%, which was reasonable for this type of sensing platform. The formation time of the antibody-antigen complex at the fiber interface was further optimized to enhance the sensitivity of the fiber sensor. The fiber samples incubated in 10 $pg.mL^{-1}$ IL-1β solution with various incubation times were collected, then the obtained samples were stained by the SPIO-IL-1β antibody conjugates to form the sandwich immunocomplex for fluorescence imaging. We observed that the time and fluorescence signal variations (Figure 3d), whereby the fluorescence signal gradually increased with increasing time. After 60 min incubation, the fluorescence signal changed only slightly, indicating the occurrence of a mild reaction to the IL-1β and antibody in the solution. Therefore, 60 min incubation was selected to ensure optimal sensitivity.

3.3 Analytical performance of the fiber sensor.

Under the optimal conditions, the analytical performance of the fiber sensor was evaluated by measuring various concentrations of the IL-1β standard in PBS containing 0.1% BSA. As previously, the z-stack method on a confocal microscope was used to collect the fluorescence signal after the fiber samples were stained by the SPIO-IL-1β conjugates. Figure 4 illustrates the increase of the fluorescence signal with increasing concentration of IL-1β which can be attributed to the formation of more of the sandwich immunocomplex at the fiber sensing surface. Furthermore, a linear correlation was obtained in the concentration range of 3.13 $pg.mL^{-1}$ to 400 $pg.mL^{-1}$ (Figure 4 c), and the observed relationship could be expressed as $F = 148290 + 865153 \log c$ ($R^2 = 0.977$). The low detection limit was calculated to be

1.12 pg.mL^{-1}. In addition, to show the ability of the fiber immunosensor in spatial localized detection of IL-1β, 1μL two different concentrations (50 pg.mL^{-1} and 250 pg.mL^{-1}) of IL-1β were spotted onto two different locations of fiber sensing surface (Figure S5). After stained by the SPIO-IL-1β antibody conjugate, the two locations were imaged by a laser scanning confocal microscope. The fluorescence intensity from 250 pg.mL^{-1} area was around 2 times larger than that of 50 pg.mL^{-1} area, which indicated the fiber immunosensor is capable to spatially discriminate between different concentrations of IL-1β. Furthermore, the analytical performances of the fiber sensor were compared with the other previously reported methods, as shown in Table S1. It could be seen that the fabricated fiber immunosensor showed a relative wider linear range (3.13-400 pg.mL^{-1}) and comparatively lower detection limit (1.12 pg.mL^{-1}) than some of the previously reported methods [13, 14, 18, 27].

To investigate the specificity of the immunosensor, the developed fiber sensor was used to detect a certain concentration of IL-1β solution (25 pg.mL^{-1}) containing a mixture of possible interfering substances including IL-6 (400 pg.mL^{-1}), IL-8 (200 pg.mL^{-1}), TNF-α (400 pg.mL^{-1}), IFN-γ (400 pg.mL^{-1}) and 0.1% serum. There was no significant change of the response fluorescence signal when it compared with the fiber sensor utilized to detect the IL-1β without these possible interfering substances, indicating the good specificity of the immunosensor (Figure S6) The reproducibility of the method was examined by using 4 batches (3 fibers per batch) of freshly prepared fibers to carry out a series of measurements of 25 pg.mL^{-1} of IL-1β. The relative standard deviation of the measurements for intra-assay and inter-assay was less than 10% indicating an acceptable reproducibility.

3.5 *ex-vivo and in vivo* detection of IL-1β

To evaluate the applicability of the proposed immunosensor, the designed fiber sensor was firstly applied to detect IL-1β in an *ex-vivo setting*. To this aim, rat macrophages seeded in a 24-well plate were stimulated by lipopolysaccharide (LPS), and the secretions collected at 2h, 4h, 7h, 10h, 24 h were analyzed by the proposed fiber sensor. For comparative purposes, a commercial ELISA kit was introduced as a reference method for validation of the results (the performance of the standard ELISA was shown in Figure S7). As shown in Figure 5a, IL-1β secreted by rat macrophages was able to be detected by the fabricated fiber sensor. The concentration of IL-1β increased over the LPS stimulation time and reached the maximum at 10 h. The results were in accordance with the secretions detected by commercial ELISA kit, suggesting that the fabricated fiber sensor was able to be used for the *ex-vivo* detection of IL-1β. Furthermore, we explored the application of the fiber sensor in detection of IL-1β at the rat spinal cord. The surgeries were carried out on the lumbar vertebrae (for details of the surgical procedure see supplementary materials), then 4 pg of recombinant rat IL-1β was injected into the thoracic region through a PE 10 tube. Subsequently, the fiber was placed at the thoracic region and then withdrawn for the SPIO-IL-1β antibody staining. The area where around 1cm away from the injected thoracic region was considered as a control area. Z-stack confocal images were taken of control and injected areas on the fiber surface. Many green fluorescent dots could be observed in the injected areas (Figure 5 b,c), with significantly greater fluorescent intensity in the injected area of than that in the control area (Figure 5 d), indicating that the fiber immunosensor was able to detect IL-1β in the spinal cord, providing the capacity to repeatedly sample from the same animal, spatially and temporally resolved cytokine release.

4. Conclusions

We reported here an immunosensor created on the fiber surface that is capable of localized measurements of IL-1β in the rat spinal cord. A stable immunocapture surface for target recognition was successfully formed through introducing the biotinylated capture antibody by a biotin-streptavidin strategy. The effectiveness biotin-streptavidin strategy for the immobilization of the capture antibody was comprehensively investigated, and excellent stability of the sensing surface was achieved. The fabricated immunosensor showed excellent responses, a wide linear range, high sensitivity and good reproducibility. This optical fiber-based immunosensor overcomes some limitations of the traditional ELISA, as it can be applied to localized detection of IL-1β also in vivo. The detection occurs within a small sample volume, which makes it possible to detect variations in local concentration of the released cytokines (i.e. at the site of injury or disease). Furthermore, the fiber immunosensor detects the released cytokines, while the standard ELISA of tissue will only assess stored and not necessarily released and hence biologically active cytokine. In the case when ELISA is used for the assessment of cerebrospinal fluid (CSF) it will assess the released fraction, but it will provide no spatial information as the CSF is irreversibly drawn from the whole intrathecal space. The application of the fiber sensor was assessed by *ex-vivo* monitoring the secretions of the rat macrophages stimulated by LPS, and the results demonstrated good correlations with commercial ELISA kit. Moreover, the fiber sensor was successfully utilized for the localized measurement of IL-1β in rat spinal cord suggesting that our system provides the capacity to repeatedly sample from the same animal, spatially and temporally resolved cytokine release. This capability is fundamentally important in research and clinical applications.

Author disclosure statement

The authors declare no conflicts of interest.

Acknowledgments

This work was supported by the ARC Centre of Excellence for Nanoscale Biophotonics (Grant CE140100003). K. Zhang acknowledges the iMQRES scholarship.

References

[1] K. Gulati, S. Guhathakurta, J. Joshi, N. Rai, A. Ray, Cytokines and their Role in Health and Disease: A Brief Overview, MOJ Immunol, 4(2016) 00121.
[2] R.M. Gibson, N.J. Rothwell, R.A. Le Feuvre, CNS injury: the role of the cytokine IL-1,. Vet. J., 168(2004) 230-7.
[3] F.L. Van de Veerdonk, M.G. Netea, C.A. Dinarello, L.A. Joosten, Inflammasome activation and IL-1β and IL-18 processing during infection, Trends Immunol., 32(2011) 110-6.
[4] A. Amarasinghe, M.S. Abdul-Cader, Z. Almatrouk, F. van der Meer, S.C. Cork, S. Gomis, et al., Induction of innate host responses characterized by production of interleukin (IL)-1β and recruitment of macrophages to the respiratory tract of chickens following infection with infectious bronchitis virus (IBV), Vet. Microbiol., 215(2018) 1-10.
[5] I. Striz, Cytokines of the IL-1 family: recognized targets in chronic inflammation underrated in organ transplantations, Clin. Sci., 131(2017) 2241-56.
[6] D. Brough, N.J. Rothwell, S.M. Allan, Interleukin‐1 as a pharmacological target in acute brain injury, Exp. Physiol., 100(2015) 1488-94.
[7] C.-C. Chio, M.-T. Lin, C.-P. Chang, Microglial activation as a compelling target for treating acute traumatic brain injury, Curr. Med. Chem., 22(2015) 759-70.
[8] P. Ruscitti, P. Cipriani, F. Carubbi, V. Liakouli, F. Zazzeroni, P. Di Benedetto, et al., The role of IL-1β in the bone loss during rheumatic diseases, Mediators Inflamm., 2015(2015).
[9] M. Jahid, D. Chawla, R. Avasthi, R.S. Ahmed, Association of polymorphic variants in IL1B gene with secretion of IL-1β protein and inflammatory markers in north Indian rheumatoid arthritis patients, Gene, 641(2018) 63-7.
[10] M. Saito, Inflammasomes and related diseases, Jpn. J. Clin. Immunol., 34(2011) 20-8.
[11] C. Zhang, L. Xi, S. Zhao, R. Wei, Y. Huang, R. Yang, et al., Interleukin-1β and tumour necrosis factor-α levels in conjunctiva of diabetic patients with symptomatic moderate dry eye: case–control study, BMJ open, 6(2016) e010979.
[12] A.A. Jesus, R. Goldbach-Mansky, IL-1 blockade in autoinflammatory syndromes, Annu. Rev. Med., 65(2014) 223-44.
[13] C.-Y. Chiang, M.-L. Hsieh, K.-W. Huang, L.-K. Chau, C.-M. Chang, S.-R. Lyu, Fiber-optic particle plasmon resonance sensor for detection of interleukin-1β in synovial fluids, Biosens. Bioelectron., 26(2010) 1036-42.
[14] T.M. Battaglia, J.-F. Masson, M.R. Sierks, S.P. Beaudoin, J. Rogers, K.N. Foster, et al., Quantification of cytokines involved in wound healing using surface plasmon resonance, Anal. Chem., 77(2005) 7016-23.
[15] J.-Y. Wu, C.-L. Tseng, Y.-K. Wang, Y. Yu, K.-L. Ou, C.-C. Wu, Detecting interleukin-1β genes using a N2O plasma modified silicon nanowire biosensor, J. Exp. Clin. Med., 5(2013) 12-6.
[16] C.E. Krause, B.A. Otieno, G.W. Bishop, G. Phadke, L. Choquette, R.V. Lalla, et al., Ultrasensitive microfluidic array for serum pro-inflammatory cytokines and C-reactive protein to assess oral mucositis risk in cancer patients, Anal. Bioanal. Chem., 407(2015) 7239-43.
[17] J. Wu, Y. Chen, M. Yang, Y. Wang, C. Zhang, M. Yang, J. Sun, M. Xie, X. Jiang, Streptavidin-biotin-peroxidase nanocomplex-amplified microfluidics immunoassays for simultaneous detection of inflammatory biomarkers, Anal. Chim. Acta 982 (2017) 138-147.
[18] R. Duer, R. Lund, R. Tanaka, D.A. Christensen, J.N. Herron, In-plane parallel scanning: a microarray technology for point-of-care testing, Anal. Chem., 82(2010) 8856-65.
[19] E.B. Aydın, M. Aydın, M.K. Sezgintürk, Highly sensitive electrochemical immunosensor based on polythiophene polymer with densely populated carboxyl groups as immobilization matrix for detection of interleukin 1β in human serum and saliva, Sensors Actuators B: Chem., 270(2018) 18-27.

[20] E. Sánchez-Tirado, C. Salvo, A. González-Cortés, P. Yáñez-Sedeño, F. Langa, J. Pingarrón, Electrochemical immunosensor for simultaneous determination of interleukin-1 beta and tumor necrosis factor alpha in serum and saliva using dual screen printed electrodes modified with functionalized double–walled carbon nanotubes, Anal. Chim. Acta, 959(2017) 66-73.
[21] A. Baraket, M. Lee, N. Zine, M. Sigaud, J. Bausells, A. Errachid, A fully integrated electrochemical biosensor platform fabrication process for cytokines detection, Biosens. Bioelectron., 93(2017) 170-5.
[22] X. Liu, X. Song, Z. Dong, X. Meng, Y. Chen, L. Yang, Photonic crystal fiber-based immunosensor for high-performance detection of alpha fetoprotein, Biosens. Bioelectron. 91 (2017) 431-435.
[23] K. Zhang, G. Liu, E.M. Goldys, Robust immunosensing system based on biotin-streptavidin coupling for spatially localized femtogram mL− 1 level detection of interleukin-6, Biosens. Bioelectron., 102(2018) 80-6.
[24] K.X. Zhang, M.V. Baratta, G.Z. Liu, M.G. Frank, N.R. Leslie, L.R. Watkins, et al., A novel platform for in vivo detection of cytokine release within discrete brain regions, Brain, Behav., Immun., 71(2018) 18-22.
[25] G. Liu, K. Zhang, A. Nadort, M.R. Hutchinson, E.M. Goldys, Sensitive Cytokine Assay Based on Optical Fiber Allowing Localized and Spatially Resolved Detection of Interleukin-6, ACS Sens., 2(2017) 218-26.
[26] N. Green, Avidin. 4. Stability at extremes of pH and dissociation into sub-units by guanidine hydrochloride, Biochem. J, 89(1963) 609.
[27] P. Dutta, J. Sanseverino, P. Datskos, M. Sepaniak, Nanostructured cantilevers as nanomechanical immunosensors for cytokine detection, Nanobiotechnology, 1(2005) 237-44.

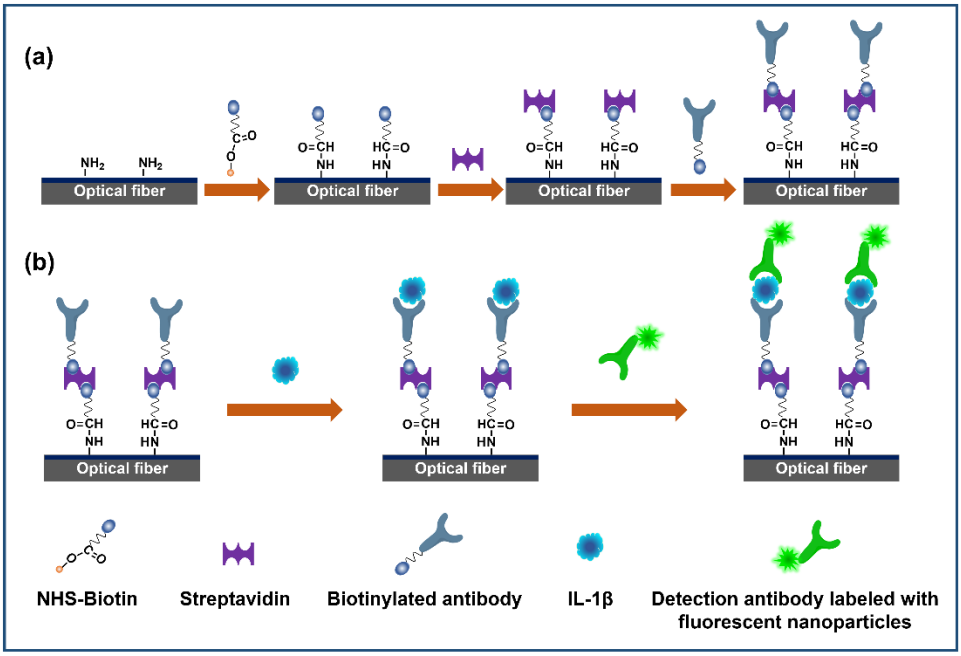

Scheme 1 (a) The procedure of the fabrication of the sensing surface. (b) The steps of preparing a fiber biosensor for the determination of IL-1β.

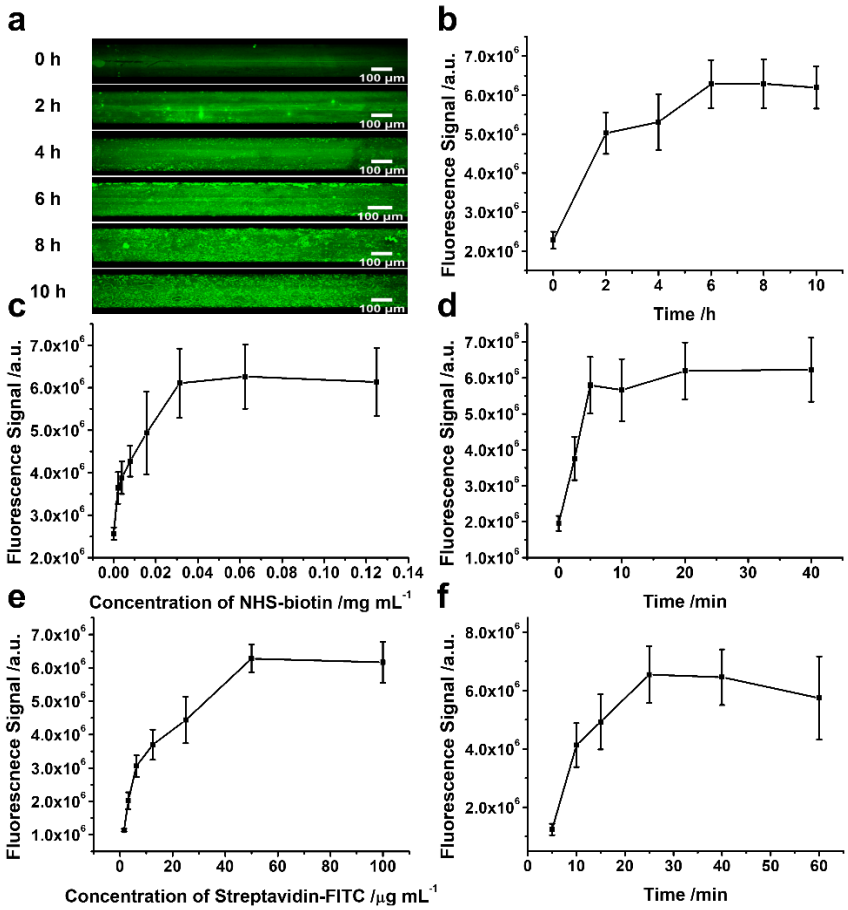

Figure 1 (a) Fluorescence image of the fiber surface treated by APTES with different incubation time after reacted with NHS-biotin and stained by streptavidin-FITC. (b) The corresponding fluorescence signal of the images from (a). (c) Optimization of NHS-biotin concentration. (d) Optimization of NHS-biotin reaction time. (e) Optimization of streptavidin concentration. (f) Optimization of streptavidin incubation time.

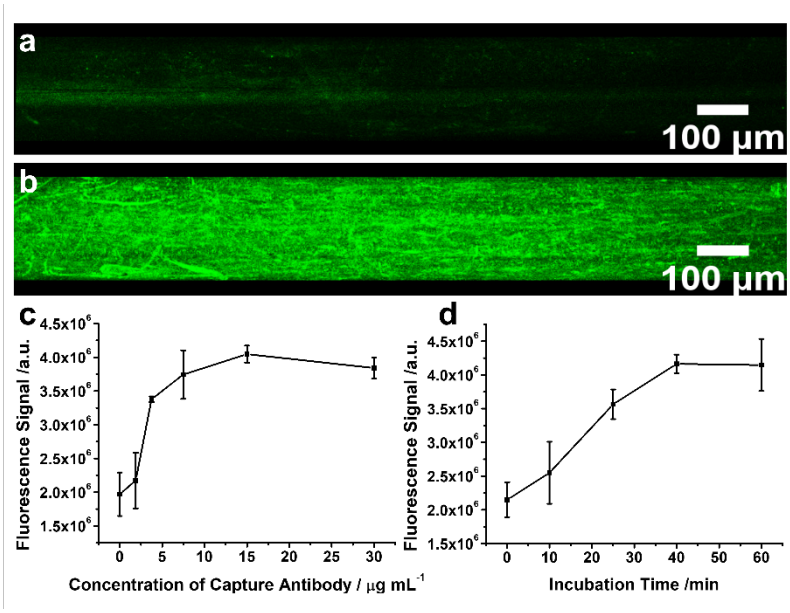

Figure 2. Fluorescence image of the fiber surface before (a) and after (b) attachment of the biotinylated capture antibody followed being stained by the fluorescent secondary antibody. (c) Optimization of the biotinylated capture antibody concentration. (d) Optimization of the incubation time of the biotinylated capture antibody.

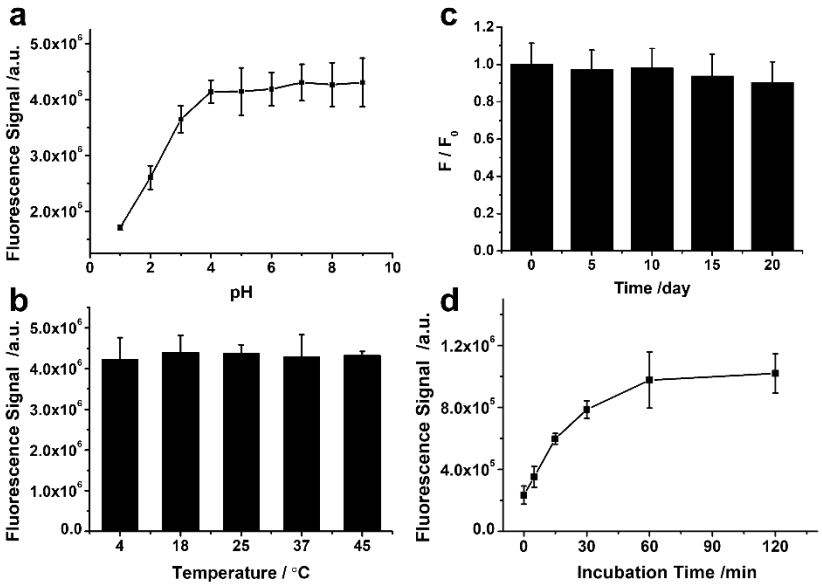

Figure 3. (a) Effect of pH on the sensing surface. (b) Effect of temperature on the sensing surface. (c) Effect of storage time on the sensing surface. (d) Optimization of the formation time of the capture antibody-antigen immunocomplex.

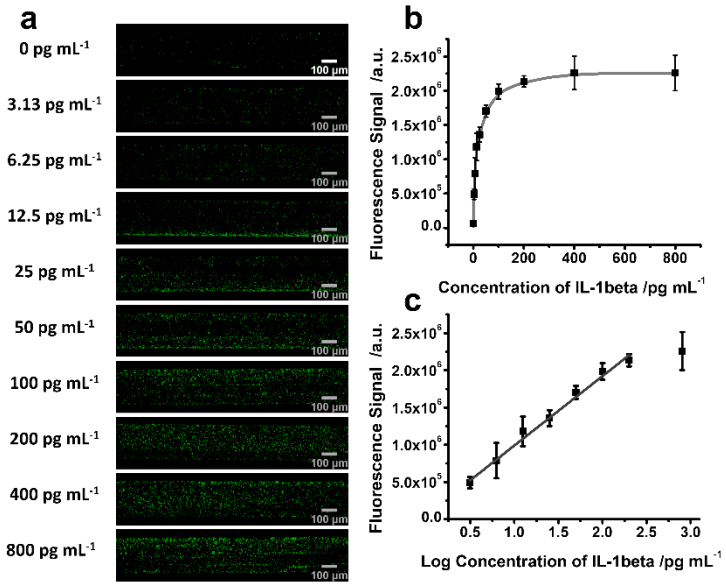

Figure 4. (a) Fluorescence images of the fiber sensor in detection of different concentration of IL1β followed being stained by SPIO-1L-1β detection antibody conjugates. (b) The corresponding fluorescence signal of the images from (a). (c) Plot of the fluorescence signal vs log concentration of IL-1β.

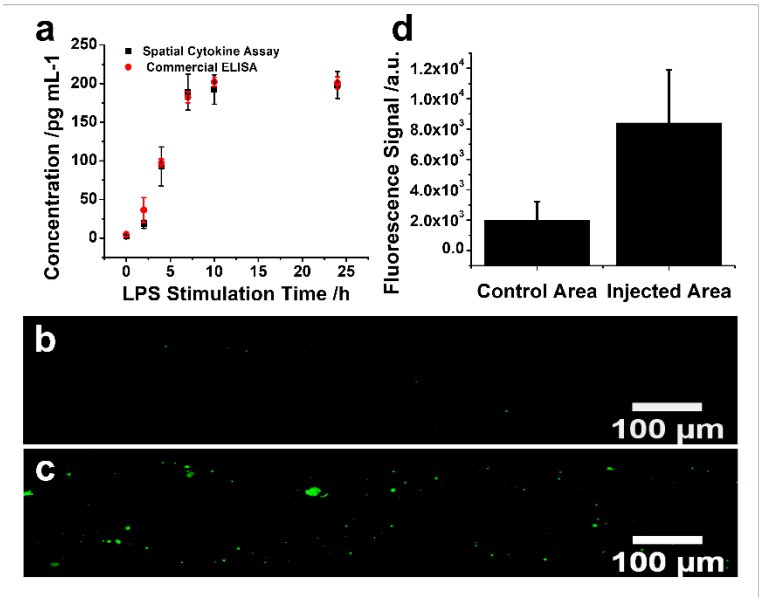

Figure 5 (a)The comparison of the IL-1β in rat macrophages secretions detected by the fiber sensor and commercial ELISA kit. (b, c) Confocal z-stack maximum intensity projection images of optical fibers taken in the spinal cord area without (b) and with (c) recombinant IL-1 β injection. (d) Mean (± SEM) fluorescent signal of fiber from the control and injected area.

Supplementary Material

Article Type: Full length Article

Title: An optical fiber based immunosensor for localized detection of IL-1β rat spinal cord

Authors: Kaixin Zhang[1,2], Azim Arman[3,4], Ayad G Anwer[1,2], Mark R Hutchinson[3,4], Ewa M. Goldys*[5]

Author Affiliations: [1]ARC Centre of Excellence in Nanoscale Biophotonics (CNBP), Macquarie University, Sydney, NSW 2109, Australia; [2]Department of Physics and Astronomy, Macquarie University, Sydney, NSW 2109, Australia; [3]ARC Centre of Excellence for Nanoscale BioPhotonics (CNBP), The University of Adelaide, Adelaide, SA 5005, Australia; [4]Institute for Photonics and Advanced Sensing (IPAS) and Adelaide Medical School, The University of Adelaide, Adelaide, SA 5005, Australia; Graduate School of Biomedical Engineering, [5]The University of New South Wales, Sydney, NSW 2052, Australia

***Corresponding Authors:** Ewa M. Goldys; Graduate School of Biomedical Engineering, The University of New South Wales, Sydney, NSW 2052, Australia

email: e.goldys@unsw.edu.au

Characterization of the SPIO-IL-1β detection antibody conjugates

To confirm the successful combination between the SPIO and the detection antibody, Zeta potential was used to monitor the charge changes on the SPIO surface. As shown in Figure 1a, SPIO showed a negative charge at around -40 mV, indicating the stability of SPIO dispersions. The value of the zeta potential shifted to -30 mV, which suggested that the detection antibody was successfully conjugated with the SPIO by the EDC/NHS coupling chemistry.

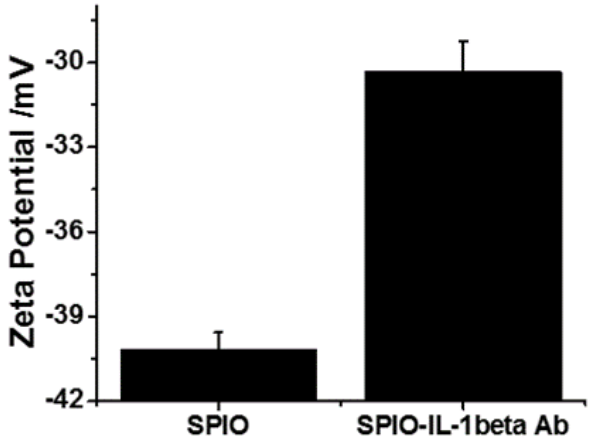

Figure S1 Zeta Potential of the SPIO and the bioconjugates of fluorescent beads antibody conjugates (SPIO-IL-1β Ab)

The effect of blocking buffer on the sensing surface

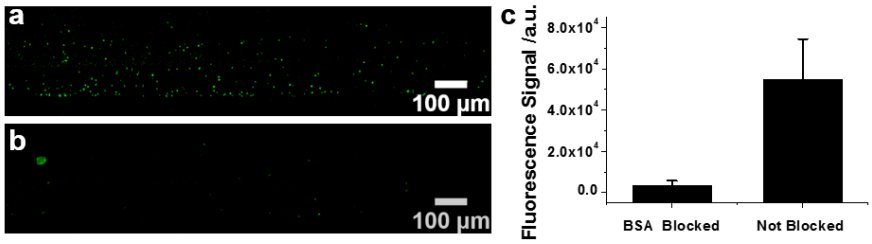

Figure S2 (a,b) The confocal microscope images of the fibre sensing surface before (a)/after (b) being treated by BSA followed incubating with SPIO-IL-1β conjugates. (c) Fluorescence intensity of (a) and (b)

To minimise the non-specific interactions of fiber sensing surface, BSA was introduced to block the sensing surface. Blocking effect of the BSA was assessed by incubating the fibers with SPIO-IL-1β antibody conjugates. As shown in figure S2, an obvious discrimination was observed between the fiber before and after being treated with BSA. Many fluorescent dots appeared on the not blocked fiber surface indicating the strong nonspecific adsorption of the sensing surface. While after the fiber treated by BSA, significant reduce of the fluorescent beads was observed which suggested that BSA effectively covered the defects of the sensing surface. The non-specific fluorescence intensity decreased from 5.5 $\times 10^4$ a.u. to 3.4 $\times 10^3$ a.u. indicating the efficiency of BSA in the elimination of protein adsorption.

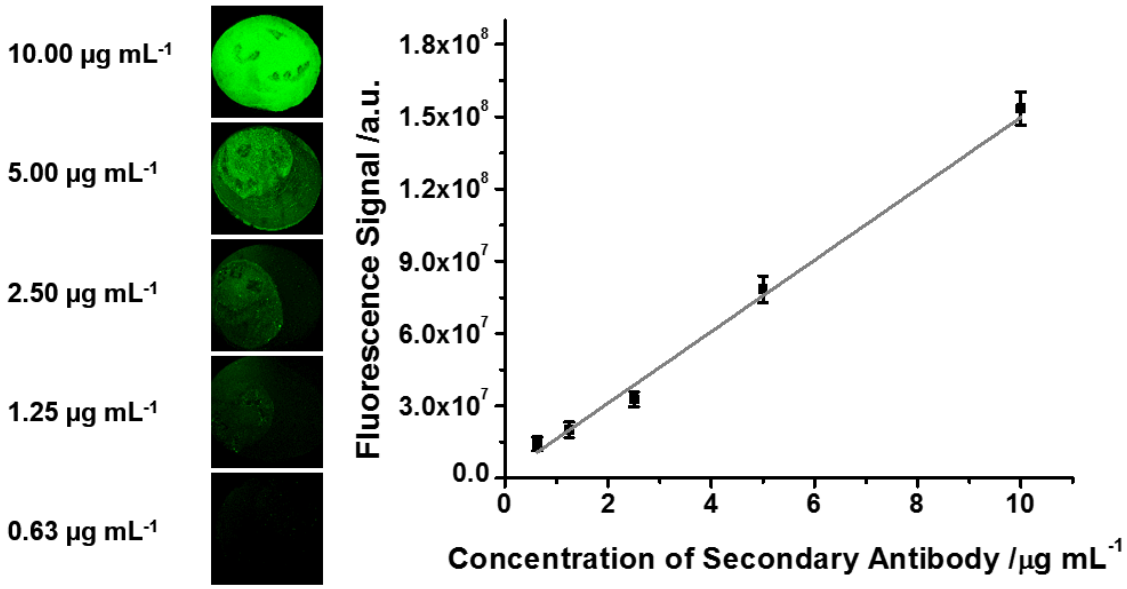

Figure S3 The calibration curve of the fluorescence intensity versus the concentration of the secondary antibody.

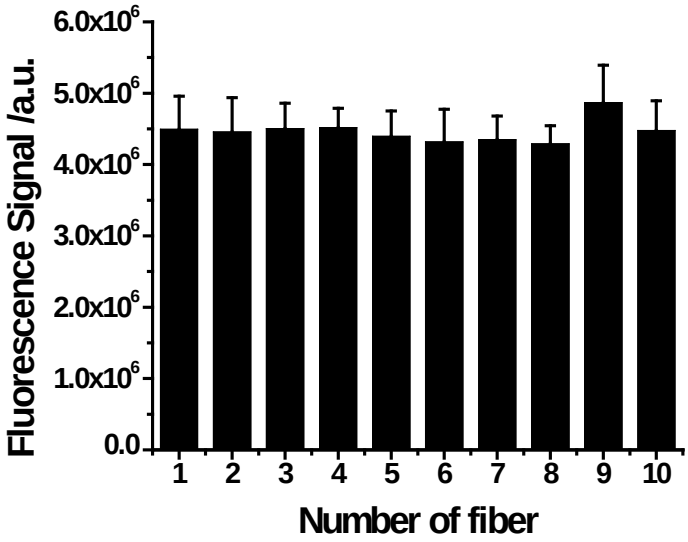

Figure S4 The reproducibility of the fabrication sensing surface

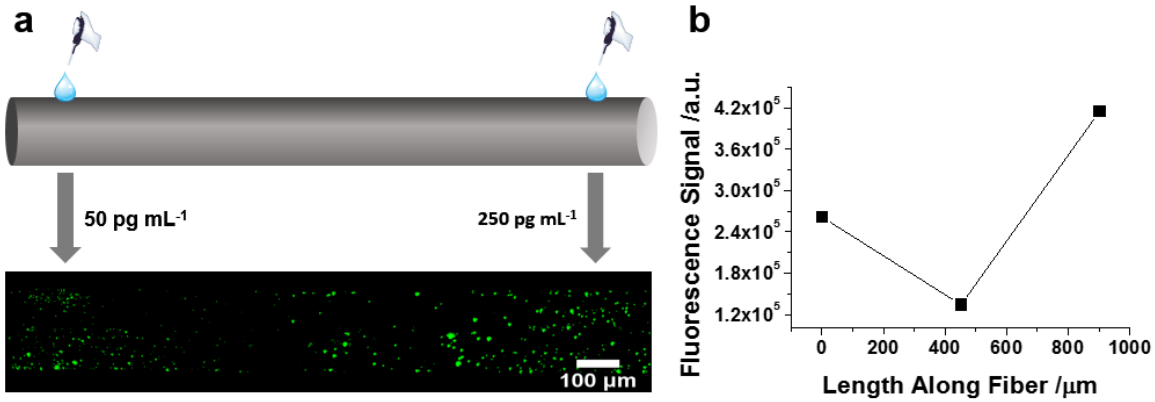

Figure S5 (a) localized determination of IL-1β by pipetting two different concentrations of IL-1β on the fiber sensing surface; (b)The changes of the fluorescence intensity along the length of fiber with the spatial resolution of 450 µm.

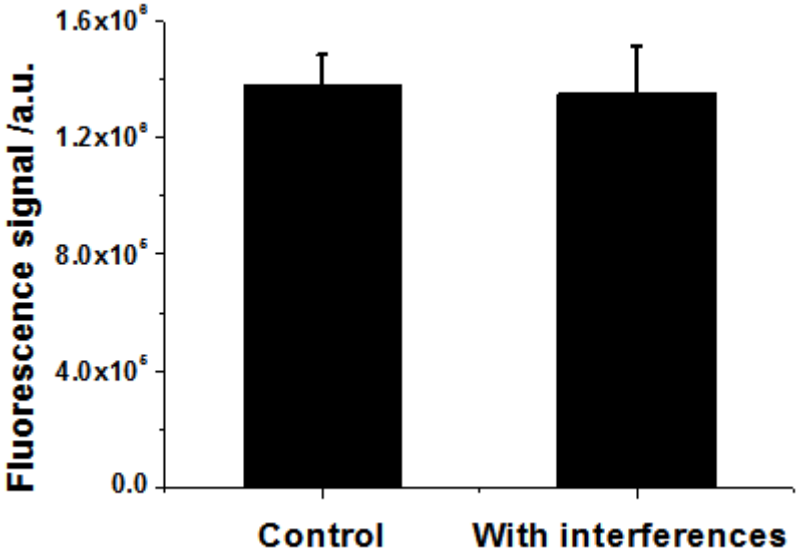

Figure S6 Fluorescence signal of the fiber immunosensor in detection of 25 pg. mL^{-1} IL-1β with and without a mixture of possible interfering substances including IL-6 (400 $pg.mL^{-1}$), IL-8 (200 $pg.mL^{-1}$), TNF-α (400 $pg.mL^{-1}$), IFN-γ (400 $pg.mL^{-1}$) and 0.1% serum.

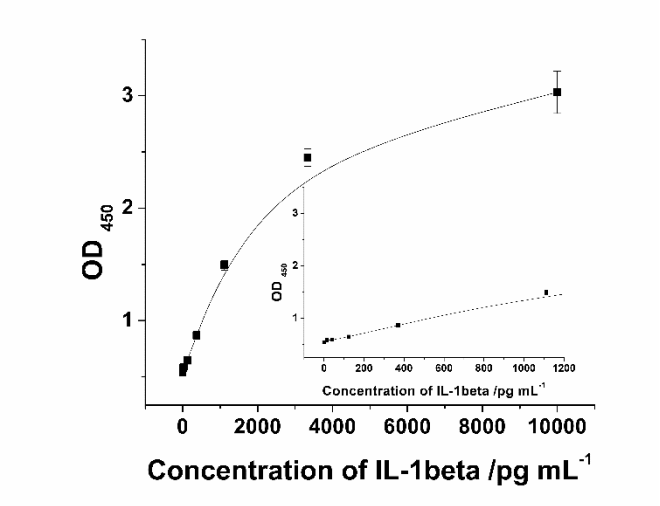

Figure S7 The performance of the ELISA kit in the detection of IL-1beta. (Linear range：41.1 pg.mL^{-1}~1111.1 pg.mL^{-1}; Detection limit: 13.7 pg.mL^{-1})

Surgical procedure

Under deep anaesthesia (initiated and maintained by inhaled isoflurane 2%), a midline skin incision was made from L2 to L5 followed by a bilateral dissection of paraspinous muscles. Subsequently, total dorsal laminectomy was performed on the lumbar vertebrae (L3-L5), with the dura matter left intact. Hemostasis was achieved by gauze packing and/or saline washing. A PE10 catheter linked to a Hamilton syringe was placed dorsally on dura matter at the level of L2 and pushed proximally up to 4 cm. 4 ng of recombinant rat IL-1β in 1 μL was injected into the thoracic region. Then, the functionalized fiber was inserted to this site and remained there for 10 minutes. After this time the fiber was withdrawn and stored in the blocking buffer (0.5%BSA+0.1% tween 20+PBS). Finally, the fiber was then processed with SPIO-IL-1β detection antibody for confocal microscope imaging.

Table S1. Comparison of the analytical characteristics of the fiber immunosensor with other previously reported techniques for determination of IL-1β.

Method	Minimum sample Volume (µL)	Linear range (pg mL^{-1})	Detection limit (pg mL^{-1})	Real sample analysis	Localized detection of IL-1β	In Ex-vivo/vivo detection of IL-1β	Reference
ELISA kit	100	68.59 - 50000	< 80	Tissue and cell culture extracts	No	No	Abcam
ELISA kit	50	31.3-2,000	4.0	Supernatants, Serum	No	No	Thermo Fisher Scientific
ELISA kit	100	15.6 - 1000	< 10	Serum, plasma, tissue and cell culture extracts	No	No	Abbexa Ltd
ELISA kit	100	31.25-2000	12.5	Supernatants, Serum	No	No	Proteintech Group Inc
Electrochemical immunosensor (Impedimetric)	NA	0.01 - 3	0.001	Serum and saliva	No	No	[1]
Electrochemical immunosensor (Amperometry)	2.5	0.5 - 100	0.38	Spiked serum	No	No	[2]
Electrochemical immunosensor (Impedimetric)	NA	1 - 15	NA	No	No	No	[3]
Electrochemical immunosensor (Amperometric microfluidic array)	5	50 - 500	0.01	Serum	No	No	[4]
Dendrimer-based assay	100	0.98-250	<1.15	No	No	No	[5]
Microarray technology	40	11.7 - 175	11.7	No	No	No	[6]
Fiber-optic particle plasmon resonance sensor	200	50 - 10000	21	Synovial fluids	No	No	[7]
Fiber-optic surface plasmon resonance sensor	NA	1000 - 100000	290	Cell culture medium	No	No	[8]
Nanostructured microcantilevers biosensor	150	10000 - 1200000	<10000	No	No	No	[9]
Fluorescence-based fiber immunosensor	1	3.13 - 400	1.12	Cell culture medium	Yes	Yes	This work

[1] E.B. Aydın, M. Aydın, M.K. Sezgintürk, Highly sensitive electrochemical immunosensor based on polythiophene polymer with densely populated carboxyl groups as immobilization matrix for detection of interleukin 1β in human serum and saliva, Sensors Actuators B: Chem., 270(2018) 18-27.

[2] E. Sánchez-Tirado, C. Salvo, A. González-Cortés, P. Yáñez-Sedeño, F. Langa, J. Pingarrón, Electrochemical immunosensor for simultaneous determination of interleukin-1 beta and tumor necrosis factor alpha in serum and saliva using dual screen printed electrodes modified with functionalized double–walled carbon nanotubes, Anal. Chim. Acta, 959(2017) 66-73.

[3] A. Baraket, M. Lee, N. Zine, M. Sigaud, J. Bausells, A. Errachid, A fully integrated electrochemical biosensor platform fabrication process for cytokines detection, Biosens. Bioelectron., 93(2017) 170-5.

[4] C.E. Krause, B.A. Otieno, G.W. Bishop, G. Phadke, L. Choquette, R.V. Lalla, et al., Ultrasensitive microfluidic array for serum pro-inflammatory cytokines and C-reactive protein to assess oral mucositis risk in cancer patients, Anal. Bioanal. Chem., 407(2015) 7239-43.

[5] H.J. Han, R.M. Kannan, S. Wang, G. Mao, J.P. Kusanovic, R. Romero, Multifunctional Dendrimer‐Templated Antibody Presentation on Biosensor Surfaces for Improved Biomarker Detection, Adv. Funct. Mater., 20(2010) 409-21.

[6] R. Duer, R. Lund, R. Tanaka, D.A. Christensen, J.N. Herron, In-plane parallel scanning: a microarray technology for point-of-care testing, Anal. Chem., 82(2010) 8856-65.

[7] C.-Y. Chiang, M.-L. Hsieh, K.-W. Huang, L.-K. Chau, C.-M. Chang, S.-R. Lyu, Fiber-optic particle plasmon resonance sensor for detection of interleukin-1β in synovial fluids, Biosens. Bioelectron., 26(2010) 1036-42.

[8] T.M. Battaglia, J.-F. Masson, M.R. Sierks, S.P. Beaudoin, J. Rogers, K.N. Foster, et al., Quantification of cytokines involved in wound healing using surface plasmon resonance, Anal. Chem., 77(2005) 7016-23.

[9] P. Dutta, J. Sanseverino, P. Datskos, M. Sepaniak, Nanostructured cantilevers as nanomechanical immunosensors for cytokine detection, Nanobiotechnology, 1(2005) 237-44.

5.3 Summary

This chapter demonstrated an immunosensor created on the fiber surface that is capable of localized measurements of IL-1β in the rat spinal cord. This is a further application extension of the fiber immunosensor. The effectiveness of the biotin streptavidin strategy for the immobilization of the capture antibody was comprehensively investigated, and excellent stability of the sensing surface was achieved. The fabricated immunosensor showed excellent responses, a wide linear range, high sensitivity and good reproducibility. The application of the fiber sensor was assessed by ex-vivo monitoring the secretions of the rat macrophages stimulated by LPS, and the results demonstrated good correlations with commercial ELISA kit. The ability of the fiber immunosensor in localized measurements of the cytokine in the spinal cord would help to define the role of the cytokine in SCI and provide useful information for SCI diagnosis and therapy.

6
Conclusions and perspectives

6.1 Summary

The work through my Ph.D. project demonstrated the cytokine immunosensor performed on the optical fiber surface and its biological applications from *in vitro* to *in vivo*. By using two kinds of antibody immobilization methods, covalent coupling with 6-mercaptohexanoic acid (MA), and biotin-streptavidin strategy, we achieved two types of sensing surface on the fiber and investigated the feasibility of the sensing fiber in cytokine detection from *in vitro* to *in vivo*.

Development of sensing surface.

Firstly, we fabricated aminopropyltriethoxysilane (APTES)-gold nanoparticle (AuNP)-6-mercaptohexanoic acid (MA) modified silica optical fiber, suitable for antibody immobilization. In our method, fiber was firstly functionalized with APTES to enable a layer of AuNPs self-assembled on the fiber surface. After attachment of AuNPs to the fiber surface, the impurities were covered by the layer of AuNPs resulting a homogeneous surface with big surface area, which is favorable for the attachment of the maximum amount of capture antibody. This strategy fabricated sensing surface firstly showed its performance in cytokine IL-6 detection with a limit of detection of 1 $pg.mL^{-1}$ and around 9 days stability in PBS solution.

To further promote the performance of the sensing surface, we introduced biotin-streptavidin coupling strategy for antibody immobilization to enhance the sensitivity and stability. In this immobilization method, the fiber surface was firstly functionalized by APTES to provide an amine-terminated polymer layer. Biotin was directly attached to the fiber surface by reacting sulfo-NHS-biotin with the amine-terminated polymer-coated fiber. Then a streptavidin layer contains two biotin-binding sites facing the optical fiber and two terminated binding sites which are available to bind capture molecules, the biotinylated capture antibody. This biotin-streptavidin coupling strategy creates a robust and ultrasensitive immunosensor for the cytokine detection, making the limit of detection from $pg\ mL^{-1}$ to $fg\ mL^{-1}$ level, and enhancing the stability up to 4 weeks.

Feasibility of the immunosensor used in different biological applications.

In order to investigate the potential applications of the fabricated immunosensor, we have carried out a series of experiments using them and obtained satisfactory results.

Firstly, we have demonstrated the application of this immunosensor in cytokine detection in the cell culture medium. The optical fiber sensor was applied for the detection of IL-6 secreted by live BV-2 cells, the concentration of IL-6 secreted into the medium increased with the LPS stimulation time and the maximum concentration was obtained after 6 h lipopolysaccharide (LPS) stimulation. This has been validated by the standard ELISA and a similar IL-6 secretion pattern for BV-2 cells was obtained, indicating the excellent detection ability of the fiber immunosensor. Similarly, we have also explored the application of the fiber sensor in *ex-vivo* monitoring the cytokine IL-1β in the secretions of the rat macrophages stimulated by lipopolysaccharide (LPS), and the results also demonstrated good correlations with a commercial ELISA kit. All these results demonstrated the protentional application of this fabricated fiber immunosensor for monitoring cytokines *ex vivo*.

To further advanced the application of the fiber immunosensor from *ex-vivo* to *in vivo*, we designed an optical fiber-based immunosensing device for repeated monitoring of spatially localized cytokine IL-1β release in the rodent brain. This immunosensing device comprises a blue cap on the fiber head and the silica optical fiber labeled with a IL-1β capture antibody on the surface interface that can be inserted into a stainless steel brain implanted cannula with micrometer-sized holes drilled along its length to enable fluid exchange between the outside and inside of the cannula. The results showed that an increase in fluorescence detection of spatially localized intrahippocampal IL-1β release was observed following a peripheral LPS challenge in Sprague Dawley rats. This novel immunosensing technology represents an opportunity for unlocking the function of neuroimmune signaling. In addition, we have carried out a simple test of the fiber immunosensor in a spinal cord of an anesthetized rat. Recombinant rat IL-1β was injected into the thoracic region, and then the fiber was inserted for the cytokine detection. Many green fluorescent dots could be observed in the injected areas, with significantly greater fluorescent intensity in the injected area than that in the control area, indicating that the fiber immunosensor was able to detect IL-1β in the spinal cord.

Moreover, it would be interesting to learn that all the sensing platforms in the thesis are based on the same sandwich immunoassay approach, the basic principle of this type sensor is based on the specific interaction between a sequence of amino acids found on an antigen(cytokine) and an antibody binding site that matches. So different cytokine-antibody pairs are corresponding to different specific sequences of amino acids, resulting in different

type of affinity ability between the antigen and the antibody. So when the fiber immunosensor was used for the cytokine detection, there will be a different formula to reflect the relationship between the detection signal (Y-axias) and the increase of cytokine concentration. The reason why the calibration curves sometimes include concentration or log(concentration) in the x-axis, was just to choose the best fitting curve for standard curve of the specific fiber immunosensor.

6.2 Future work

The performance of the developed cytokine immunosensor in this thesis can be further enhanced in terms of fabrication procedure, stability and application of the immunosensor, to better enable translation into commercial products. From the user perspective, the major issues that need to be addressed include:

(1) The procedures for the fabrication of immunosensor in this thesis are a little bit complex, which is unpleasant for users especially if they had never worked in the chemistry area. The complex protocol and long analysis time will hinder the wide application of the fiber immunosensor in various fields, so an alternative design with simple protocol shortening the analysis time should be envisaged. This might be improved by using more commercially available materials to reduce the fabrication procedure. For example, amine-terminated polymer-coated fibers are able to be purchased from some fiber manufacturers, and the detection antibody-fluorescent beads conjugates can be obtained from the antibody or nanoparticle manufacturers (eg: R&D system, Bangs Laboratories, Inc. Spherotech etc.). As a result, an immunosensing platform simpler than the one reported in the thesis will be targeted in the future.

(2) The sensing surface fabricated by biotin-streptavidin strategy can be stable in the PBS for around 4 weeks, this might be not satisfactory enough for a commercially available product. To solve this issue, one way might be shortening the fabrication procedure and finding an easier and faster way to prepare the immunosensor so that people can use the freshly prepared fiber sensor at the time they need. Another way is improving the storage conditions, the fiber sensor surface might be able to be stored in a dry state rather than in the PBS solution as mentioned in the thesis. Some storage experience of commercial products (eg: antibody coated ELISA plate) should be able to offer some useful reference for improving this issue. To enable these immunosensors to be commercially available for practical work, it is also critical to make the preparation of the immunosensor sufficiently well standardized so that the prepared immunosensor can be highly reproducible to be

reliable. Finally, alternative bioreceptors, such as DNA aptamers, could also be proposed to improve the storage stability, as well as to facilitate simple and fast regeneration of the sensing surface, contributing to the potential future use of the sensor for continuous monitoring purposes.

(3) A problem we met is that when we explore the application of this fiber immunosensor, the silica glass optical fiber was easy to break, especially when the fiber was applied to the cytokine detection in behavior animals. This drives us to find a more flexible type of fiber to replace the current silica glass fiber. The plastic fiber might be a good choice to solve this issue, as there is a lot of flexible polymer fibers (eg: PMMA, PS, PDMS, PC) available in the market.

In addition to these issues, further advances can be made in multiplex-cytokine sensing based on the optical fiber. The ability to measure multiple cytokines simultaneously is extremely important in various physiological conditions because the release of the cytokine is often in a cascade type and the concentration fluctuations of one cytokine often induce changes in other networked cytokines [1-3]. Most of the current developed multiplex-cytokine sensing is generally based on the multiplexed bead systems. In bead-based multiplex immunoassays, identifiable bead sets (multi-colored) are functionalized with desired and specific capture antibodies. These beads are then incubated with the samples allowing the analytes of interest specifically captured by individual functionalized beads. Following this, labeled detection antibodies bind to the analyte-capture antibody-bead complex to make a multimember solid phase sandwich that when passed through the detection system allows the identification and quantification of the desired immunocomplex. This beads system has offered a solid foundation for the multiplex analyte signaling strategy which can be briefly introduced on the optical fiber system to realize multiplex-cytokine sensing. The difficulty for fabrication a multiplex-cytokine immunosensor on the optical fiber might be the immobilization of various antibodies in their native conformation. The microarray protein fabrication technologies might offer useful experiences on the antibody immobilization. Immobilization methods like UV photolithography and microcontact printing method (where proteins can be immobilized by a stamping action with a micro-patterned elastomeric stamp) [4-6] or a non-contacting method that employs ink jetting [7, 8] or the electrospray deposition method [9, 10] should be able to solve the problems for the fabrication of the multiplex-cytokine sensing surface on the optical fiber. As a result, by combinating the smart signaling strategy from the beads-based system and the developed

microarray protein fabrication technologies, it is expected that the multiplex-cytokine sensing performed on the fibre surface would be realized soon.

Apart from the multiplex cytokine sensing, it would be promising to develop the fiber immunosensor into a point-of-care (POC) device. In this case, the signal read-out system should be miniaturized, to achieve this goal, one way is to create a laser-CMOS image sensor system to realize the collection of the fluorescence signal when the detection antibody labeled with fluorescence particles/dyes is excited by the relevant laser. Until now, people have made great efforts to promote the development of the miniaturization of the sensor read-out system, as this signal read-out system is an indispensable requirement for the POC testing applications such as in the field of the product quality control, environmental monitoring, safety monitoring for foods and beverages, and the rapid detection against the bio-terrorism. In particular, the development of Spreeta, a miniature version of a commercially available surface plasmon resonance (SPR) biosensor has offered solid foundation for the fabrication of the minimized read-out system for the fiber immunosensor, as the image sensing system for the SPR sensor chip can be easily transferred to the fiber surface for imaging and many system parameters' set-up are universally compatible, as both of them might involve in a similar system (Figure 6-1) that a laser beam from a diode laser (as the incident light source for SPR/excitation laser beam for the fiber immunosensor) was modulated with a rotating mirror, where a part of the reflected and diverged light from the centre of the rotating mirror is focused on the imaging sensor chips/fibers, and then the reflected light/excited fluorescence signal from the sensor chip/fibers is captured by a CMOS image sensor, which is controlled by a notebook PC via a USB interface [11].

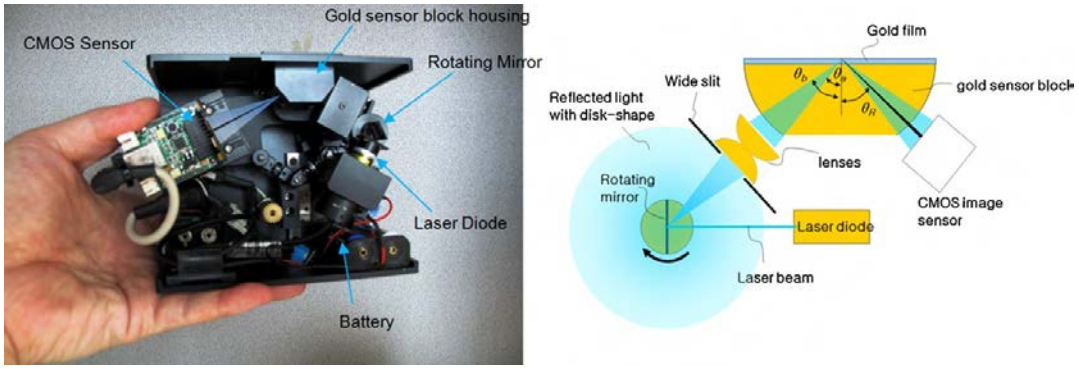

Figure 6-1. Interior (left) and a scheme (right) of the palm-sized SPR biochemical sensor system are based on the modulation of laser light by a rotating mirror [11].

This fiber immunosensor technology provides a new strategy for monitoring spatially varying concentration of cell secreting products, apart from that it has the potential to be

developed as a point-of-care device for multiple health conditions, it is also of great potentional to be developed for the spinal cord injury diagnosis and therapy, as cytokines are considered as signaling proteins that play important roles in the pathophysiology of spinal cord injury [12]. It is evidenced that cytokines have homeostatic physiologic and neuromodulatory functions in the central neuro system (the brain and spinal cord), and they are able to contribute to neuronal damage and destruction when their concentration exceeds a certain threshold. In addition, the upregulation of these cytokines, together with the consequent cellular infiltration they cause, can cause a significant effects in the determination of the extent of the secondary tissue damage and neural degeneration observed after the injury [13-15].Therefore, the study of cytokine release in spinal cord could bring to light novel potential therapeutic targets that could reduce the degenerative processes that occur after spinal cord injury. Moreover, as this type immunosensor has the ability to capture interstitial cytokine levels or cytokine release in discrete brain regions and holds great promise for selective, rapid and serial measurement of cytokine release in the central neuro system, it also offers an opportunity for unlocking the function of neuroimmune signalling and provides the potential to elucidate pathological dynamics underlying neuropsychiatric disease.

6.3 Reference

[1] R.C. Bone, Toward a theory regarding the pathogenesis of the systemic inflammatory response syndrome: what we do and do not know about cytokine regulation, Critical care medicine 24(1) (1996) 163-172.
[2] F. Balkwill, F. Burke, The cytokine network, Immunology today 10(9) (1989) 299-304.
[3] M.C. Cohen, S. Cohen, Cytokine function: a study in biologic diversity, American journal of clinical pathology 105(5) (1996) 589-598.
[4] A. Bernard, E. Delamarche, H. Schmid, B. Michel, H.R. Bosshard, H. Biebuyck, Printing patterns of proteins, Langmuir 14(9) (1998) 2225-2229.
[5] C. Donzel, M. Geissler, A. Bernard, H. Wolf, B. Michel, J. Hilborn, E. Delamarche, Hydrophilic poly (dimethylsiloxane) stamps for microcontact printing, Advanced materials 13(15) (2001) 1164-1167.
[6] M. Blees, Micro-contact printing method, Google Patents, 2005.
[7] L. Pardo, W.C. Wilson, T. Boland, Characterization of patterned self-assembled monolayers and protein arrays generated by the ink-jet method, Langmuir 19(5) (2003) 1462-1466.
[8] A. Roda, M. Guardigli, C. Russo, P. Pasini, M. Baraldini, Protein microdeposition using a conventional ink-jet printer, Biotechniques 28(3) (2000) 492-496.
[9] S. Kavadiya, P. Biswas, Electrospray deposition of biomolecules: applications, challenges, and recommendations, Journal of Aerosol Science (2018).
[10] B. Lee, J. Kim, K. Ishimoto, Y. Yamagata, A. Tanioka, T. Nagamune, Fabrication of protein microarrays for immunoassay using the electrospray deposition (ESD) method, Journal of chemical engineering of Japan 36(11) (2003) 1370-1375.
[11] Y.-B. Shin, H.M. Kim, Y. Jung, B.H. Chung, A new palm-sized surface plasmon resonance (SPR) biosensor based on modulation of a light source by a rotating mirror, Sensors and Actuators B: Chemical 150(1) (2010) 1-6.
[12] E. Garcia, J. Aguilar-Cevallos, R. Silva-Garcia, A. Ibarra, Cytokine and growth factor activation in vivo and in vitro after spinal cord injury, Mediators of inflammation 2016 (2016).
[13] J. Glaser, R. Gonzalez, V.M. Perreau, C.W. Cotman, H.S. Keirstead, Neutralization of the chemokine CXCL10 enhances tissue sparing and angiogenesis following spinal cord injury, Journal of neuroscience research 77(5) (2004) 701-708.
[14] S.I. Lee, S.R. Jeong, Y.M. Kang, D.H. Han, B.K. Jin, U. Namgung, B.G. Kim, Endogenous expression of interleukin‐4 regulates macrophage activation and confines cavity formation after traumatic spinal cord injury, Journal of neuroscience research 88(11) (2010) 2409-2419.
[15] J.R. Plemel, V.W. Yong, D.P. Stirling, Immune modulatory therapies for spinal cord injury–past, present and future, Experimental neurology 258 (2014) 91-104

7
List of publications

Peer-reviewed publications:

1. **Kaixin Zhang,** Azim Arman, Ayad G Anwer, Mark R Hutchinson, Ewa M. Goldys, An optical fiber based immunosensor for localized detection of IL-1β in rat spinal cord. Sensors and Actuators B: Chemical 282 (2019): 122-129.
2. **Kaixin Zhang**, Michael V. Baratta, Guozhen Liu, Matthew G. Frank, Nathan R. Leslie, Linda R. Watkins, Steven F. Maier, Mark R. Hutchinson, and Ewa M. Goldys, A novel platform for in vivo detection of cytokine release within discrete brain regions. Brain, Behavior, and Immunity, 71 (2018): 18-22.
3. **Kaixin Zhang**, Guozhen Liu, and Ewa M. Goldys. ”Robust immunosensing system based on biotin-streptavidin coupling for spatially localized femtogram mL−1 level detection of interleukin-6.” Biosensors & Bioelectronics 102 (2018): 80-86.
4. Guozhen Liu*, **Kaixin Zhang**, Annemarie Nadort, Mark R. Hutchinson, and Ewa M. Goldys. "Sensitive Cytokine Assay Based on Optical Fiber Allowing Localized and Spatially Resolved Detection of Interleukin-6." ACS sensors 2 (2017): 218-226.
5. Li, Jiawen, Heike Ebendorff-Heidepriem, Brant C. Gibson, Andrew D. Greentree, Mark R. Hutchinson, Peipei Jia, Roman Kostecki, Guozhen Liu, Antony Orth, Martin Ploschner, Erik P. Schartner, Stephen C. Warren-Smith, **Kaixin Zhang**, Georgios Tsiminis, and Ewa M. Goldys. "Perspective: Biomedical sensing and imaging with optical fibers—Innovation through convergence of science disciplines." APL Photonics 3, no. 10 (2018): 100902.

Conference proceedings and abstracts:

1. **Kaixin Zhang**, Guozhen Liu, Ewa M. Goldys. Development of a robust immunosensing

platform for sensitive detection of interleukin-6. 28th World Congress on Biosensors, Miami, Florida, USA (June 2018)

2. Ewa M. Goldys, Guozhen Liu, Ayad Anwer, **Kaixin Zhang**. nanoparticle-based strategy for ultrasensitive cytokine detection. International Conference on Biophotonics V Perth, Australia (30 April - 1 May 2017)
3. Ewa M. Goldys, Guozhen Liu, **Kaixin Zhang**. An optical fibre based ex-vivo detection device allowing localised and spatially resolved detection of cytokines. International Conference on Biophotonics V Perth Perth, Australia (30 April - 1 May 2017)
4. **Kaixin Zhang**, Annemarie Nadort, Mark R. Hutchinson, and Ewa M. Goldys. A spatial ELISA based on gold nanoparticle modified optic fiber for probing cytokine IL-6. SPIE BioPhotonics, Australia (October 2016)
5. Fei Wang, Nicole Cordina, **Kaixin Zhan**g, Iron oxide based particles for dual-modal targeted cancer imaging. SPIE BioPhotonics, Australia (October 2016)

Statement of Contribution

Chapter 2 Detection of Interleukin-6 on APTES -AuNP-MA Modified Glass Fiber

Guozhen Liu did the experiment set-up, sample preparation, data collection and analysis and main part of manuscript preparation. Kaixin Zhang and Annemarie Nadort involved in the experiments on the fiber surface and the sample preparation and data collection and analysis. Mark R. Hutchinson and Ewa M. Goldys did critically revising on this manuscript and involved in the design of the experiments.

Chapter 3 Detection of Interleukin-1β on APTES -AuNP-MA Modified Glass Fiber

Kaixin Zhang designed and carried out all the in vitro experiments and did the data collection, analysis and in vitro part of manuscript preparation. Moreover, Kaixin Zhang and Michael V. Baratta and Nathan R. Leslie did the collection of the in vivo data and did the data analysis together. Michael V. Baratta designed the in vivo experiments and integrated the in vitro and in vivo part together, and finally drafted the whole manuscript. Guozhen Liu, Matthew G. Frank, Linda R. Watkins, Steven F. Maier, Mark R. Hutchinson, Ewa M. Goldys involved in the revision of the manuscript. Matthew G. Frank, Steven F. Maier, Mark R. Hutchinson, Ewa M. Goldys involved in the design of the whole experiment and did critically revising on the manuscript and response to the reviewers' comments.

Chapter 4 Detection of Interleukin-6 on Biotin-Avidin System Modified Glass Fiber

Kaixin Zhang designed and carried out all the experiments and did the analysis and interpretation of the related data and finally drafted the significant part of the manuscript. Guozhen Liu helped to revise the manuscript. Ewa M. Goldys did critically revising on the manuscript, and supervised on how to response the reviewer's comments, and supervised the experiments during the revising step.

Chapter 5 Detection of Interleukin-6 on Biotin-Avidin System Modified Glass Fiber

Kaixin Zhang designed and carried out most of the in vitro experiments, moreover Kaixin Zhang did the analysis and interpretation of the related data and finally drafted the significant parts of the article. Ayad G. Anwer did the cell work part, and confocal imaging help on data collection and processing. For the in vivo part, Azim Arman did the animal experiment and collected the data. Mark R. Hutchinson, and Ewa M. Goldys supervised the whole experiment work and did critical revising on the manuscript and the response to the reviewers' comments.